Investigating the non-genomic actions of the glucocorticoid receptor

A thesis submitted to the University of Manchester for the degree of Doctor of Philosophy in the Faculty of Biology, Medicine, and Health

2018

Stephen Kershaw

School of Medical Sciences

Division of Diabetes, Endocrinology, and Gastroenterology

The University of Manchester

Oxford Road

Manchester

M13 9PL

United Kingdom

Table of Contents

List of Figures

List of Tables

Publications arising from this thesis

- Kershaw, S., Morgan, D., Boyd, J., Iqbal, M., Zindy, E., Hunter, L., Baxter, M., Knight, A., Krakowiak, K., Spiller, D., Brass, A., Matthews, L & Ray, D. Glucocorticoids inhibit cell migration by a non-transcriptional pathway involving HDAC6. In preparation for submission Nature Cell Biology 2018.
- Kershaw, S., Pfaendar, P., Poolman, T., Matthews, L & Ray, D. In preparation for submission to Cell Reports 2018.

Presentations arising from this thesis

Oral presentations

- Society of Endocrinology conference, Harrogate, UK: Glucocorticoids rapidly inhibit migration through a novel, non-genomic mechanism involving HDAC6. Kershaw, S., Morgan, D., Boyd, J., Spiller, D., Brass, A., Iqbal, M., Zindy, E., Matthews, L., Ray, D. 2017.
- Gene Expression and Chromatin Signalling Seminar Series, Manchester, UK: Glucocorticoids rapidly inhibit migration through a novel, non-genomic mechanism involving HDAC6. Kershaw, S., Morgan, D., Boyd, J., Spiller, D., Brass, A., Iqbal, M., Zindy, E., Matthews, L., Ray, D. 2017.
- Medical Research Council Doctoral Training Partnership conference, Manchester, UK: Glucocorticoids inhibit cell migration through a novel, non-transcriptional pathway. Kershaw, S., Morgan, D., Boyd, J., Spiller, D., Brass, A., Iqbal, M., Zindy, E., Matthews, L., Ray, D. 2017.
- Biological Timing Seminar Series, Manchester, UK: Glucocorticoids rapidly inhibit migration through a novel, non-genomic mechanism involving HDAC6. Kershaw, S., Morgan, D., Boyd, J., Spiller, D., Brass, A., Iqbal, M., Zindy, E., Matthews, L., Ray, D. 2017.
- Society of Endocrinology conference, Edinburgh, UK: Glucocorticoids stabilise the microtubule network to inhibit cell migration. Kershaw, S., Morgan, D., Brass, A., Iqbal, M., Zindy, E., Matthews, L., Ray, D. 2015.

Poster presentation

- Nuclear Receptors Research Network, Amsterdam, Netherlands: Glucocorticoids rapidly inhibit migration through a novel, non-genomic mechanism involving HDAC6. Kershaw, S., Morgan, D., Boyd, J., Spiller, D., Brass, A., Iqbal, M., Zindy, E., Matthews, L., Ray, D. 2016.

List of Abbreviations

A549	Human lung adenocarcinoma epithelial cells
ACN	Acetonitrile
AF1	Activation function 1
AF2	Activation function 2
αTAT1	α-tubulin acetyltransferase-1
ACTH	Adrenocorticotrophic hormone
AMD	Actinomycin D
AP1	Activating-protein 1
BSA	Bovine serum albumin
cAMP	Cyclic adenosine monophosphate
CALD1	Caldesmon-1
CBG	Corticosteroid binding globulin
CBP	CREB-binding protein
CDF	Cumulative distribution function
CHiP	Chromatin immunoprecipitation
cGR	Cytosolic glucocorticoid receptor
cGRE	Composite glucocorticoid response element
COPD	Chronic obstructive pulmonary disease
COX	Cyclooxygenase

cPLA2	Cytosolic phospholipase A2
CREB	CBP binding protein
CRH	Corticotropin-releasing hormone
CRM	Chromosomal maintenance
CVZ	Cortivazol
CYP	P450 heme-containing monooxygenase
DAC	Deacetylcortivazol
DBD	DNA-binding domain
Dex	Dexamethasone
DMEM	Dulbecco's modified eagle's medium
DMSO	Dimethylsulfoxide
DTT	Dithiothreitol
DUSP1	Dual specificity phosphatase-1
EB3	End-binding protein-3
ECL	Enhanced chemiluminescence
EDTA	Ethylenediaminetetraacetic acid
eGFP	Enhanced green fluorescent protein
E/R/M	Ezrin/Radixin/Moesin
ER	Oestrogen receptor
FBS	Foetal bovine serum
cFBS	charcoal-stripped foetal bovine serum
FASP	Filter-aided sample preparation
FCCS	Fluorescence cross-correlation spectroscopy
FF	Fluticasone furoate
FITC	Fluorescein isothiocyanate

FKBP ..... FK506-binding protein

FP ..... Fluticasone propionate

G6P Glucose-6-phosphate

GAPDH ..... Glyceraldehyde 3-phopshate dehydrogenase

GC ..... Glucocorticoid

Gdmcl ..... Guanidine hydrochloride

GILZ ..... Glucocorticoid-induced leucine zipper

GFP ..... Green fluorescent protein

GR ..... Glucocorticoid receptor

GR^{dim} ..... Dimerisation-deficient glucocorticoid receptor

GRE ..... Glucocorticoid response element

GRIP1 ..... Glucocorticoid receptor interacting protein-1

GSK ..... Glycogen synthase kinase

H2B ..... Histone 2B

HAT ..... Histone acetyltransferase

HDAC ..... Histone deacetylase

HeLa ..... Human cervical carcinoma cells

HPA ..... Hypothalamic-pituitary-adrenal

HRP ..... Horse radish peroxidase

HSD ..... 11-β-hydroxysteroid dehydrogenase

Hsp ..... Heat shock protein

ID ..... Intrinsically disordered

IκBα ..... Inhibitor of nuclear factor κB (NFκB)

IFN ..... Interferon

IL ..... Interleukin

JNK	c-Jun N-terminal kinase
LBD	Ligand-binding domain
LC-MS/MS	Liquid chromatography-mass spectrometry
Luc	Luciferase
MAPK	Mitogen-activated protein kinase
MF	Mometasone furoate
mGR	Membrane-bound glucocorticoid receptor
MMTV	Mouse mammary tumour virus
MR	Mineralocorticoid receptor
mRNA	Messenger ribonucleic acid
MT	Microtubule
NAD	Nicotinamide adenine dinucleotide
NES	Nuclear export signal
NF-κB	Nuclear factor-κB
nGRE	Negative glucocorticoid response element
NLS	Nuclear localization sequence
NPC	Nuclear pore complex
NR	Nuclear receptor
NRE	NF-κB response element
NSG	Non-steroidal glucocorticoid
NTD	N-terminal domain
OCN	Osteocalcin
p/CAF	p300/CBP-associated factor
PBS	Phosphate buffered saline
PDF	Probability distribution function

Pepck	Phosphoenolpyruvate
PFA	Paraformaldehyde
pHT	HaloTag
PKA	Protein kinase A
PKC	Protein kinase C
PMA	Phorbol 12-myristate 13-acetate
POMC	Pro-opiomelanocortin
PR	Progesterone receptor
Pred	Prednisolone
pTEFB	Positive transcription elongation factor
PTM	Post-translational modification
qPCR	Quantitative polymerase chain reaction
RA	Rheumatoid arthritis
RIPA	Radioimmunoprecipitation
RLU	Relative light unit
RMS	Root mean square
RT	Room temperature
RXR	Retinoid X receptor
SDS	Sodium dodecyl sulfate
SEGRA	Selective glucocorticoid receptor agonist
SILAC	Stable isotope labelling with amino acids in cell culture
siRNA	Small interfering RNA
STAT	Signal transducer and activator of transcription
SUMO-1	Small ubiquitin-related modifier-1

THN.....Tetrahydronapthalene

TF.....Transcription factor

TFA.....Trifluoroacetic acid

TFE.....Trifluoroethanol

tGRE.....Tethering glucocorticoid response element

TMR.....Tetramethylrhodamine

TNF.....Tumour necrosis factor

tPA.....Tissue plasminogen activator

TPR.....Tetratricopeptide repeat

TSA.....Trichostatin A

UTR.....Untranslated region

VEGF.....Vascular endothelial growth factor

X2K.....Expression to kinase

Word count: 32,871

Declaration

I declare that no portion of the work in this thesis has been submitted in an application for another degree or qualification of this or any other university or other institute of learning.

Copyright Statement

Alternative Format Thesis

This thesis is presented in the alternative format in accordance with the University of Manchester guidelines. Chapters three and four present my findings which are in preparation to be submitted for publication and have been adapted to a coherent style suitable for this thesis. My contributions to each publication are described below.

Chapter 3: Glucocorticoids inhibit cell migration by a novel non-transcriptional mechanism involving HDAC6

In review at Nature Communications

I performed the live-cell migration assays (Fig 3.1D-H, Fig 3.2E-G, Fig 3.3D, Fig 3.5B-E, Fig 3.5I, Fig S3.1E, Fig S3.2C), scratch wound assays (Fig S3.1F), FCCS imaging and analysis (Fig 3.6A-G), siRNA knockdown experiments (Fig 3.1F-G, Fig 3.5A-B), real-time GR trafficking (Fig 3.2A-B), reporter gene assays (Fig S3.1C), real-time HDAC6 imaging (Fig S3.4A), HaloTag pulldown assay (Fig S3.4B), colocalisation imaging (Fig S3.4C-D). Dr David Morgan performed the initial set of cell migration experiments (Fig 3.1A-C, Fig S3.1A-B) and alpha stable distribution parameterisation in collaboration with Professor Andy Brass (Fig S3.2A-F, Fig S3.3A-F). Dr David Morgan also performed the western blots and immunofluorescence of acetylated α-tubulin and the live-cell EB3-GFP imaging and analysis (Fig 3.4A-E). Dr Mudassar Iqbal conducted the mathematical analysis of cell migration kinetics (Fig 3.3C). Dr Egor Zindy developed the wavelet plugin used for tracking cell migration in brightfield microscopy. Dr James Boyd and Dr David Spiller helped with the acquisition and analysis of FCCS samples I prepared (Fig 3.6B-F). My supervisors Dr Laura Matthews and Professor David Ray provided advice and guidance on all experimental work and analysis. I wrote the initial draft of the manuscript, which was reviewed by my supervisors before additional comments from the co-authors. The subsequent final draft incorporated the suggested comments.

Chapter 4: Non-genomic approach to investigate novel glucocorticoid mechanism of action

In preparation for submission to Scientific Reports

I performed the luciferase reporter gene assays (Fig 4.1A-B, Fig S4.1), real-time GR trafficking assays (Fig 4.2), SILAC phosphoproteomics and quantification (Fig 4.3A-D, Fig S4.2, Fig S4.3, Fig S4.4), and pathway analysis of phosphoproteomics data (Fig 4.4A-C).Pauline Pfaendar performed the western blots for SILAC validation (Fig 4.5). Dr Toryn Poolman helped with the phosphoproteomics processing and analysis. My supervisors Dr Laura Matthews and Professor David Ray provided advice and guidance on all experimental work and analysis. As first author on this paper, I was responsible for writing the text of the manuscript, the first draft of which was reviewed by my supervisors before additional comments from the co-authors. The subsequent final draft incorporated the suggested comments.

Acknowledgements

I would like to thank my supervisors Prof David Ray and Dr Laura Matthews for their guidance and support during my PhD. Special thanks to Laura for her words of wisdom and listening to my rambling over the years. I'd also like to thank everyone in the Ray group and at the University who helped and supported me during my time there. I am thankful to the Medical Research Council for providing the funding for my PhD. Finally, I'm incredibly grateful to my friends and family for being amazing to me through all the highs and lows of my PhD, you're all saints! I'd especially like to dedicate this thesis to my sister, mother, grandparents, and family for their unwavering love and support.

Abstract

Glucocorticoids (GCs) are a class of steroid hormone that play essential roles in development, glucose homeostasis, and reducing inflammation. Clinically, GCs are potent anti-inflammatory and immunosuppressive agents used to treat a variety of diseases. However, the therapeutic benefit of GCs is negatively impacted by the induction of severe side effects. In this thesis, I present two studies that have contributed to the understanding of the non-genomic actions of GCs.

GCs inhibit cell migration by a non-transcriptional pathway involving HDAC6: A negative side effect of GC therapy is impaired wound healing which is ascribed to inhibited cell migration. Using live-cell microscopy, I show that GCs inhibit cell migration within 30 minutes of administration. GCs alter the dynamics of the microtubule network through rapid induction of tubulin acetylation (by inhibition of HDAC6) which increases microtubule stability and slows cell movement. The inhibitory effect of GCs on cell migration is reversed by overexpressing HDAC6. Using quantitative imaging, I identified a rapid ligand-dependent association of the GR and HDAC6 within the cytoplasm that is absent in the nucleus. However, a very small proportion of HDAC6 enters the nucleus post-GC treatment, suggesting that HDAC6 accompanies the GR during nuclear translocation. This study demonstrates that GCs rapidly inhibit cell migration by a non-transcriptional mechanism involving HDAC6.

Investigating the rapid effects of GCs on the phosphoproteome: Non-steroidal GCs are useful tool compounds to dissect glucocorticoid receptor (GR) activity. Here, I investigated the early, rapid effect of GCs on the phosphoproteome of A549 cells using SILAC-based phosphoproteomics. A consistent spectrum of phosphoproteins was differentially regulated by GC within 10 minutes of administration, notably including regulators of RNA polymerase II, chromatin remodifying proteins, transcription factors, cytoskeletal modifiers, regulators of intracellular calcium signalling and endocytosis. These phosphoproteins were validated by western blotting. This study shows a clear early effect of GCs on the phosphoproteome with implications for non-specific, non-transcriptional activity of GCs.

Chapter 1: Introduction

1.1. Glucocorticoid Physiology

Glucocorticoids (GCs) are a class of steroid hormones that are involved in a variety of critical processes within the human body, including bone turnover, glucose metabolism, and regulation of the immune system and inflammatory response (Buttgereit and Scheffold, 2002). GCs are secreted from the adrenal cortex after activation of the hypothalamic-adrenal-pituitary (HPA) axis in a diurnal and pulsatile manner, with additional release in response to stress (Gratsias et al., 2000).

1.1.1. Glucocorticoid synthesis and release

Upon stimulation, the hypothalamus releases corticotrophin-releasing hormone (CRH), which then acts on the anterior pituitary gland to stimulate the synthesis of adrenocorticotropic hormone (ACTH). ACTH then acts on the adrenal cortex to induce the secretion of GCs by up-regulating the transcription of genes involved in steroidogenesis through the induction of a cyclic AMP (cAMP)/protein kinase A (PKA)-dependent signalling pathway. The naturally occurring GC within humans, cortisol, is synthesised from cholesterol by cells of the *zona fasciculata* within the adrenal cortex by the action of ACTH-induced P450 heme-containing monooxygenases (CYPs) and 3β-hydroxysteroid dehydrogenase (HSD) enzymes (Lucki et al., 2012) (Figure 1.1). Each step of the steroidogenesis process is subject to negative feedback regulation by cortisol that prevents the release of excessive corticosteroids.

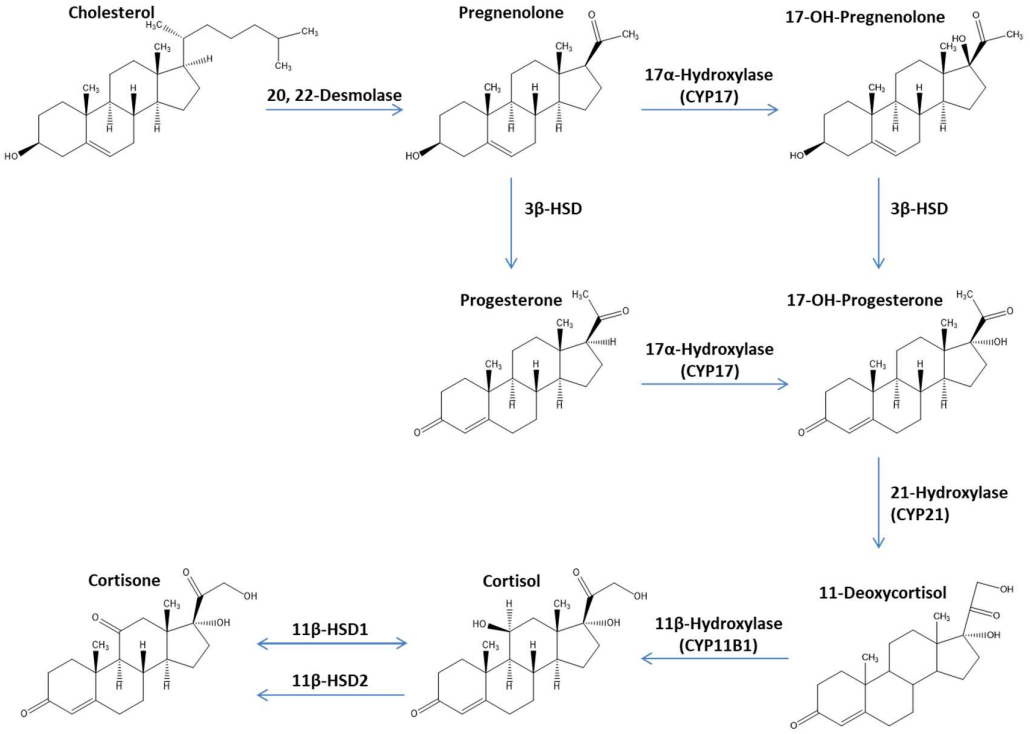

Figure 1.1. **Cortisol biosynthesis pathway**. Representation of the cortisol biosynthesis pathway beginning with the conversion of cholesterol to pregnenolone by cytochrome p450 side-chain cleavage enzymes (CYPs) located on the inner mitochondrial membrane. Subsequent hydroxylation and dehydrogenation reactions by hydroxysteroid dehydrogenase (HSD) enzymes convert pregnenolone into cortisol as an active GC. After secretion, 11β-HSD1 interchangeably converts cortisol into inactive cortisone, whereas 11β-HSD2 only converts cortisol to cortisone, both of which act to regulate cortisol availability in the circulation. Cortisol and its hormonal precursors share a common chemical structure and are composed of 21 carbon atoms that form a cyclopentanoperhydrophenanthrene backbone. This backbone is divided into three cyclohexane rings (labelled A, B, and C) and one cyclopentane ring (labelled D). Images were made via Java Molecular Editor applet (http://www.changbioscience.com/mis/chemdraw.html) (Adapted from (Freel and Connell, 2004)).

1.1.2. Glucocorticoid availability

Synthesised cortisol is then released into the circulation where it exists in three main forms: free cortisol (~5%), protein-bound (90-95%), and as cortisol conjugates (George et al., 2009). The protein-bound cortisol constitutes the majority within the circulation and forms pools of available cortisol upon binding to either high-affinity, low-capacity cortisol-binding globulins (CBG) or to low-affinity, high-capacity albumin. In addition to this, cortisone, which is also synthesised from

cholesterol, can be interchangeably converted into active cortisol by the action of 11-β-hydroxysteroid dehydrogenase type-1 enzymes (HSD1) thus providing another mechanism of altering GC availability in the circulation (Chapman et al., 2006). Cortisol availability is also regulated by the HSD2 enzyme that solely converts cortisol back into cortisone in the presence of NAD+ (Hardy et al., 2014). The local modulation of cortisol availability is integral to the swift resolution of local inflammation and promote rapid resolution, with HSD1 expression being enhanced by pro-inflammatory cytokines (Chapman and Seckl, 2008).

The interaction of protein-bound cortisol with protease enzymes then stimulates the release of active cortisol, where it is free to diffuse across cellular membranes and bind to the glucocorticoid receptor (GR) and exert a variety of cell- and tissue-specific effects, including the brain, liver, muscle, adipose tissue, and lungs. As lipophilic hormones, GCs can diffuse freely across the plasma membrane of cells and exert their regulatory effects on target genes through binding to the glucocorticoid receptor (GR). As the GR is ubiquitously expressed in all cell types and tissues, the systemic effect of GCs is quite profound and stimulates physiological changes within a relatively fast period at both the genomic and non-genomic levels (Stahn and Buttgereit, 2008; Croxtall et al., 2000).

1.2. Glucocorticoids in Health and Disease

Endogenous GCs play an essential role in energy homeostasis (metabolism) within humans, where they act on various tissues to increase the concentration of glucose within the circulation to provide the energy to maintain brain function under stressful conditions (Patel et al., 2014).

1.2.1. Regulation of glucose metabolism

GCs provide the substrates for glucose production by inducing the transcription of genes involved in gluconeogenesis in the liver, increasing amino acid release by protein catabolism in muscle tissue, increasing fatty acid release by lipolysis in adipose tissue, and reducing glucose re-uptake by inhibiting the release of insulin from pancreatic β-

cells (Patel et al., 2014). Stress-induced activation of the HPA axis and the release of GCs may provide a short burst of energy to the body by mobilising circulating glucose, which allows it to overcome the stressful stimulus. However, the prolonged activity of GCs, as seen with high doses of synthetic GCs or in Cushing's syndrome (pathological GC excess), elevates blood glucose concentration beyond homeostatic levels, which has a deleterious metabolic effect resulting in hyperglycaemia, obesity, and insulin resistance.

In the liver, elevated GC levels increase the transcription of the phosphoenolpyruvate carboxykinase (Pepck) and glucose-6-phosphate (G6P) enzymes, both of which catalyse the final rate-limiting steps in gluconeogenesis, thereby causing an increase in blood glucose beyond homeostatic levels (Waltner-Law et al., 2003). GCs also act to directly impair the insulin signalling pathway and oppose the action of insulin on regulating blood glucose levels.

1.2.2. Regulation of immunity

GCs are also potent regulators of the inflammatory response within humans and their repression of pro-inflammatory genes encoding cytokines, chemokines, and cell adhesion molecules. GCs can achieve this through binding and activation of the cytosolic GR (cGR), which directly and indirectly down-regulates pro-inflammatory gene expression and up-regulates the expression of anti-inflammatory proteins. GCs can also regulate inflammation through interaction with membrane proteins, the membrane-bound GR (mGR), and kinases independent of gene expression, all of which are attributed to the non-genomic actions of the GR. The anti-inflammatory effects of GCs are very potent and act quickly to resolve points of local inflammation with incredible speed (Baschant and Tuckermann, 2010).

GCs modulate primary and secondary immune cells to exert their immunosuppressive effects. GCs can suppress the immune system by shifting the balance between the innate-adaptive activation pathways in macrophages (van de Garde et al., 2014). Here, GCs enhance the innate immune response whilst suppressing the adaptive immune response, by modulating the proliferation and activity of macrophages, cytokine-secreting T cells, and monocytes in a dichotomous manner (Kino et al.,

2000; Niraula et al., 2018; Tu et al., 2017). This has downstream effects on the synthesis of pro-inflammatory mediators secreted through macrophages, including prostaglandins, cyclooxygenase (COX)-2, and cytokines, and contributes to the anti-inflammatory activities of GCs. The importance of GC immunosuppressive activity is notably demonstrated in the poor survival rates of adrenalectomised *in vivo* models challenged with bacterial lipopolysaccharide (LPS) (Goodwin et al., 2014).

GCs inhibit the production of various pro-inflammatory molecules, including arachidonic acid, tumour necrosis factor-α (TNFα), signal transducer and activator of transcription-1 (STAT1), interleukin-6 (IL-6), IL-1α, prostaglandins, fibronectin (Ballegeer et al., 2018; Ito et al., 1999; Chivers et al., 2004; Huang et al., 2018; Khan et al., 2005). GCs also inhibit the activity of pro-inflammatory transcription factors including NFκB and AP-1 prior to nuclear entry, the former by up-regulation of the NFκB inhibitor IκB (van der Burg et al., 1997), and the latter by antagonising TNFα-mediated induction of AP-1 (Gonzalez et al., 2000).

In addition to their profound anti-inflammatory effects, GCs also induce the expression of anti-inflammatory mediators such as transforming growth factor-β and IL-10 (Gonzalez-Robayna et al., 2000; Ogasawara et al., 2018). Moreover, GR directly activates the expression of the anti-inflammatory glucocorticoid-induced leucine zipper (GILZ) protein, which suppresses the action of many pro-inflammatory molecules including TNFα, NFκB, and inducible nitric oxide synthase (iNOS) (Aguilar et al., 2013; Esposito et al., 2012; Beaulieu and Morand, 2011)

1.3. Synthetic Glucocorticoids

Due to the potent anti-inflammatory and immunosuppressive activity of GCs, the development of synthetic GCs capable of selectively activating these pathways is an attractive prospect for treating inflammatory and autoimmune disorders. The development of potent GCs through manipulation of the chemical structure of cortisol, such as dexamethasone (Dex), prednisolone (Pred), and fluticasone propionate (FP), have been successful in the treatment of asthma, rheumatoid arthritis, haematological cancers, and immune suppression (Hirst and

Lee, 1998; Krause et al., 2011; Inaba and Pui, 2010; Oehling et al., 1997). The chemical structures of the synthetic GCs have been altered to optimise local anti-inflammatory potency, such as modification of the steroid D-ring in FP to treat respiratory diseases of an inflammatory nature such as asthma and rhinitis (Cosio et al., 2005). Despite the powerful applications of GCs, the caveat of adverse side effects is invariably observed after administration at high doses over a long period of time (Longui, 2007). These effects, including osteoporosis, hyperglycaemia, muscle atrophy, and hypertension, are characteristic of the systemic effects of GC action (Wust et al., 2009; Schakman et al., 2013; Lund et al., 1985; Goodwin and Geller, 2012; Weinstein et al., 1995). The prevalence of such side effects presents a major contraindication to prolonged high dose GC therapy in treating inflammatory and autoimmune diseases.

It is therefore important to understand the molecular effect of GC binding upon the glucocorticoid receptor (GR) to develop GCs that retain anti-inflammatory activity whilst avoiding the induction of severe side effects. The body of this introduction will therefore provide an analysis of the current literature surrounding the structure and function of the GR and novel ligands developed with this paradigm in mind. An emphasis will be placed on the interaction of novel ligands with the GR and how ligand binding is able to induce conformational changes within the receptor that alter its ability to interact with non-genomic and genomic signalling networks and regulate target gene expression.

1.4. Glucocorticoid Receptor

The biological actions of GCs are mediated through the glucocorticoid receptor (GR), a ubiquitously expressed, ligand-activated transcription factor. As part of the nuclear receptor (NR) family, GR shares structural and functional similarity to other NR members, including the oestrogen (ER), progesterone (PR), mineralocorticoid (MR), androgen (AR), and retinoid X receptors (RXR) (Pawlak et al., 2012).

In its resting state, GR forms complexes with heat-shock proteins and immunophillins, including Hsp90, Hsp70, Hop, FKBP51, and p23, which promote the cytoplasmic retention of GR and maintain the ligand-

binding domain (LBD) in a high-affinity binding state (Ebong et al., 2016; Paakinaho et al., 2010). Upon ligand binding, the GR undergoes a conformational change that facilitates receptor activation, interaction with cytoplasmic proteins to initiate non-genomic effects, and nuclear translocation along microtubules leading to regulation of GC-target genes (Boldizsar et al., 2010; Iwasaki et al., 1997; Chien et al., 2016; Teng et al., 2013).

1.4.1. *GR* gene

The gene encoding the human GR protein is 9 exons in length and located on human chromosome 5q31-32 (Strehl et al., 2011). Each exon of the *GR* gene, excluding exon 1, contains the coding sequences for the GR protein. The GR exists in multiple isoforms and splice variants resulting from altered initiation of GR gene transcription and differential splicing of the exons within the GR gene (Lu and Cidlowski, 2004). Each isoform presents different signal transduction potentials and, along with post-translational modifications, contributes to the molecular diversity and possibility to the variety of GR effects (Figure 1.2).

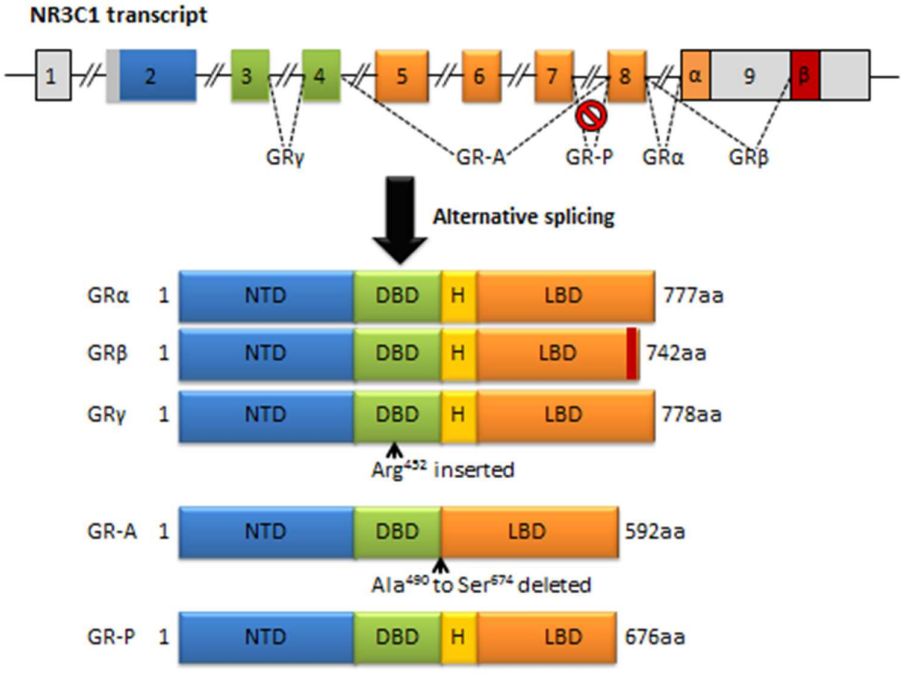

Figure 1.2. ***GR* splice variants**. Alternative splicing of the primary *NR3C1* transcript with dashed lines representing exon splicing. Transcript exons and resulting domains are matched by colour (N-terminal domain [blue], DNA-binding domain [green], hinge region

[yellow], ligand-binding domain [orange]. Predominant GRα results from splicing of exon 8 to the start of exon 9. GRβ results from an alternate splicing acceptor site within the LBD thus encoding a unique 15 amino acid sequence at positions 728-742. GRγ results from an alternate splice donor site in the intronic region between exons 3 and 4 leading to an insertion of arginine at position 452 within the DBD. GR-A results from alternate splicing between exons 4 and 8 which deletes exons 5-7 from the LBD. GR-P results from a failure to splice exon 7 to exon 8 causing truncation of the LBD.

Exon 1 encodes the 5'-untranslated region (UTR) of the *GR* and contains several transcription initiation sites that result in the generation of multiple mRNA transcripts. The alternative exon 1 transcripts (1A1, 1A2, 1A3, 1B, and 1C) are differentially expressed in different cell types and each is controlled by different upstream regions (promoters 1A, 1B, and 1C). Each of the different exon 1 transcripts joins to the same acceptor site on exon 2 yielding transcripts containing various 5'-UTRs (Russcher et al., 2007). As exon 1 only contains untranslated regions, any splice variants of this region do not have subsequent effects on the coding of the GR polypeptide but do have downstream effects on the expression of the *GR* gene within specific cell types (Zhou and Cidlowski, 2005). Exon 2 contains the acceptor site for exon 1 recognition and encodes the N-terminal domain of the GR, including the activation function 1 (AF-1) domain that is involved in the recruitment of co-regulatory molecules during gene regulation. Exons 3 and 4 encode the two zinc finger motifs that constitute the DNA-binding domain (DBD) of the GR and are involved in GR dimerization and binding to GREs within target genes. Exons 5 to 9 each encode part of the ligand-binding domain (LBD) of the *GR* that facilitates ligand-dependent activation of the GR. Exons 5 to 9 subsequently encode the sites for the activation function 2 (AF-2) domain that permits ligand-dependent gene transcription and recruitment of co-regulatory molecules (Oakley and Cidlowski, 2011). Exon 9 also encodes the 3'UTR and is subject to alternate splicing to yield the exon 9α and exon 9β variants, both of which ultimately encode two separate GRs, GRα (by exon 9α) and GRβ (by exon 9β).

1.4.1.1. GR isoforms

The majority (~90%) of cellular GR exists as the classical GRα isoform located predominantly in the cytoplasm, with GRβ accounting for 0.2-1% of the total GR transcript (Kino et al., 2009). GRα and GRβ both have identical polypeptide structures up to amino acid 727 of the LBD

where they differ in their C-termini; GRα encodes an additional 50 amino acids whereas GRβ encodes an additional 15, each of which is unique to the splice variant (Lu and Cidlowski, 2004).

GRβ has been described as a functionally inactive isoform of GR and is implicated in GC resistance in chronic obstructive pulmonary disorder (COPD) and small cell lung cancer (Lewis-Tuffin and Cidlowski, 2006), although it has been demonstrated that GRβ is capable of regulating distinct GRβ-responsive genes independent of GRα (Kino et al., 2009). GRβ can form transcriptionally inert heterodimers with GRα that suppresses GR-target gene expression in a dominant-negative manner. This mechanism has been implicated in the development of GC resistant and reduced sensitivity in health and disease states (Fruchter et al., 2005). However, due to the relatively low levels of GRβ in cells compared to GRα both in healthy and disease states, coupled with the high degree of variability in GC sensitivity between different cells and tissues, the role of GRβ in GC resistance is disputed (Lewis-Tuffin and Cidlowski, 2006).

Furthermore, the addition of three nucleotides from the intronic region between exons 3 and 4 (constituting the DBD) results in an additional arginine amino acid at position 452 and forms the GRγ isoform (Lu and Cidlowski, 2004; Matthews et al., 2011; Morgan et al., 2016). GRγ has been implicated in GC resistance owing to the reduction in transactivation activity compared to GRα (Duma et al., 2006). Other splice variants are also formed from truncations of the GR gene, with GR-A lacking exons 5 to 7 and GR-P lacking exons 8 and 9, both of which are functionally inactive and have been implicated in GC resistance in leukaemia and myeloma (Sanchez-Vega et al., 2006).

The initiation of translation at alternative downstream start sites (ATG codon; Methionine residue) by leaky ribosomal scanning of the GR gene can also add an additional level of translational variation (Smith et al., 2005). The predominant GRα-A product is formed from the initiation of mRNA translational at the first start codon (Met1). Additional GR isoforms, GRα-B and GRβ-B, are formed from the alternate initiation of translation at an extra start codon (Met27) within exon 2 of the GR gene, both of which have distinct regulatory effects on target gene expression that are separate to GRα (Dong et al., 2015). Each GR isoform and splice variant also undergoes post-translational

modifications that alter activity, structure, and interactions with other proteins and DNA, which is described in further detail in the following section.

1.4.2. GR structure

The GR is a modular protein and contains three main functional domains: the N-terminal domain (NTD), DNA-binding domain (DBD), and ligand-binding domain (LBD) as shown in Figure 1.4 (Giguere et al., 1986). Each of these domains acts independently to mediate GR action and each domain is independently subject to post-translational modifications that affect overall GR activity.

1.4.2.1. N-terminal domain

The NTD is the main site of post-translational modifications including phosphorylation, SUMOylation, acetylation, and ubiquitination (Figure 1.4). The NTD also contains the activation function-1 (AF1) domain that mediates the protein-protein interaction between the GR and co-regulatory proteins, subsequently altering gene expression (Kumar and Thompson, 2012). Co-regulator binding is mediated through the recognition of the α-helical LXXLL motif (where L represents a Leucine residue and X represents any amino acid residue), or NR box, within the co-regulator promoter region (Savkur and Burris, 2004).

1.4.2.2. DNA-Binding Domain

The DBD has a highly conserved sequence homology and contains two zinc finger motifs that facilitates receptor dimerization and binding to specific GREs in the promoter region of target genes thus allowing the GR to directly regulate gene expression (Lundback et al., 1993). The GRE is an imperfect palindrome composed of a pair of hexameric DNA sequences (half-sites) separated by three random amino acid residues (GAGAACAnnnTGTTCT) and is located in the 5' promoter region of GR-target genes (Dokoumetzidis et al., 2002). The first zinc finger (P box) contains amino acids that are primarily involved in recognition of response elements, whether GR- or transcription factor-targeted, whereas the second zinc finger (D box) is integral to GR homo- and/or hetero-dimerization thus indicating a delegation of function within the DBD (Kumar and Thompson, 2005). The hinge region connects the DBD

to the LBD and is the main site of lysine residue acetylation that affects GR activity (Yoshikawa et al., 2008).

1.4.2.3. Ligand-Binding Domain

The LBD is responsible for the ligand-receptor interaction that results in activation of receptor activity. In its nascent state, the LBD of the GR is associated with a multi-protein chaperone complex that comprises heat-shock proteins (hsp) and immunophilins, including hsp70, Hsp90, FKBP51, CyP-40, and p23, which promote cytoplasmic retention and maintain the LBD in a high-affinity binding state (Bertorelli et al., 1998; Dittmar et al., 1997; Grad and Picard, 2007). The LBD initially associates with hsp40 and hsp70 to induce a low-affinity receptor conformation within the cytoplasm. Upon recruitment of the hsp70-Hsp90 organising protein (HOP) to the LBD by recognition of its tetratricopeptide (TPR) repeats, the GR re-associates with Hsp90, p23, and FKBP51 to enable the receptor to fold into a high-affinity conformation and facilitate ligand binding following cellular entry (Grad and Picard, 2007).

It was previously believed that upon ligand binding, conformational changes in the receptor would trigger its dissociation from the multi-protein complex. More recent evidence has shown that Hsp90 remains bound to the LBD of the GR after ligand binding and accompanies the receptor during nuclear import where it interacts with nuclear proteins, thus indicating that Hsp90 has a more regulatory role in GR activity (Silverstein et al., 1997). The binding of Hsp90 to the GR alters its conformation to expose the nuclear localisation signals (NLS1 and NLS2) contained within the hinge region between the DBD and NTD and thus initiate nuclear translocation (Bledsoe et al., 2004). This is accompanied by the replacement of FKBP51 with FKBP52 that binds the microtubule motor protein, dynein, and enables retrograde transport of the GR along cytoskeletal tracts leading to the nucleus (Galigniana et al., 2001; Galigniana et al., 2004).

Ligand-binding to the GR changes the orientation of helix 12 of the LBD and creates the surface for co-regulator recruitment, called the activation function-2 (AF-2) domain. Both the AF-1 domain (located within the NTD of the GR) and AF-2 domains acquire a folded conformation upon ligand binding which allows the GR to regulate gene

transcription through tethering to co-regulatory proteins. The recruitment of co-regulatory proteins by the AF-1 and AF-2 domains is also determined by post-translational modifications, such as phosphorylation-induced stability of the GR LBD and subsequent association with MED14 (Chen et al., 2006).

1.4.3. Dimerization and oligomerization of the GR

GR binding to cognate response elements can have profound effects on receptor structure and function. NMR chemical-shift difference mapping of the GR-DNA interaction has shown that glucocorticoid binding sequences (GBS) drives distinct conformational changes in the rat GR, including the DBD and dimerization interface (Watson et al., 2013). The same study showed that mutational ablation of the GR dimer interface alters its DNA-binding kinetics and transcriptional activity, highlighting the importance of GR dimerization for its activity.

The generation of a GR mutant mouse model (GR^{dim}), in which the GR contains a mutation that impairs dimerization, fails to affect the transrepression of tGREs but successfully prevents the transactivation of simple GREs (Kleiman et al., 2012; Jewell et al., 2012). In addition, ChIP-exo sequencing in the mouse liver under endogenous GC exposure demonstrate the prevalence of GR monomer vs dimer binding to GR half site motifs (Lim et al., 2015). The same study also showed that GR monomers colocalise with other lineage-specific transcription factors whilst occupying GR half sites (half-site tethering), and that GR monomers enhance gene expression. However, under high concentrations of exogenous GC, the GR monomer population on DNA is usurped by GR dimer binding to palindromic GRE sequences, suggesting a dichotomous action of GCs (either low endogenous or high exogenous levels) on the GR monomer/dimer formation and thus GR transcriptional activity. Although these studies highlight the importance of GR monomers in resolving inflammation, conflicting studies challenged the GR^{dim} model, demonstrating that GR^{dim} forms homodimers in response to over-expression of GFP/YFP-tagged GR^{dim} (Presman et al., 2014). Moreover, a recent study elegantly showed that DNA binding at cognate response elements induces GR tetramerisation, suggesting that the GR may exist in multiple oligomers that dictates its transcriptional activity (monomer/dimer/tetramer) (Presman et al., 2016). At minimum, these

studies show that the GR can exert different genomic effects through dimerization-dependent and –independent mechanisms, although additional research into the active form of DNA-bound GR need to be conducted.

Crystal structures of the GR are used to visualise the ligand-receptor interaction and allows for a more in-depth analysis of conformational changes that are induced upon ligand binding (Biggadike et al., 2009). Such conformational changes may have profound impacts on both non-genomic and genomic signalling cascades induced by activated GR and must be understood to develop novel ligands that selectively suppress inflammation yet avoid the induction of side effects.

The crystallisation of the GR LBD is difficult due its low solubility, with the original crystal structure containing a point mutation at F602 (F602S) to improve protein stability (He et al., 2014). Such surface entropy mutations that affect residues away from the LBD (e.g. K669A/K703A for the mineralocorticoid receptor or E684A/E688A for cortisol) do not affect ligand-bound GR activity and allow the creation of receptor-ligand complexes that retain their solubility and form crystals.

The structure of the ligand-bound GR LBD comprises a three layer helical ligand-binding pocket consisting of 12 α-helices and 4-β strands in which the ligand-binding cavity is found on the lower part of the bundle (Bledsoe et al., 2002; He et al., 2014). Agonist binding induces a conformational change of the AF-2 helix within the LBD, which stabilises the GR in an active state thus enabling the recruitment of co-regulatory proteins, facilitated through interaction with multiple LXXLL motifs (Moraitis et al., 2002). Figure 1.3 shows an example of GR homodimerisation of two ligand/bound GRs that have both recruited a co-regulator molecule (TIF2).

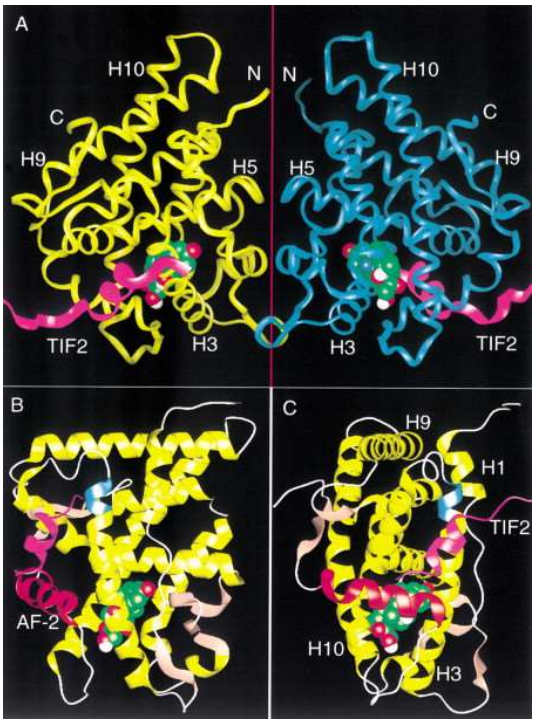

Figure 1.3. **Crystal Structure of the GR ligand binding domain bound to dexamethasone and nuclear receptor coactivator TIF2**. (A) Structure of the GR homodimer with the yellow and blue worms representing the LBDs, the purple ribbons representing the nuclear receptor coactivators 2 (TIF2), and two dexamethasone molecules represented as a collection of carbon (green), hydrogen (white), and oxygen (red) atoms, connected by the DBDs of the two GRs. Helices (H) of importance are noted and the C-terminus (C) and N-terminus (N) identified as appropriate. (B and C) Two 90° angle views of the monomeric GR/Dex/TIF2 complex representing the helices (yellow), β strands (gold), AF-2 helix (pink), TIF2 (purple), Dex (as above), and the charge clamp composed of K579 from helix 3 (blue) which facilitates the recognition and binding of the LXXLL motifs within promoter regions of co-regulatory proteins (Taken from (Bledsoe et al., 2002)).

Several unique properties of the LBD have been characterized using the crystal structure as a point of reference, including the presence of an additional charge clamp (Bledsoe et al., 2002). The crystal structure of the LBD shows us that ligand binding induces a closed conformation of Helix 12 position, which closes over the ligand and provides a surface for the binding of co-regulatory proteins (Kumar and Thompson, 2005). Mutations in the dimer interface (composed of a β sheet) that ablate LBD dimerization result in a loss of GR transactivation activity but leave its transrepressive ability unaffected (Kumar and Thompson, 2005). This suggests that transrepression of GR-target genes is not dependent on GR homodimerisation, signifying the importance of the GR monomer

either directly repressing pro-inflammatory gene expression or tethering to other pro-inflammatory mediators.

1.4.4. GR protein

The predominant GRα protein consists of many modifiable residues that alter its structure, function, and activity. The intrinsically disordered N-terminal domain contains the majority of modifiable sites, frequently serine/threonine phosphorylation. The other modular GR domains contain sites for other, less frequent, post-translational modifications, including ubiquitination, acetylation, and SUMOylation, each of which will be discussed in greater detail in the following section.

1.4.4.1. Post-translational modifications

Post-translational modifications of the GR affect many aspects of GR activity including sub-cellular localisation, functional activity, and protein-protein interactions (Duma et al., 2006; Giguere et al., 1986; Kumar and Thompson, 2005). Figure 1.4 outlines the amino acid residues that are subjected to modification, each of which affects GR activity in a distinct way.

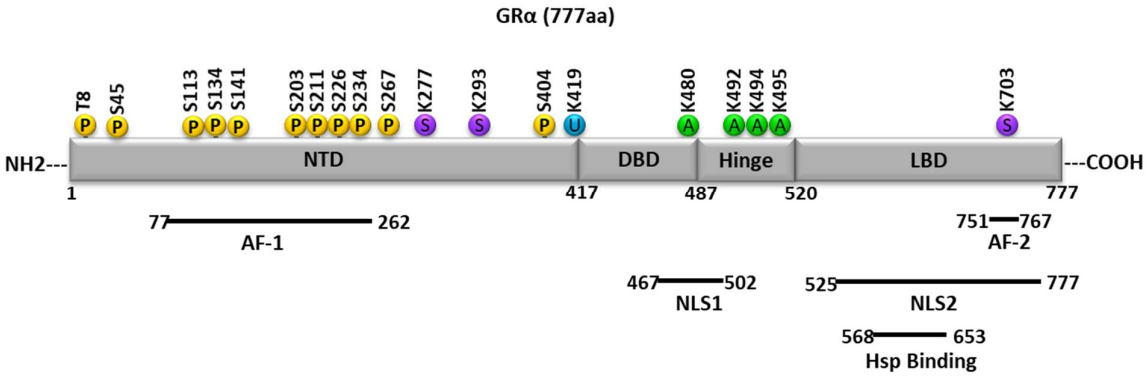

Figure 1.4. **GRα polypeptide with post-translational modifications**. The GRα contains 3 modular domains (NTD, DBD, and LBD) and a hinge region. GRα post-translational modifications are included in the appropriate domains; phosphorylation (P), SUMOylation (S), ubiquitination (U), and acetylation (A), with each respective residue named above. Below each domain are the relative sites for AF-1 and AF-2 (co-regulator recruitment), NLS1 and NLS2 (nuclear import), and Hsp binding (maintains a high-affinity, ligand-binding state) (Adapted from (Bledsoe et al., 2004)).

The diversity of post-translational modifications contributes to the genomic and non-genomic actions of GR and helps to explain how the single GR protein can exert a plethora of effects.

1.4.4.1.1. Phosphorylation

Phosphorylation involves the transfer of a phosphate group to an acceptor amino acid that is catalysed by kinases and reversed by phosphatases. Multiple amino acids have been identified in the GR that are the targets of kinases, many of which are found in the N-terminal domain of the GR. The phosphorylation of each of these amino acids results in distinct changes to GR function. For example, the glycogen synthase kinase (GSK)-3 enzyme phosphorylates serine 404 (S404), the ablation of which impairs the ability of GR to bind co-regulatory proteins (CBP/p300 and the p65 subunit of NFκB) and attenuates GR-mediated transrepression (Galliher-Beckley et al., 2008). For transcription factor proteins, a high number of phosphorylation sites are localised to the intrinsically disordered (ID) region (White et al., 2018). The ID AF1 domain of the GR contains a trio of residues (serine-203, serine-211, serine-226) that upon phosphorylation induce the GR to adopt a functionally active conformation (Khan et al., 2017). Phosphorylation of serines 203 (S203) and 211 (S211) by the p38 mitogen-activated protein kinase (MAPK) and cyclin/cdk2 complexes is also required for GR-interacting protein (GRIP)-1 recruitment that facilitates the induction of GR-transactivated genes such as glucocorticoid-induced leucine zipper (GILZ) (Avenant et al., 2010). The phosphorylation of S203 and S211 regulates GR-target gene transcription by inducing a conformational change in the receptor structure to reveal a novel surface for the recruitment of co-regulatory proteins, known as the activation function-1 (AF-1) domain (Chen et al., 2008; Mukudai et al., 2018). This site-specific phosphorylation is integral to GR function and directs other forms of post-translational modification of the GR such as ubiquitination (Wallace and Cidlowski, 2001). Interestingly, phosphorylation of serine 226 (S226) by the c-Jun N-terminal kinase (JNK) induces a conformational change in the GR that attenuates its transcriptional activity (Itoh et al., 2002). The differences observed by phosphorylating different amino acids demonstrate the complexity and diversity of post-

translational modifications in modulating the structure and activity of the GR.

1.4.4.1.2. Ubiquitination

Ubiquitination is the process by which ubiquitin molecules, either singly or in chains, are covalently attached to proteins which targets them for proteolytic degradation by the proteasome (Lecker et al., 2006). Moreover, chronic GC exposure causes down-regulation of GR through ubiquitin-proteasome pathways mediated by the carboxyl terminus of hsp70 (CHIP) E3 ligase, one of the chaperone proteins that bind to cytosolic GR (Belova et al., 2006). CHIP E3 ligase overexpression was found to restore GC-dependent down-regulation of GR in HT22 hippocampal cells that normally resist GR down-regulation (Wang and DeFranco, 2005). Ubiquitination of the GR therefore prevents GR signalling and is induced by GCs as a form of self-regulation (Wallace and Cidlowski, 2001).

1.4.4.1.3. SUMOylation

SUMOylation involves the covalent attachment of a small ubiquitin-related modifier (SUMO)-1 molecule onto the GR polypeptide catalysed by the SUMO-conjugating enzyme Ubc9 (Le Drean et al., 2002). Although similar in structure to ubiquitin, the role of SUMO-1 is not related to proteolytic degradation but rather works to enhance GR-mediated transcription of promoters containing multiple GR-response elements (GREs) (Le Drean et al., 2002; Paakinaho et al., 2014a; Druker et al., 2013). The same study also demonstrated that SUMO-1 dramatically reduces the stability of GR, which contradicts its enhancing effect on gene transcription. This dichotomy of SUMOylation has also been demonstrated in gene expression profiling of cells expressing wild-type GR and SUMOylation-deficient GR (Paakinaho et al., 2014b). Here, SUMOylation was demonstrated to have a negative effect on cell proliferation whilst also up-regulating the activity of the GR in a target locus-selective manner. The physiological role of SUMOylation may therefore be as a form of control for GR activity particularly during cell proliferation.

1.4.4.1.4. Acetylation

Acetylation is the process by which acetyltransferase enzymes transfer an acetyl group onto an amino acid residue and influences the transcriptional activity of GR. Studies have shown that GR is under direct control of the circadian system within humans and that the circadian rhythm-transcription factor "Clock" possesses inherent acetyltransferase activity (Charmandari et al., 2011; Kino and Chrousos, 2011). The circadian system is an internal timing mechanism that synchronises to the daily light/dark cycle (24 hours) and allows organisms to respond to environmental changes (Gibbs et al., 2014). Clock was found to acetylate lysine amino acids containing a KXXKK motif (Figure 1.4), which causes repression of the transcriptional activity of the GR in an inverse phase to GC release by the HPA axis (Kino and Chrousos, 2011). Further investigation into Clock regulation of GR demonstrated that regulation occurs at local tissues and works to decrease tissue sensitivity to GCs during the morning (when circulatory GC concentration is highest) and increase GC sensitivity at night (when GC concentration is at its lowest) (Charmandari et al., 2011). Acetylation therefore represents a regulatory mechanism to the diurnal fluctuations of GCs.

1.5. GR trafficking

The GR exists in a high-affinity ligand-binding state within the cytoplasm, facilitated by the interaction between the GR and its co-chaperones (Hinds et al., 2014; Stavreva et al., 2004; Rajapandi et al., 2000). Upon ligand binding, the GR undergoes a series of conformational changes in receptor structure leading to its translocation to the nucleus, whereby the GR can interact with GC-target genes, other components of the transcription machinery, and other transcription factors (Conway-Campbell et al., 2011). As such, the kinetics of GR trafficking dictate the occupancy of the GR within the nucleus and thus GR transcriptional activity. Furthermore, prolonged residency of the GR within the cytoplasm may alter its interaction with other proteins within that sub-cellular space (Trebble et al., 2013). Any perturbations in GR

trafficking would therefore have profound downstream effects on GR genomic and non-genomic activity.

1.5.1. Nuclear Import

The GR is in a constant state of dynamic shuttling between the nucleus that is dependent upon tetratricopeptide (TPR) repeat chaperone proteins, such as Hsp90 and immunophilins, as well as cell cycle phase (Matthews et al., 2011; Wu et al., 2004). Nuclear import involves the interaction of GR with the macromolecular nuclear pore complex (NPC), with importin-α and importin-7 facilitating the entry of large molecular weight proteins (>40kDa) (Matthews et al., 2011). The multi-protein GR-chaperone complex also interacts with importin-β and the integral nuclear pore glycoprotein Nup62 of the NPC in an importin-α-independent manner (Echeverria et al., 2009). Import is mediated through the association of NPC proteins with the NLS1 and NLS2 sequences within the GR that are revealed through conformational changes induced upon ligand binding. The kinetics of GR trafficking are also influenced by the ligands that bind the GR, as shown in (Trebble et al., 2013), where the actions of a non-steroidal GR ligand caused a change in electrostatic charge on the surface of the GR. This change in surface charge was caused by displacement of arginine at position 611 of the GR ligand-binding domain, which resulted in slowed phosphorylation and kinetics of nuclear import and subsequently delayed the transactivation of GR-target genes.

1.5.2. Nuclear Export

Upon ligand dissociation, the unliganded GR is recycled to the cytoplasm albeit with a prolonged rate of export. A study by (Liu and DeFranco, 2000) used a chimeric GR expressing containing a heterologous, leucine-rich nuclear export signal (NES) sequence that utilises the exportin-1/CRM-1-dependent nuclear export pathway. (Liu and DeFranco, 2000) found that leptomycin-B inhibited the rapid export of the chimeric GR but had no effect on the wild-type GR; therefore, GR nuclear export occurs independently of exportin-1/CRM-1. The nuclear export of GR is instead mediated by the actions of serine/threonine phosphatase type 5 (PP5) (Wang et al., 2007), which associates with Hsp90 to drive GR transport into the cytoplasm in a process reliant on kinesin motor proteins (Dean et al., 2001). However, despite evidence

that PP5 inhibition by okadaic acid enhances GR transcriptional activity by nuclear retention, the exact mechanism of PP5-mediated nuclear export remains unclear (Zhou and Cidlowski, 2005). Nuclear export of GR is also dependent on site-specific phosphorylation, as seen with JNK-mediated inhibition of GR activity by enhancing the rate of nuclear export (Itoh et al., 2002). Interestingly, the accumulation of unliganded GR in the nucleus appears to serve as a nuclear export storage area; the GR is able to rebind ligand and re-associate with chromatin, thus retaining its functionality (Yang et al., 1997).

1.6. Genomic Signalling

The classical mechanisms of GR target gene regulation explain direct transactivation and/or transrepression of GR-targeted genes. The genes regulated by the GR are numerous and account for ~1% of the human genome thus providing evidence for the multi-faceted role of GR in multiple processes within the human body.

Once in the nucleus, the GR is able to activate (transactivation) or inhibit (transrepression) GR-targeted genes both through direct interaction with GREs within the promoter regions of target genes as a dimerised receptor or by interaction with co-regulator proteins (which can function as coactivators, corepressors, anti-activators, and anti-repressors) as a monomeric receptor that can bind to GREs or other regulatory transcription factors, such as NFκB and AP-1, in a process termed "tethering" (Kumar and Thompson, 2005) (Figure 1.5).

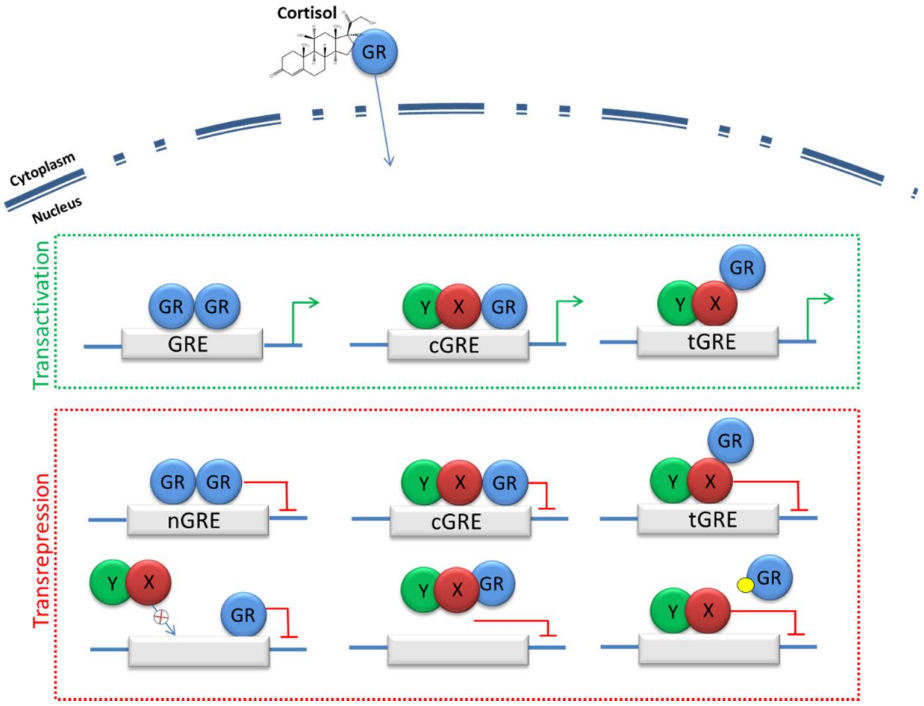

Figure 1.5. **Genomic mechanisms of GR action**. GC-GR binding induces nuclear import and interaction with GR-responsive promoter regions in target genes in the nucleus. GR directly binds to GC-responsive elements (GREs) of target genes on simple GREs (+GREs), negative GREs (nGREs), and composite GREs (cGREs). GR is also recruited to other DNA-binding sequences by protein-protein interactions (tGREs). Transactivation or transrepression of target genes is dependent on the co-regulator molecules (X and Y) recruited to the GR and the type of GRE the GR interacts with (Adapted from (Bellavance and Rivest, 2014)).

GREs are varied amongst different genes and are divided into simple (+GRE), negative (nGRE), composite (cGRE), and tethering (tGRE) response elements (Bellavance and Rivest, 2014; Hua et al., 2016). The following section describes the transcriptional activity of ligand-activated GR with respect to each of these GREs.

1.6.1. Glucocorticoid Response Elements

The binding of a GR homodimer to simple GRE-containing genes recruits many transcriptional co-regulators that remodel chromatin and are essential for proper gene regulation. The co-regulators induce the assembly and/or disassembly of transcription complexes on transcription start sites of genes associated with enhancer and silencer elements (Wu

et al., 2014). GR co-regulators function in a gene-specific manner and can regulate different pathways controlled by the GR.

1.6.1.1. Simple GREs

GR and co-regulatory proteins are also able to regulate gene transcription through their respective response elements by chromatin remodelling induced through acetylation and/or deacetylation of histone proteins leading to transactivation or transrepression of gene transcription respectively (Kurihara et al., 2002). When GR is bound to simple GREs, following chromatin structural modifications, the recruited co-regulators are then able to modulate gene transcription through recruitment of the basal transcriptional machinery (including RNA polymerase II) and conversion into a pre-initiation complex which interacts with the targeted promoter region; examples of which include the steroid receptor coactivator-1 (SRC-1) family, cAMP response element binding protein (CREB) binding protein (CBP), p300/CBP associated factor (p/CAF), and the vitamin D_3 receptor/thyroid hormone receptor (DRIP/TRAP) complex (Jenkins et al., 2001; Shao et al., 2000). Co-regulator proteins involved in transactivation also recruit histone acetyltransferase (HAT) enzymes which work by transferring acetyl groups onto histone proteins, that permits the unfolding of chromatin structures and allows more GR molecules to access promoter sequences, bind GREs, and potentiate gene transcription (Kagoshima et al., 2001). The genes subject to transactivation include anti-inflammatory mediators, such as IκBα (the inhibitor of the pro-inflammatory transcription factor NFκB), interleukin (IL)-10, Annexin-1, and other regulatory enzymes, including tyrosine aminotransferase (TAT) and serine dehydrogenase (Stahn and Buttgereit, 2008).

1.6.1.2. Negative GREs

GR action to repress transcription has always been controversial, with many potential mechanisms provided. GR occupancy of nGREs results in direct transrepression of target gene transcription through the recruitment of a transrepression complex composed of specific co-regulator proteins. These co-regulators interfere with the basal transcriptional machinery of target genes and inhibit their transcription (Ki et al., 2005; Stevens et al., 2003; Zhou and Cidlowski, 2005; Surjit

et al., 2011). The co-regulators also recruit histone deacetylase (HDAC) enzymes to the repression complex, which act in opposition to the HAT enzymes involved in transactivation. HDACs deacetylate histone proteins resulting in a reversion of the chromatin structure to a closed conformation thus restricting the access of GR to target promoters resulting in transrepression of gene expression (Ito et al., 2006). The molecular mechanisms underpinning GR-mediated transrepression are still to be conclusively determined, and much of the theory ascribed to this process remains unexplored (Ayroldi et al., 2014). Examples of genes subject to direct transrepression include pro-inflammatory genes, such as IL-1/2/6/8, vascular endothelial growth factor (VEGF), and cyclooxygenase (COX)-2, prostaglandins, tumour necrosis factor (TNF)-α, and interferon (IFN)-γ. However, the transrepression of inverse repeat nGRE-containing genes can lead to the suppression of certain genes involved in many homeostatic functions within humans, the perturbation of which that can lead to undesirable side effects (Surjit et al., 2011). Corticotrophin-releasing hormone (CRH), and pro-opiomelanocortin (POMC) also contain nGRE sites in their promoter regions leading to transrepression and suppression of the HPA axis; an unwanted side effect of excessive GC activity (Goodman et al., 1996; Turney and Kovacs, 2001; Przybycien-Szymanska et al., 2011). GR also transrepresses the expression of the serotonin gene via nGRE occupancy that results in the down-regulation of serotonin levels in the brain and contributes to the depression and psychosis exhibited in patients being treated with high doses of GCs (Ou et al., 2001; Pariante, 2009). Activated GR represses the gene expression of many inflammatory genes, and the mechanism involves transrepression of the activity of NFκB and AP-1 transcription factors, and although this mechanism is still under investigation it is proposed that GR is tethered to DNA-bound NFκB, and thereby recruits a repressor complex to block transactivation (Smoak and Cidlowski, 2004; Oh et al., 2017).

1.6.1.3. Chimeric GREs

cGREs are chimeric sequences that are recognised by a GR monomer associated with other transcription factors and are contained within a more select number of genes, such as the thyrotrophin-releasing hormone (Diaz-Gallardo et al., 2010). Activation of cGREs and tGREs

can result in both transactivation and transrepression of genes which is dependent on the transcription factor tethered to the GR (Bellavance and Rivest, 2014).

1.6.1.4. Tethering GREs

tGREs do not contain binding sites for GR but instead have binding sites for other DNA-bound regulators that recruit GR. In this manner, the GR tethers to other transcription factors through protein-protein interactions, resulting in the inhibition of its transcriptional activity and indirect transrepression of its target genes. Such transcription factors include NFκB, AP-1, nuclear factor of activated T cells (NF-AT), and signal transducer and activator of transcription (STAT)-5, each of which regulates their own set of distinct tGRE genes (Stahn and Buttgereit, 2008). As the downstream targets of these transcription factors include pro-inflammatory genes encoding cytokines, chemokines, cellular adhesion molecules, and prostaglandins, this method of transrepression is proposed to contribute much of the anti-inflammatory activity of GCs, although there is currently little evidence supporting the GR monomer-dominant anti-inflammatory action (Figure 1.6).

Emerging research has challenged the importance of tethering in GC-mediated transrepression of pro-inflammatory factors. ChIP-sequencing and structural biology analysis of GR at AP-1 response elements results in transrepression by direct DNA binding and not tethering (Weikum et al., 2017). In addition, an elegant study by (Oh et al., 2017) showed that, upon challenge with bacterial LPS, GCs craft an "inflamed epigenome" that restricts the access of pro-inflammatory NFκB with chromatin by inducing the expression of inhibitors of both NFκB and AP-1, again without the need for tethering. Other studies have largely debunked the dichotomous action of GR monomer and dimers, even demonstrating the existence of a GR tetramer in live cells (Presman et al., 2014; Presman and Hager, 2017; Presman et al., 2016). These findings also call into question whether the model used to design the dissociated GCs favouring the monomeric GR is indeed promoting the anti-inflammatory action of GCs or if repression of pro-inflammatory inhibitors and direct DNA interactions are involved.

This suggests that the role of tethering may be less important than previously thought and may continue to be challenged in future research.

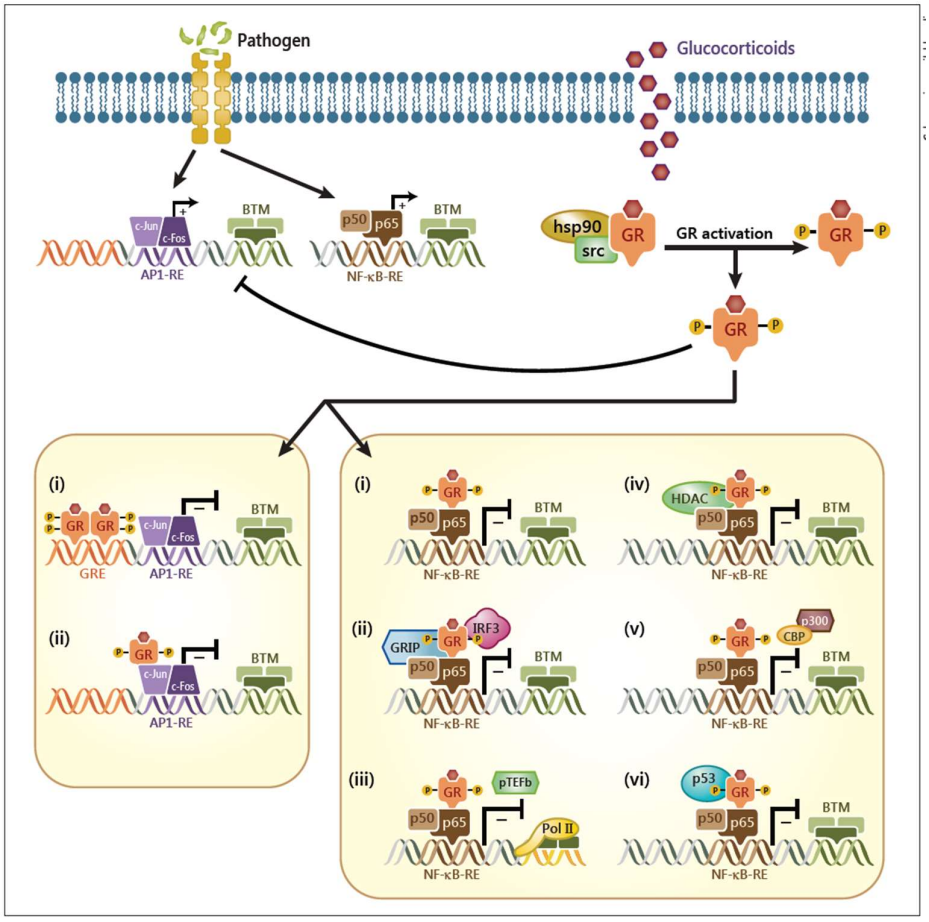

Figure 1.6. **Anti-inflammatory actions of the GR at pro-inflammatory transcription factor promoters.** Pathogens induce the expression of the pro-inflammatory transcription factors, NFκB and AP-1. In response, GCs are secreted into the circulation, enter the cytoplasm, and bind to the GR in an inactive complex with chaperone proteins. GC binding to GR stimulates its activation and translocation to the nucleus where it acts to repress the inflammatory response. The mechanism of GR-mediated repression depends on the target promoter, ligand and GR concentrations, and GR kinetics. GR represses AP-1 transcriptional activity using the following mechanisms: (i) GR binds to simple GREs and simultaneously interacts with c-Jun to repress AP-1 activity. (ii) GR physically tethers to c-Jun to repress AP-1 activity. GR represses NFκB transcriptional activity using the following mechanisms: (i) GR physically interacts with the p65 subunit of NFκB to repress its activity. (ii) GR can recruit the GR interacting protein-1 (GRIP-1) which blocks the formation of the p65/IRF3 NFκB heterodimer. (iii) GR prevents the phosphorylation and activation of RNA polymerase II (Pol II) by blocking the recruitment of the positive transcription elongation factor (pTEFb). (iv) GR recruits HDACs to repress NFκB by limiting its occupancy at chromatin and NFκB-target promoters. (v) GR prevents the interaction between NFκB and Creb-1 binding protein (CBP) and p300 that normally induce

transactivation of target genes. (vi) GR interacts with p53 that alters the transcriptional activity of NFκB. Taken from (Cruz-Topete and Cidlowski, 2015).

Alternatively, GR can indirectly regulate gene transcription through steric hindrance of DNA sequences overlapping the GRE site (Figure 1.5). The GR can also sequester transcription factors from DNA, compete for coactivator binding, and ligand-bound GR can occupy alternate response elements by binding to overlapping GREs (Bellavance and Rivest, 2014).

The various methods that GR uses to regulate the expression of its target genes add to its complexity of action and explain how the single receptor can interact with a large number of genes.

1.6.2. GR and Chromatin

Chromatin proteins are composed of a highly organised structure of nucleosomes, with each nucleosome consisting of an octamer of two core histone proteins (H2A, H2B, H3, and H4) (Bornelov et al., 2018). The conformation of chromatin dictates transcriptional responses by either restricting or facilitating the access of the basal transcription machinery (RNA polymerase II) to DNA sequences, initiating gene transcription. A closed chromatin conformation is associated with repression of gene expression and an open conformation with increased gene expression (Lu et al., 2018). Co-regulators and transcription factors locally modify chromatin structure by recruiting histone modifying enzymes (HATs or HDACs) or ATP-dependent nucleosome remodellers (Singh et al., 2018). Genome-wide analyses show that transcription factors only occupy a small percentage of consensus target gene sequences at any given time, suggesting a transient, dynamic mode of action (Zaret and Carroll, 2011). Chromatin immunoprecipitation (ChIP) and *in vivo* footprinting identified "pioneer" transcription factors, including FoxA, GATA, and the SWI/SNF ATPase BRG1, which directly bind target DNA sequences (e.g. enhancer elements) on nucleosomes for a stable period and opens local chromatin structures by increasing methylation of histone 3 lysine-4 (H3K4) (Hoffman et al., 2018). The action of pioneer factors facilitates the binding of GR and other chromatin remodifiers, as shown by the ability of FOXA1 and FOXA2 to assist GR loading in human endometrial cells (Whirledge et al., 2017) and assisted loading of the GR to cognate GBS

mediated by the ER and AP-1 (Karmakar et al., 2013). Chromatin accessibility therefore represents an additional level of complexity to the regulation of GC-target gene expression.

1.7. Non-Genomic Signalling

The speed at which activated GR induces a portion of its anti-inflammatory and immunosuppressive effects occurs at a rate that is too fast to be attributed to changes in gene expression. It is therefore the consensus that cytosolic GR induces the activation of non-genomic signalling cascades prior to nuclear entry. Three mechanisms of non-genomic signalling by GCs have been proposed: activation of membrane-bound GR (mGR) which induces separate signalling cascades to the cytosolic GR (cGR); a direct effect of GC action on proteins within the plasma membrane; and interaction of the GR with other proteins within the cytoplasm of cells after GC-mediated activation (Buttgereit and Scheffold, 2002). The cytosolic GR also rapidly stabilises the microtubule network and inhibits cell migration within minutes of GC administration, although the mechanism underlying this process remains unclear (Akner et al., 1995).

1.7.1. Membrane-Bound Glucocorticoid Receptor

The functional activity of mGR action is poorly understood owing to its scarcity compared to cGR. However, more recent evidence demonstrates that the mGR can activate downstream p38 mitogen-activated protein kinases (MAPKs) that may initiate non-genomic signalling cascades independently of the cGR (Strehl et al., 2011). The same study also showed using shRNA-targeted knockdown of the human GR gene that both the mGR and cGR are encoded by the same gene and that the mGR is not produced due to alternative mRNA splicing. It has been postulated that the mGR is localized to the plasma membrane following post-translational modification of a small fraction of the initial GR gene product after shuttling through the endoplasmic reticulum and Golgi apparatus (Strehl and Buttgereit, 2014). The relevance of mGR appears to be in priming the cell for genomic regulation by cGR, as initial entry of GCs will quickly activate non-genomic signalling pathways upstream

of the nucleus, although further functional analysis is warranted to prove this hypothesis.

1.7.2. Glucocorticoids and Plasma Membrane Proteins

GC interaction with the plasma membrane has been demonstrated in studies of the mGR in mast cells, keratinocytes, and lymphoma cells to name a few (Gametchu et al., 1991; Oppong et al., 2014; Stojadinovic et al., 2013). However, high concentrations of GCs have also been found to alter the physiochemical properties of proteins within the plasma membrane itself, causing an impairment of cation (Na^+, K^+, and Ca^{2+} cycling across the plasma membrane and increased proton leak across the mitochondrial membrane through inhibition of oxidative phosphorylation (Stahn and Buttgereit, 2008). Both effects cause alterations in Na^+/K^+-ATPase activity within immune cells that are involved in the immunosuppressive and anti-inflammatory activity of GCs, along with some GC-associated side effects (Song and Buttgereit, 2006).

1.7.3. Cytosolic Glucocorticoid Receptor and Cytoplasmic Proteins

Rapid GC effects within the cytoplasm occur independent of engagement with nuclear targets (Chien et al., 2016; Deng et al., 2015). Activated GR engages and alters the activity of various cytoplasmic proteins, including phosphatidylinositol-3-phosphate (PI3K), Akt, protein kinases B and C, Janus kinases (JNKs), mitogen-activated protein kinases (MAPKs), G-protein-coupled receptors (GPCRs), and (Liu et al., 2017; Bruna et al., 2003; Zou et al., 2015; Leis et al., 2004; Kino et al., 2005). This emerging field highlights the importance of early GC effects on parallel intracellular signalling cascades, leading to the indirect induction of downstream nuclear targets outside canonical GREs (Alangari, 2010).

The dissociation of the multi-protein complex from the GR upon ligand binding allows some proteins, such as src, to exert non-genomic effects on cytosolic proteins, for example src inhibits the EGFR activation of cytosolic phospholipase A2 (cPLA2) which prevents the formation of arachidonic acid from membrane phospholipid precursors (Alangari,

2010). This effect occurred outside of the classical genomic signalling pathway for the GR, as (Croxtall et al., 2000) demonstrated that cPLA2 down-regulation is GR-dependent (ablated by treatment with the selective GR antagonist RU486) and transcription-independent (no effect following application of the transcription inhibitor actinomycin D).

1.8. Glucocorticoids and Wound Healing

Wound healing is a complex physiological response to repair damaged tissue, characterised by inflammation, epithelial reorganisation, and tissue remodelling (Zeng et al., 2018). Each stage of the wound healing process is dependent on the directed migration of cells (platelets, leukocytes, and keratinocytes) to the site of injury, ultimately resulting in the resolution of inflammation and deposition of extracellular matrix components (collagen, elastin) to finalise wound repair (Kunkemoeller and Kyriakides, 2017; Solomon, 2002). GCs are commonly known to impair wound healing as an off-target clinical effect, albeit through an unknown mechanism of action (Carolina et al., 2018; Bitar et al., 1999; Beck et al., 1993; Dahmana et al., 2018). GCs are also known to inhibit the migration of various cell types, again through an undetermined mechanism, suggesting a causal link between the two processes (Kisanga et al., 2018; Fietz et al., 2017; Murakami et al., 1998). Moreover, whilst these studies show a transcriptional response of migratory genes to GCs after prolonged treatment (24 hours), the early response is neglected and may yield greater insight into the mechanism by which GCs inhibit cell migration and, by extension, impair wound healing (Drebert et al., 2017). Emerging research is taking note of the GC effect on cell migration, with a recent study demonstrating the dependence of dexamethasone-induced GILZ expression in up-regulating expression of Annexin-1, a protein implicated in cytoskeletal remodelling and regulation of cell migration (Ricci et al., 2017; Belvedere et al., 2014).

Although less evidence exists for the GR, the role of the GR co-chaperone Hsp90 in regulating cell migration has been extensively studied owing to the use of Hsp90 inhibitors as therapeutic agents for the treatment of cancer (Min et al., 2018; Thanomkitti et al., 2018; Pfeiffer et al., 2018; Memmel et al., 2017; Peng et al., 2015). The

chaperone function of Hsp90 is tightly regulated by the cytoplasmic histone deacetylase-6 (HDAC6) enzyme, which also has consequences on GR maturation and activity (Yu et al., 2017; Kramer et al., 2014; Ai et al., 2009; Kekatpure et al., 2009; Rao et al., 2008; Kovacs et al., 2005). A recent study found that silencing the expression of HDAC6 disrupted the function of Hsp90 in oesophageal squamous cell carcinoma suppressed proliferation and migration, indicating a functional link between the two proteins and, by extension, between HDAC6 and the GR (Tao et al., 2018). Indeed, the GR was reported to have significantly impaired translocation kinetics and inhibited transcriptional activity in *in vivo* HDAC6-knockout mice (Winkler et al., 2012). Moreover, inhibition of HDAC6 deacetylase activity at α-tubulin K-40 is known to alter the dynamics of the microtubule network in an EB-1 dependent manner, with downstream effects on polarized cell migration (Zhang et al., 2014; Deakin and Turner, 2014; Li et al., 2011; Valenzuela-Fernandez et al., 2008). Investigating the role of HDAC6 in the GC effect on cell migration could therefore provide a novel route for therapeutic intervention of impaired wound healing, thus minimising the off-target effect of clinical GCs and improving therapeutic benefit.

1.9. Therapeutic Glucocorticoids

The use of synthetic GCs such as dexamethasone, prednisolone, and fluticasone propionate to treat inflammatory and autoimmune diseases is well known. These drugs have been developed to mimic the anti-inflammatory and immunosuppressive actions of endogenous GCs with improved potency and efficacy (Figure 1.7).

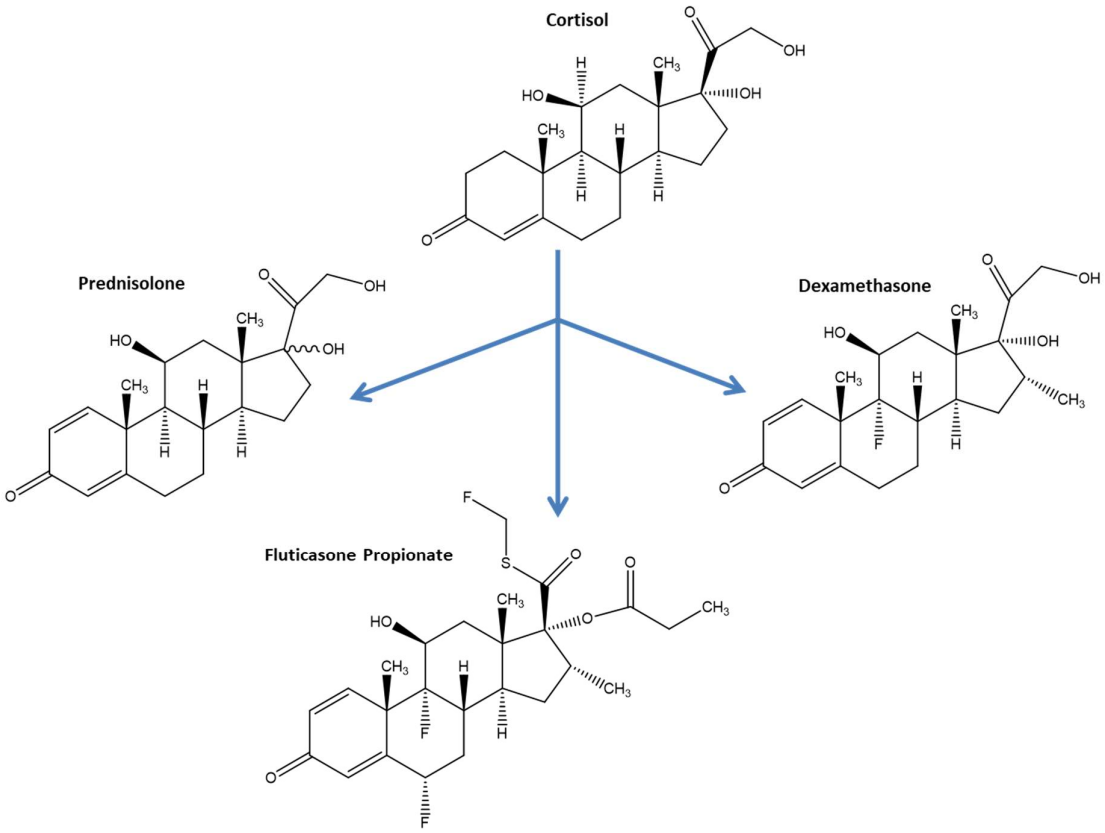

Figure 1.7. **Chemical structures of therapeutic GCs**. Each compound is structurally related to the endogenous GC cortisol, with subtle additions and alterations that improve potency and efficacy in the treatment of inflammatory and autoimmune diseases. Images were made via Java Molecular Editor applet (http://www.changbioscience.com/mis/chemdraw.html).

Altering the chemical structure of synthetic GCs can cause changes in the size, shape, and electrostatic profile of the ligand-binding pocket of the ligand-bound GR, which affects both the potency and efficacy of the ligand (Wang et al., 2008). Common GC structures that infer good GR binding include the carbonyl groups at C3 and C20, the β-hydroxyl group at C11, and the $\Delta^{4,5}$ double bond at C1 (Derbyshire et al., 1996; He et al., 2014). The double bond at C1 increases ligand selectivity for the GR over other NRs, which prevents off-target activation of side effects and increases the anti-inflammatory activity of the ligand. A similar effect is observed after halogenation of C6/C9 with a chloro (Cl) or fluoro (F) group, or with α/β-methylation at C16, which increases the binding affinity for GR (Mehta et al., 2016).

The goal of these alterations is to create a potent GC that can be used for the treatment of inflammatory and autoimmune disorders with high

potency and efficacy. A prime example is fluticasone propionate (FP), a highly potent GC that is commonly used in the treatment of asthma. FP exhibits a greater therapeutic profile compared to the endogenous GC, cortisol, through its various chemical additions. The fluticasone backbone of FP contains a second double bond in the C1, C2 position which slows its metabolism and prolongs its activity at the GR. In addition, FP is halogenated at the C6 and C9 positions with F groups and contains a C11β-hydroxyl group, all of which enhance its topical activity (Daley-Yates, 2015). The α-methyl substituent at C16 eliminates any mineralocorticoid activity and the esterified lipophilic group at C17α improves its lipophilicity, leading to an increased ratio of topical to systemic potency (Crim et al., 2001).

However, a caveat soon emerged with GC-induced side effects, which are caused by pleiotropic GC action on metabolism and the immune system. Soon enough, patients given high doses of synthetic GCs and/or over a prolonged period began to contract these side effects, which impaired their use in the clinic. A concerted effort has therefore been put forward to develop newer, safer GCs that retain the anti-inflammatory activity of conventional GCs without the induction of side effects. Unfortunately, this search has proven more difficult in practice, with newer drugs displaying improved potency and efficacy compared to conventional GCs yet still inducing the same side effects. Nevertheless, the pharmacological improvement imparted by subtle changes in their chemical compositions does not restrict their use in the clinic and allows a more controlled dosing to help minimise side effects. The following section will describe these newer GCs in more detail and will highlight the growing field of "selective GR modulators" that has provided promising breakthroughs in the creation of safer therapeutic GCs.

1.9.1. Furoate Compounds

To enhance the therapeutic profile of FP, further subtle additions were made to its chemical structure, which resulted in profound improvements in its binding affinity for the GR and its anti-inflammatory activity. The addition of a furoate ester group at the C17α position enabled an improved therapeutic profile and lead to the generation of the furoate compounds, mometasone furoate (MF) and fluticasone furoate (FF) (Figure 1.8).

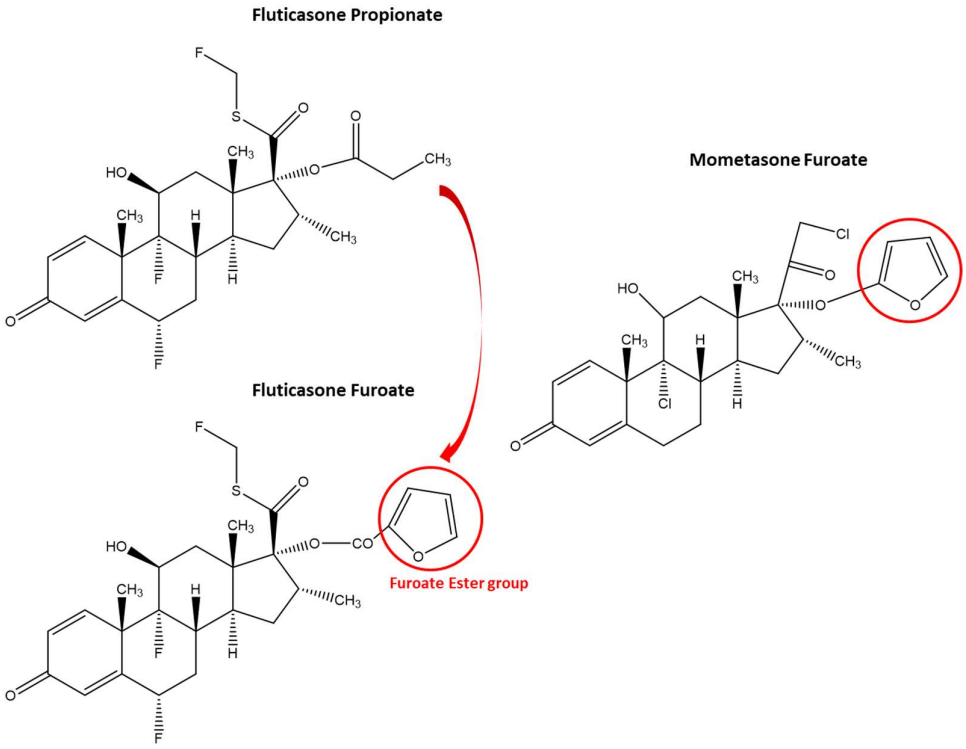

Figure 1.8. **Furoate glucocorticoids.** Examples include: mometasone furoate (MF), fluticasone propionate (FP), and fluticasone furoate (FF), with the furoate ester group highlighted in red. Images were made via Java Molecular Editor applet (http://www.changbioscience.com/mis/chemdraw.html) (Adapted from (Salter et al., 2007)).

Compounds such as mometasone furoate (MF) and FF are used as potent GR agonists in the treatment of inflammatory skin conditions and asthma (He et al., 2014). The high anti-inflammatory potency of both compounds is conferred by the substituted lipophilic furoate ester group on the C17α position of the steroid D-ring. The furoate ester group enhances the binding affinity and lipophilicity of MF and FF over other conventional GCs that retain a hydroxyl group at C17α. The C17α furoate group sticks out at a 90° angle that expands the ligand-binding pocket and fills the empty cavity above the steroid D-ring that is typically left unoccupied. Within the cavity, MF and FF make extensive hydrophobic interactions with surrounding residues to form a ball-anchored-to-socket joint that increases its affinity for GR over conventional GCs (e.g. Dex) that fail to occupy the cavity. FF also displays a slower dissociation from the GR leading to prolonged activity and enhanced anti-inflammatory activity (Biggadike, 2011; Salter et al., 2007).

More importantly, MF and FF cause movement of the Q642 residue that normally rests perpendicular to helix 7 and forms hydrogen bonds with the C17α-hydroxyl group to tether the bound ligand in position with the ligand-binding pocket. GR binding to MF and FF causes Q642 to bend at a 90° angle to the helix 7 axis and pushes it away from the lipophilic C17α group. This alteration perturbs helices 5, 6, and 7, leading to expansion of the loop between helices 5 and 6 and changes the orientation of the AF-2 helix (Bijsmans et al., 2015). A subtle change in the AF-2 helix orientation can have profound effects on the co-regulator molecules recruited to the GR, which ultimately modulates the transcriptional activity of the GR. This effect is also observed in compounds containing C17α-hydroxyl groups replaced with the C17α-furoate ester, such as the DAC moiety VSG24. The C17α-furoate group therefore serves as an anchor point to position low-affinity ligands precisely and firmly in the ligand-binding pocket that consequently improves ligand potency and efficacy (Khan and Lee, 2008).

1.9.2. Pyrazole Compounds

A cause of off-target pharmacology with steroidal GR agonists is due to cross –reactivity with other NR members (especially the PR, AR, and MR). This off-target activation, along with high GC dose, has been implicated in the pathogenesis of side effects associated with GCs. It was therefore hypothesised that the creation of non-steroidal GR agonists would exhibit greater selectivity for the GR over other group I NRs. A series of GR agonists containing a tetrahydronapthalene (THN) group were generated where NR and transrepressive selectivity are achieved (Barnett et al., 2009). These pyrazole compounds contain an aryl aminopyrazole group that is a competent replacement for the steroidal cyclohexadione A-ring, with the x-ray crystal structure of deacylcortivazol (DAC)-bound GR LBD showing that the space occupied by the A-ring can open to accommodate the arylpyrazole structure (Figure 1.9). The position of the pyridine N atom at C5 and C6 forms hydrogen bonds with the amino acids Gln570 and Arg611 of the GR thus mimicking the action of the steroid A-ring.

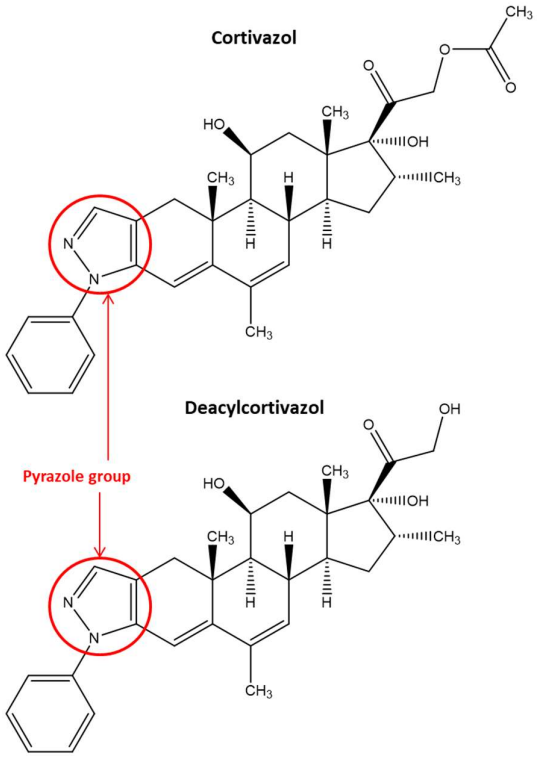

Figure 1.9. **Arylpyrazole glucocorticoids**. Examples include: deacylcortivazol (DAC) and cortivazol (CVZ), with the bulky phenylpyrazole group highlighted in red. The pyrazole groups are linked to benzamide groups to improve potency. Images were made via Java Molecular Editor applet (http://www.changbioscience.com/mis/chemdraw.html).

This aryl group is designed to occupy the hydrophobic pocket populated by the 17α furoate ester group as seen with FP and fluticasone furoate (FF). The aryl aminopyrazole pharmacophore can also be linked to a benzamide bearing a trigger group (provided by an angular alkyl group) to give potent agonists selective for the GR that do not exhibit a dissociated profile. The pyrazole compounds also lack the same interactions with the AF-2 domain helix of the GR LBD and are therefore not optimal for stabilizing the GR in an active conformation, which may explain their reduced transactivation activity.

1.9.3. Dissociated Ligands

To circumvent the induction of side effects, a heightened effort has been made to develop dissociated ligands which transrepress pro-inflammatory mediators like NFκB and AP-1 but do not transactivate genes that regulate homeostatic functions, e.g. metabolic effects (Schacke et al., 2004; Mylka et al., 2018; Meyer et al., 2018; van den

Heuvel et al., 2016; Mammi et al., 2016). However, more recent studies have shown that the GR can exert its anti-inflammatory effects at both transcriptional and post-transcriptional levels via both transrepression and transcriptional activation. It is therefore important to gain a deeper understanding of the molecular mechanisms underlying ligand-bound GR activity to develop agonists that selectively inhibit inflammation. Selective GR agonists (SEGRAs) are examples of ligands that were developed based on the "dissociated activity" hypothesis. SEGRAs interact with the GR similarly to conventional GCs but are also able to induce subtle conformational changes in the receptor's structure that promote the protein-protein interaction of GR to pro-inflammatory transcription factors (transrepression) over direct GR-DNA binding (transactivation) (Schacke et al., 2004). This is in direct opposition to the action of steroidal GR agonists that induce the complete transcriptional activity of the GR, which leads to off-target pharmacology and the induction of side effects.

However, the perfect separation of transrepression from transactivation is not always possible and this may reflect deficits in understanding the molecular mechanism of transrepression. Furthermore, much of analysis into transactivation and transrepression activity of SEGRAs are performed *in vitro* and many fail to recapitulate their dissociated profiles *in vivo*. Many of the SEGRAs that were initially dissociated have now been found to transactivate GR-target genes, thus invalidating the dissociated status of these ligands. Despite these drawbacks, a few SEGRAs have successfully shown to dissociate transactivation from transrepression in both cellular and animal models, with select ligands currently being tested in clinical trials (Table 1.1).

SEGRA Name	Therapeutic Target	Mode of Action	Owning Company	References
Mapracorat **(BOL-303242-X)** **(ZK245186)**	Ocular inflammation Dermatitis (Phase II)	Attenuation of NFκB signalling and up-regulation of anti-inflammatory RelB. Inhibits pro-inflammatory cytokine release (TNF) by reducing mitogen-activated protein kinase (MAPK) and NFκB phosphorylation and activation. Topical anti-inflammatory action in skin.	Bayer Healthcare Pharmaceuticals	(Baiula and Spampinato, 2014; Spinelli et al., 2014; Vollmer et al., 2012; Baiula et al., 2011; Baumer et al., 2017)
GW870086X	Asthma Atopic dermatitis Chronic obstructive pulmonary disorder (COPD) Ocular hypertension	Inhibition of cyclooxygenase (COX)-2 expression and up-regulation of MAPK phosphatase (MAPK)-1. Increases tissue plasminogen activator (tPA) to favour matrix turnover.	GlaxoSmithKline	(Bareille et al., 2013; Uings et al., 2013; Leaker et al., 2015)
AZD5423	Asthma COPD	Attenuates allergen-induced	AstraZeneca	(Gauvreau et al., 2015; Melin et al., 2017;

		sputum eosinophilia.		Kuna et al., 2017; Backman et al., 2017; Werkstrom et al., 2016)
DE-110	Allergic conjunctivitis Dry eye syndrome		Santen Inc.	

Table 1.1. **Selective GR agonists (SEGRAs) undergoing evaluation in clinical trials**. The therapeutic target, mode of action, and owning company are displayed alongside each SEGRA.

The anti-inflammatory potential of dissociated ligands has been demonstrated through selective repression of AP-1 and NFκB-inducible pro-inflammatory genes such as IL-6, IL-1β, and TNFα (Vanden Berghe et al., 1999; Schacke et al., 2002), but with only weak transactivation of GRE-dependent genes such as glucocorticoid-induced leucine zipper (GILZ) protein (Wust et al., 2009; Schacke et al., 2004; Du et al., 2011; Trebble et al., 2013). The method by which each dissociated ligand induces transrepression over transactivation depends on their interaction with the GR, with subtle changes in the chemical composition of each compound modulating the GR differently. However, the proposed model of transactivation versus transrepression has been shown to be a simplistic representation of GR activity. Some genes encoding anti-inflammatory proteins (e.g. GILZ and DUSP1) are induced through transactivation, which suggests that dissociated ligands may not exert the full anti-inflammatory effects of conventional GCs. Furthermore, GR is capable of rapidly activating kinase signalling cascades outside of the nucleus, some of which have protective effects on cells and tissues in inflammation (Limbourg and Liao, 2003). Structural changes to the GR structure induced through binding of SEGRAs may therefore result in a conformation that has profound effects on the ability of GR to recruit kinases and as an extension may affect its anti-inflammatory activity on the non-genomic level (Stahn et al., 2007).

The earliest dissociated ligands to be developed include RU24858, AL-438, and ZK-245186 (Ayroldi et al., 2014). The non-steroidal

dissociated ligands GSK47867A and GSK47869B cause a reduction in the kinetics of GR nuclear phosphorylation and nuclear import, thus prolonging GR activity (Trebble et al., 2013). This effect is due to the addition of a patch of positive charge onto the amino acid surface that normally associates with Hsp90 through movement of Arg611; the extra charge disrupts the link between the GR and Hsp90 and results in all of the aforementioned actions, which demonstrates that Hsp90 has an integral role for multiple stages of GR activity (Trebble et al., 2013). The ability of GSK47867A and GSK47869B to slow the kinetics of cellular response results in a delayed onset of GR-target gene regulation, demonstrating that modulation of receptor kinetics is an effective regulator of GR activity.

GW870086X is a novel GR agonist that extends into the 17α pocket of the GR LBD, presenting with a selective transcriptional profile at GC-responsive genes that is finding promise as an inhaled glucocorticoid in the treatment of asthma (Leaker et al., 2015). Furthermore, GW870086X shares similar potency to dexamethasone and favours extracellular matrix turnover in *in vitro* models of conventional outflow (Stamer et al., 2013). Although a mode of action has been proposed for GW870086X that involves dual inhibition of cyclooxygenase-2 (COX-2) and activation of MAPK phosphatase-1 (MPK-1), comprehensive next-generation analysis (RNA-sequencing, proteomics) of the compound's activity *in vitro* has not been studied (Uings et al., 2013).

The pyrazole compound DAC, a potent GR ligand, is able to expand the size of the GR LBD and allow the recruitment of additional non-steroidal ligands, although the mechanism of GR conformational change remains unclear (Suino-Powell et al., 2008). Crystallographic analysis of the GR LBD-DAC complex reveals the presence of a novel "meta" channel in the GR that extends beyond the typical A-ring region of the ligand binding pocket and is created after binding with non-steroidal GR agonists containing an aminopyrazole moiety (D-prolinamide and D-alaninamide), including DAC, which explains its ability to expand the LBD (Figure 1.10) (Biggadike et al., 2009). The ability of the expanded GR pocket to dock both steroidal and non-steroidal ligands allows an efficient method for investigating the molecular mechanisms of dissociated GCs, thus aiding the discovery of better and safer GR drugs.

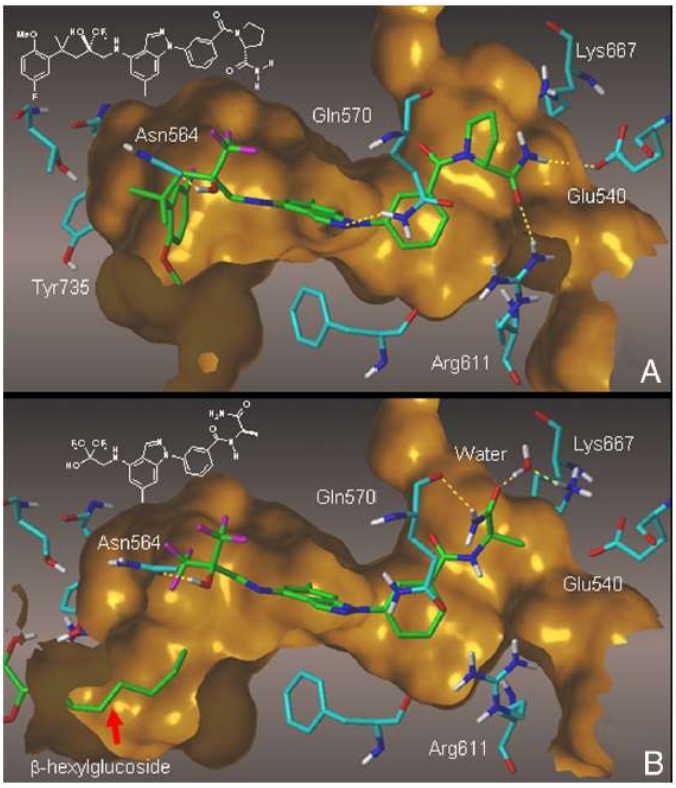

Figure 1.10. **Crystal structures of the GR ligand-binding domain and "meta" channel**. The A-ring is formed between Asn564 and Gln570 residues. (A) D prolinamide GR-LBD structure. (B) Truncated D-alaninamide GR-LBD structure. Bottom left is the crystallographic adduct β-hexylglucoside tail incorporated into the crystal structure of GR pushing into the unoccupied 17α pocket that generates an additional meta channel (Taken from (Biggadike et al., 2009)).

The formation of this "meta" channel delivers enhanced GR potency and dissociated transrepression activity (Biggadike et al., 2009). Furthermore, ligands that occupy the meta channel do not require binding to the typical steroid pocket to activate the GR, demonstrating that full binding is not essential for potent agonist activity, thus offering significant opportunities for the delivery of ligands with selective transrepressive activity (Biggadike et al., 2009).

SEGRAs represent a novel class of GR ligands that have the potential to revolutionize GC treatment by selective modulation of GR transcriptional and non-genomic activity. However, more detailed information must be gathered regarding the specific targets (both at the gene and protein level) to provide a full profile of SEGRA activity.

1.10. Summary

Glucocorticoids are the most potent anti-inflammatory drugs known yet there is still much to understand about their mechanism of action. GCs exert their cellular effects by binding and activating the ubiquitously expressed GR, a ligand-activated transcription factor. Upon ligand binding the GR activates signalling cascades in the cytoplasm within minutes and translocates to the nucleus to regulate gene expression over hours. GR has a dynamic structure and adopts different conformations depending on the ligand it binds. The shape of the GR dictates its stability, compartmentalisation, and activity. The side effects of GCs are diverse due to the pleiotropic action of the GR in glucose homeostasis, immune regulation, and bone turnover. Understanding how the GR mediates its cellular effects will allow the development of new GCs with maximal therapeutic benefit. An emphasis is placed on the importance of the non-genomic actions of the GR, which are relatively unexplored when compared to GR transcriptional activity.

1.11. Hypothesis and Aims of PhD

1.11.1. Investigating non-genomic actions of GCs

This work aims to investigate the non-genomic mechanism of GC action in two contexts: induction of off-target effects (wound healing) and early changes in protein phosphorylation induced by GCs. The findings of this investigation will shed light on the cellular response to GCs and provide a foundation for further research into this comparatively unexplored area of GC biology.

Hypothesis

Glucocorticoids impair wound healing by rapidly inhibiting cell migration, through a non-genomic mechanism of action linked to the dynamics of the microtubule network.

Aims

1) To determine the capacity for glucocorticoids (conventional agonist, antagonist, and selective agonists) to inhibit cell migration using live-cell imaging.
2) To demonstrate whether the GR is required for the glucocorticoid effect using small interfering RNA (siRNA) GR knockdown assays.
3) To identify the earliest time point at which cell migration is significantly reduced following glucocorticoid treatment using statistical analysis of migration data.
4) To assess the role of αTAT1 and HDAC6 (as regulators of tubulin acetylation) in the glucocorticoid effect on cell migration using αTAT1 siRNA knockdown assays and HDAC6 inhibition/overexpression assays (HDAC6 siRNA knockdown negatively impacts the function of Hsp90 which is integral for GR maturation and activity (Kekatpure et al., 2009; Kovacs et al., 2005)).
5) To demonstrate an interaction between the GR and αTAT1/HDAC6 using HaloTag pulldown and co-immunoprecipitation following glucocorticoid treatment. Fluorescence cross-correlation spectroscopy will be used to provide a dynamic measure of this interaction in live cells using fluorophore-labelled plasmid constructs (HaloTag-GR and HDAC6-eGFP).

1.11.2. Investigating early changes in protein phosphorylation in response to GCs

Hypothesis

Rapid GC treatment phosphorylates proteins whilst the GR is localised within the cytoplasm. Non-steroidal GR agonists (tool compounds), designed to minimise the induction of off-target GC effects, will differentially regulate protein phosphorylation due to changes in GR conformation adopted upon ligand binding.

Aims

1) To assess the pharmacology of each GR agonist using dose-response luciferase reporter gene assays chosen for convenience for high-throughput screening (Paguio et al., 2010).
2) To evaluate the pharmacokinetics of GR trafficking using live-cell imaging assays of HaloTag-GR to determine sub-cellular distribution of the GR upon ligand activation. Any differences in GR trafficking kinetics will affect GR occupancy at target gene promoters, which will affect the rate of target gene regulation.
3) To identify the changes in protein phosphorylation in response to GCs using SILAC-based phosphoproteomics and validation by western blotting.
4) Pathway analysis will be used to infer protein-protein interactions and build a network of proteins differentially regulated by rapid GC exposure.

Chapter 2: Methods

2.1. Cell culture

Human lung epithelial carcinoma (A549) and human cervical adenocarcinoma (HeLa) cells (ATCC, Teddington, UK) were cultured in high glucose (4500 mg/l) Dulbecco's modified Eagle's medium (DMEM; D6429, Sigma) with L-glutamine, sodium bicarbonate, sodium pyruvate and supplemented with 10% heat-inactivated foetal bovine serum (FBS; F9665, Invitrogen, Paisley, UK) or 10% charcoal-stripped foetal bovine serum (cFBS; #12676029, Invitrogen, Paisley, UK) at 37°C in 5% CO_2.

2.2. Stable isotope labelling with amino acids in cell culture (SILAC)

A549 cells were subjected to stable isotope labelling with amino acids in cell culture (SILAC) to generate "light", "medium", and "heavy" labelled cell lines. "Light" cells were labelled with L-arginine (Arg^0) and L-lysine (Lys^0), "medium" cells with L-arginine-U-$^{13}C_6$ (Arg^6) and L-lysine-$^2H_4$ (Lys^4), and "heavy" cells with L-arginine-U-$^{13}C_6$-$^{15}N_4$ (Arg^{10}), and L-lysine-U-$^{13}C_6$-$^{15}N_2$ (Lys^8). Three separate SILAC media were prepared per cell line (DMEM for SILAC; #88364; ThermoFisher Scientific) supplemented with 10% dialyzed foetal bovine serum (#26400044; ThermoFisher Scientific) and appropriate amino acids. Cells were grown in the appropriate SILAC media for 10x doublings and L-arginine incorporation was tested in each cell line before further testing (>98%).

2.3. Transfection

Transfections were performed with Fugene 6 reagent (E2691; Promega) used at a ratio of 3:1 volume/weight ratio with DNA. Fugene 6 was pre-mixed with RPMI media (serum-free) for 5 minutes prior to incubation with DNA for 15 minutes at room temperature. Transfections were performed over 24 hours at 37°C/5% CO_2.

Small interfering RNA (siRNA) transfections were performed with Lipofectamine RNAiMAX reagent (#13778150; ThermoFisher Scientific) as described in the manufacturer's instructions and allowed to occur over 48 hours at 37°C/5% CO_2.

2.4. Western blotting

Cells were treated as described in the results and lysed on ice for 30 minutes with modified RIPA buffer (50mM Tris-HCl, pH7.4, 1% NP-40, 0.25% sodium deoxycholate, 150mM NaCl, 1mM EDTA) supplemented with protease inhibitor (#04693124001, Roche) and phosphatase inhibitor cocktails (P5726; P0044; Sigma). Cell lysates were scraped into 1.5mL Eppendorf tubes, cleared by centrifugation at 14000xg for 10 minutes at 4°C. Supernatants were collected and protein concentration determined by Bradford assay #23236; ThermoFisher Scientific). Lysates were resuspended to 1mg/mL in 1x Laemmli buffer (0.125M Tris-HCl, pH6.8, 0.1% SDS, 20% glycerol, 0.2% β-mercaptoethanol, 0.001% bromophenol blue) and boiled at 95°C for 10 minutes. Lysates were electrophoresed on Tris-Glycine (4-20%) Mini-PROTEAN TGX precast polyacrylamide protein gels (15-well, 15µL per lane) (#4561096, BioRad, Hertfordshire, UK) using 1x Tris/Glycine running buffer (#1610732; BioRad) and run at 130V for 60 minutes at room temperature. Gels were transferred onto nitrocellulose membranes using transfer buffer (192mM glycine, 25mM Tris Base, 20% methanol) and run at 90V for 60 minutes at 4°C. Membranes were blocked in blocking buffer (2% skimmed milk, 150µM NaCl, 0.1% Tween-20) for 2 hours at room temperature and incubated with relevant primary antibodies diluted in blocking buffer overnight at 4°C. Membranes were washed 3x in wash buffer (0.3% milk, 48mM Tris-HCl, 24.8mM Tris Base, 0.1% Tween-20) for 10 minutes and incubated with relevant horse-radish peroxidase (HRP)-tagged secondary antibodies diluted (1:5000) in wash buffer for 1 hour at room temperature. Membranes were washed 3x in wash buffer and exposed to enhanced chemiluminescence (ECL) Clarity reagent (#1705060; BioRad) for 2 minutes. Protein bands were visualised using BioMax MR photographic film (#V8572786; GE Healthcare).

2.5. HaloTag pulldown assay

A549 cells were seeded onto 15cm^2 dishes at 300,000 cells per mL in CSM and left to incubate for 24 hours at 37°C/5% CO_2. Cells were transiently transfected with either HaloTag-GR (10µg) or HaloTag-HDAC6 (10µg) and left to incubate for 24 hours. Cells were treated with vehicle (DMSO) or

dex (100nM) for 1 hour and washed 2x with ice-cold 1xPBS. Cells were gently scraped into conical tubes and centrifuged at 2000xg for 10 minutes at 4°C. Supernatant was discarded and cell pellets were stored overnight at -80°C prior to lysis. Before cell lysis, HaloTag resin (G1912; Promega) was mixed to obtain uniform suspension and 200µL resin was dispensed into 1.5mL Eppendorf tubes per treatment condition. Tubes were centrifuged at 800xg for 1 minute, supernatant discarded, and resuspended in 800µL resin equilibration buffer (100mM Tris-HCl, 150mM NaCl, 0.005% IGEPAL CA-630). Tubes were centrifuged at 800xg for 2 minutes and supernatant discarded. Resin was washed an additional 3x in equilibration buffer. Cell pellets were thawed on ice and resuspended in 300µL lysis buffer (50mM Tris-HCl pH7.5, 150mM NaCl, 1% Triton X-100, 0.1% sodium deoxycholate) supplemented with 6µL of 50x protease inhibitor cocktail (800µ/mL benzamidine HCl, 500µg/mL phenanthroline, 500µg/mL aprotinin, 500µg/mL leupeptin, 500µg/mL pepstatin A, 50mM PMSF). Cells were passed 5x through a 25G needle to complete lysis and centrifuged at 14000xg for 5 minutes at 4°C. Cleared lysates (300µL) were transferred to new 1.5mL tubes and diluted in 700µL 1xTBS (100mM Tris-HCl pH7.5 and 150mM NaCl). 1mL diluted lysates were mixed with the washed HaloTag resin and left to incubate overnight on a tube rotator at 4°C. Tubes were centrifuged at 800xg for 2 minutes and supernatant discarded. Pellets were washed 4x in resin equilibration buffer. After the last wash, resin was resuspended in 50µL HaloTEV Protease (G6601; Promega) and incubated at room temperature for 1 hour with constant shaking. Tubes were centrifuged at 800xg for 2 minutes and eluates transferred to new 1.5mL tubes.

2.6. Scratch wound assay

A549 cells were seeded onto 96-well ImageLock plates (#4379; Incucyte) at 100,000 cells per well in CSM and left to adhere overnight to ensure the formation of a confluent monolayer. Once each well contained a confluent monolayer, scratches of uniform size and shape were induced in each well simultaneously using a WoundMaker device (Incucyte). The wells were washed twice in fresh CSM to remove debris from the scratch sites. The wells were filled with 100µL of new CSM containing the appropriate concentration (0.1nM, 1nM, 10nM, 100nM, 1µM, 10µM) of

Dex, RU486, hydrocortisone, or vehicle (DMSO) control. The plate was immediately placed into the Incucyte Zoom live-cell microscope which couples as a temperature and CO_2 controlled incubator (37°C/5% CO_2). Duplicate images were acquired from each well using a 20x/0.61 SPlan Fluor ELWD objective at 30-minute intervals over 24 hours. Incucyte Zoom scratch wound analysis software was used to determine the wound width (µm), wound confluence (%) and relative wound density (%) of each well over the 24-hour time course.

2.7. Luciferase reporter assay

HeLa cells were seeded onto 10cm^2 dishes at 50,000 cells per well in CSM and left to adhere overnight. Cells were transiently transfected with luciferase tagged-mouse mammary tumour virus (MMTV-Luc; 2µg) or luciferase tagged-nuclear factor-κB response element (NRE-Luc; 2µg) using Fugene 6 reagent (3:1 volume/weight ratio with DNA) for 24 hours. Cells were re-seeded onto 24-well plates at 50,000 cells per well in CSM and left to adhere overnight at 37°C/5% CO_2. Cells were treated as specified in the results and 18 hours later each well was washed twice with 1xPBS. 100µL of Bright Glo lysis buffer (Promega, E2620) was added to each well and left to lyse on ice for 30 minutes. Cell lysates were transferred to a white, flat-bottomed 96-well plate and luciferase absorbance was read using a luminometer (Glomax, Promega). 10x 1-second reads were taken of each well and the average relative light unit (RLU) determined. Background wells were included that only contained lysis buffer. IC_{50} and EC_{50} values were extrapolated from the resulting dose response curves using non-linear regression analysis in GraphPad Prism software, with the following equation:

Y=Bottom + (Top-Bottom) / (1+10^((LogIC50-X) *HillSlope))

Where X: log of dose or concentration; Y: Response; Top and Bottom: Plateaus; LogIC_{50} interchangeable with LogEC_{50}; HillSlope: Slope factor or Hill slope, unitless.

2.8. Microscopy

2.8.1. Fixed immunofluorescence

A549 or HeLa cells were seeded onto glass coverslips (13mm diameter) within 12-well plates and treated as required. Cells were rinsed twice in 1xPBS and fixed with pre-warmed 4% paraformaldehyde (PFA; #441244; Sigma) for 1 hour at room temperature. Cells were rinsed three times in 1xPBS and washed for 5 minutes (three times) with 1xPBS. Cells were permeabilised in PBS containing 0.1% Triton X-100 (T8787; Sigma) for 10 minutes at room temperature, rinsed three times in 1xPBS, and blocked in PBS containing 2% bovine serum albumin (BSA; #12827172; ThermoFisher Scientific) for 1 hour at room temperature. Cells were incubated with relevant primary antibodies diluted in blocking buffer overnight at 4°C. Cells were washed for 5 minutes in 1xPBS (three times) and incubated with relevant secondary antibodies (diluted in 1xPBS) and appropriate dyes (e.g. SiR-actin or rhodamine-phalloidin) for 1 hour at room temperature (protected from light). Cells were washed for 5 minutes (three times) in 1xPBS and stained with Hoeschst (#33258; Sigma; 1:10000) where appropriate. Coverslips were washed for 5 minutes (three times) in 1xPBS and mounted onto glass slides using prolong gold anti-fade reagent (P36930; Thermo) and left to set overnight at room temperature (protected from light). Slides were stored at 4°C in the dark after the mountant had set.

2.8.2. Live brightfield

A549 cells were seeded onto glass-bottomed 24-well plates (#662892; Greiner) at 25,000 cells per well in CSM and left to adhere overnight. Cell movement was captured at 10-minute intervals over 24 hours in response to treatment with appropriate ligand. Cells were maintained at 37°C/5% CO_2 for the duration of image capturing. Images were acquired on an Eclipse Ti inverted microscope (Nikon) using a 20x/0.45 SPlan Fluar objective in brightfield. The images were collected using a Retiga R6 (Q-Imaging) camera and resulting images were compiled into time-lapse movies using ImageJ software.

Cell movement was tracked using Imaris 8.0 software (Media Cybernetics, Ltd) using an autoregressive motion algorithm, with cells filtered by size (>25μm) and from tracks filtered by minimum movement speed (>2.5μm/min) to discount stationary debris. XY co-ordinates of each cell between each time frame were used to calculate the step length (displacement; μm) by Pythagoras: **SQRT of $a^2 + b^2 = c$**, where **a** is position of the cell along the X axis, **b** is position of the cell along the Y axis, and **c** is the step length.

2.8.3. Live immunofluorescence

A549 or HeLa cells were seeded onto glass-bottomed 24-well plates (#662892; Greiner) at 25,000 cells per well in CSM and left to adhere overnight. Cells were transiently transfected as described in the results and live-cell imaging was performed using an Eclipse Ti inverted microscope (Nikon). Images were acquired with a 20x/0.45 SPlan Fluar objective or 40x/0.6 SPlan Fluor objective as required. Nikon filter sets for GFP and mCherry and a pE-300 LED (CoolLED) fluorescent light source were used to visualise GFP- or rhodamine-tagged proteins. Cells were maintained at 37°C/5% CO_2 throughout imaging. Images were collected using a Retiga R6 (Q-Imaging) camera and images compiled into time-lapse movies using ImageJ software.

2.8.4. Fluorescence cross-correlation spectroscopy (FCCS)

A549 cells were seeded onto glass-bottomed 35mm dishes (#627965; Greiner) at 25,000 cells per well in CSM and left to adhere overnight. Cells were transiently co-transfected with HaloTag-GR (500ng) and HDAC6-eGFP (500ng) using Fugene 6 reagent (3:1 v/w ratio with DNA) for 24 hours. 6 hours later, cells were treated with 100nM HaloTMR Direct ligand (G2991; Promega) overnight to visualise HaloTag-GR. The following morning, cells were washed once with CSM before being treated with GCs. FCCS was performed using either a Zeiss LSM780 or Zeiss LSM880 with Confocor 3 mounted on an AxioObserver Z1 microscope with a 40x C-apochromat, 1.4 NA oil-immersion objective. Zen 2010B software was used for data collection and analysis. eGFP fluorescence was excited with 488nm laser light and emission collected between 500 and 530nm. Rhodamine was excited with 561nm laser light and emission collected

between 580 and 630nm. 10x10 second runs were used for each experiment. Single-point FCCS measurements were taken within the cytoplasm and nucleus of individual cells.

2.9. SILAC-based phosphoproteomics

SILAC-labelled cells were grown to sufficient quantities in 15cm^2 dishes and serum starved by washing twice in serum-free SILAC DMEM (serum-free) and left overnight in SFM. "Light" cells were treated with vehicle (DMSO) control. "Medium" cells were treated with dex (100nM). "Heavy" cells were treated with GRT7 (3nM) or GW870086X (100nM). All ligands were made up in SILAC SFM. Three biological replicates were tested per condition. Cells were washed 3x in ice-cold 1xPBS and cells scraped into 1.5mL Eppendorf tubes, with cell pellets being collected by centrifugation at 2000xg for 10 minutes at 4°C and stored at -80°C. Cell pellets were re-suspended in 200µL guanidine hydrochloride (GdmCl) lysis buffer (6M guanidine hydrochloride, 100mM Tris-HCl pH8.5, 10mM dithiothreitol [DTT], 40mM iodoacetamide – made up in MilliQ Ultrapure water) and heated at 95°C for 5 minutes, cooled on ice for 15 minutes, sonicated for 20-30 seconds at 30% amplification, and re-heated at 95°C for 5 minutes. Lysates were centrifuged at 3500xg for 30 minutes at 4°C, a 100µL aliquot transferred to a new 1.5mL Eppendorf tube, diluted 50% in MilliQ water, and precipitated by adding 4x volume of ice-cold (-20°C) 80% acetone and left overnight at -20°C. Precipitates were collected by centrifugation at 2000xg for 15 minutes at 4°C and washed 2x in -20°C 80% acetone, then air dried upside-down at room temperature for ~10 minutes (until acetone odor dissipated). Pellets were re-suspended in 500µL 2, 2, 2-trifluoroethanol (TFE) digestion buffer (10% TFE, 100mM ammonium bicarbonate) with sonication until a homogenous suspension was formed. Peptide concentrations were determined by Nanodrop, samples were diluted to equal concentration in TFE buffer, and samples stored at -80°C prior to processing. Peptides were re-sonicated to ensure homogenous suspension and digested overnight in sequencing-grade trypsin at a 1:100 dilution of enzyme:protein (Promega; V5111). The following day, samples were diluted 1:1 in 80% ACN and phosphopeptides enriched using a combination of $Ti0_2$ (0.25mg) and Ti-IMAC (0.75mg) magnetic beads and the automated phosphopeptide enrichment method (APE) on the

KingFisher Flex system (Tape et al., 2014). TiO_2 (MR-TID002) and Ti-IMAC (MR-TIM002) beads were purchased from MagReSyn Biosciences.

Deep-well 96-well plates (VWR; #733-3004) were prepared for each position in the KingFisher Flex system (500µL per well). Magnetic beads were washed for 5 minutes in wash buffer 1 (80% ACN/5% TFA/1M glycolic acid) and incubated with peptide samples for 20 minutes at room temperature. Samples were subsequently washed in three separate wash buffers for 2 minutes each – wash buffer 1, wash buffer 2 (80% ACN/1% TFA), and wash buffer 3 (10% ACN/0.2% TFA). Phosphopeptides were eluted in 200µL of 1% ammonium hydroxide. Beads were passed through the KingFisher Flex system an additional two times to ensure complete collection of all available phosphopeptides. Samples were concentrated in a SpeedVac centrifuge to ~50µL per sample and acidified by the addition of 100µL of 0.1% formic acid. Light, medium, and heavy SILAC samples were mixed 1:1:1 and desalted in C18 microcolumns containing OLIGO R3 resin (Life Technologies; #1-1339-03) prewashed in 50% ACN and 2x in 0.1% formic acid. After passing through the columns, the samples were washed 2x in 0.1% formic acid, eluted into 100µL of 50% ACN/0.1% formic acid, and run on a liquid chromatography-mass spectrometer (LC-MS/MS).

Digested samples were analysed by LC-MS/MS using an UltiMate® 3000 Rapid Separation LC (RSLC, Dionex Corporation, Sunnyvale, CA) coupled to a Q Exactive HF (Thermo Fisher Scientific, Waltham, MA) mass spectrometer. Peptide mixtures were separated using a multistep gradient from 95% A (0.1% FA in water) and 5% B (0.1% FA in acetonitrile) to 7% B at 1 min, 18% B at 58 min, 27% B in 72 min and 60% B at 74 min at 300 nL min^{-1}, using a 75 mm x 250 µm i.d. 1.7 □M CSH M-Class C18, analytical column (Waters). The top 8 precursors were selected for fragmentation automatically by data dependant analysis during each cycle.

Resulting LC-MS/MS data was processed by MaxQuant software (Max Planck Institute, Denamrk) and analysed by Perseus software as discussed in the results (Max Planck Institute, Denmark).

2.10. Statistical analysis

Statistical tests were performed using GraphPad Prism software, with parametric data represented as mean ± standard deviation and non-parametric data represented as median ± interquartile range unless stated otherwise. Parametric data was analysed for statistical significance using student's t-test (between 2 groups) or one-way analysis of variance (ANOVA) (between >2 groups). Non-parametric data was analysed by Mann Whitney test (between 2 groups) or Kruskal-Wallis followed by Dunnett's multiple comparison tests (between >2 groups). Experiments were performed in triplicate unless stated otherwise in the results.

Chapter 3: Glucocorticoids and Cell Migration

Glucocorticoids inhibit cell migration through a non-transcriptional pathway involving HDAC6

Stephen Kershaw[1], David J. Morgan[1], James Boyd[2,5], David G. Spiller[3], Egor Zindy[4], Mudassar Iqbal[4], Andrew Brass[4], Laura C. Matthews[6] & David W. Ray[1,7]

[1]Division of Diabetes, Endocrinology, and Gastroenterology, [2]Division of Infection, Immunity, and Respiratory Medicine, [3]Platform Sciences, Enabling Technologies, and Infrastructure, [4]Division of Informatics, Imaging, and Data Sciences, Faculty of Biology, Medicine, and Health, University of Manchester, Manchester M13 9PT, UK. [5]Division of Cellular and Molecular Physiology, University of Liverpool, Liverpool, L69 3BX, UK. [6]Leeds Institute of Cancer and Pathology, Faculty of Medicine and Health, University of Leeds, Leeds, LS2 9JT, UK, [7]Oxford Centre for Diabetes, Endocrinology and Metabolism, University of Oxford, Oxford, OX37LE, UK.

In review at Nature Communications (2018)

3.1. Abstract

Glucocorticoids (GCs) act through the ubiquitously expressed glucocorticoid receptor (GR) to regulate immunity, energy metabolism, and tissue repair. Upon ligand binding, activated GR mediates cellular effects by regulating gene expression, but some GR effects can occur rapidly without new transcription. We now show GCs rapidly inhibit cell migration, and unexpectedly both GR agonist and antagonist ligands exert the same effect. The inhibitory effect on migration is prevented by GR knockdown with siRNA, confirming GR specificity, but not by actinomycin D treatment, suggesting a non-transcriptional mechanism. Immunoblotting and immunofluorescent microscopy reveal a rapid increase in tubulin acetylation upon GC treatment – a marker of microtubule stability- and live-cell imaging uncovers rapid tubulin polymerisation and thereby stabilisation of the microtubule network upon GC treatment. HDAC6 overexpression, but not aTAT1 siRNA rescued the GCs effect, implicating HDAC6 as the GR effector. Consistent with this hypothesis, ligand-dependent cytoplasmic interaction between GR and HDAC6 was demonstrated using fluorescent cross correlation spectroscopy. Taken together, we propose that activated GR inhibits HDAC6 function, driving hyper-acetylation of microtubules, and thereby increasing the stability of the microtubule network to reduce cell motility. We therefore report a novel, non-transcriptional mechanism whereby GR agonists and antagonists mediate similar effects, through inhibition of HDAC6 resulting in rapid reorganization of the cell architecture.

3.2. Introduction

Glucocorticoids (GCs) are steroid hormones that regulate a range of biological functions essential for life, including normal homeostasis, glucose metabolism, resolution of inflammation, and development (McMaster et al., 2008; Tu et al., 2018; Tanaka et al., 2017). GCs exert their biological effects through the ubiquitously expressed glucocorticoid receptor (GR), a ligand-inducible transcription factor of the nuclear hormone receptor superfamily (Hollenberg et al., 1985). Synthetic GCs (including dexamethasone, fluticasone furoate, and prednisolone) are powerful anti-inflammatory and immunosuppressive drugs that are widely prescribed in the clinic to treat a variety of ailments (Donn et al., 2007; Smoak and Cidlowski, 2004; Xing et al., 2015). However, the pleiotropic action of GCs leads to severe off-target effects that severely limits prolonged clinical use, including osteoporosis, diabetes, and impaired wound healing (Zhou and Cidlowski, 2005; Abell et al., 2015). For this study we investigated the mechanism underlying GC impairment of wound healing and by extensions the inhibition of cell migration which is implicated in impaired wound healing (Matsubayashi et al., 2004)

GCs are known to inhibit the migration of various cell types yet with an unrecognised mechanism of action (Fietz et al., 2017; Murakami et al., 1998) Regulation of cell motility has often been attributed to reorganization and stabilisation of the actin and microtubule networks (Akhshi et al., 2014; Yumura et al., 2013; George et al., 2013; DeFea, 2013; Yang et al., 2010). The actin network generates the propulsive force necessary for front-end protrusion and rear-end retraction of cells facilitating cell movement (Kaverina and Straube, 2011; Ridley et al., 2003). The actin and microtubule networks can cross-talk which impacts persistent cell movement through myosin convergence and focal adhesion turnover (Wu and Bezanilla, 2018; Schneider and Persson, 2015; Juanes et al., 2017). Cell movement is highly dependent on the state of microtubule dynamic stability (Pitaval et al., 2017). Microtubule stability is regulated by acetylation of lysine-40 (K40) on α-tubulin, with acetylated α-tubulin being most abundant in stable microtubules (Piperno et al., 1987; Zhang et al., 2003). Deacetylation of α-tubulin is catalysed by histone deacetylase-6 (HDAC6) and modulation of HDAC6 activity impacts cell migration by altering the dynamics of the microtubule network

(Hubbert et al., 2002; Zhang et al., 2007; Shi et al., 2015). Overexpression of HDAC6 increases cell motility by regulating microtubule-dependent migration [19, 20]. Glucocorticoids are known to interact with the cytoskeleton to facilitate ligand-induced nuclear translocation amongst other functions (Mayanagi et al., 2008; Hong et al., 2011; Fitzsimons et al., 2008; Dvorak et al., 2004; Akner et al., 1995). In addition, HDAC6 deacetylates heat shock protein-90 (Hsp90), which is vital for GR maturation and maintaining the receptor in a ligand-binding state (Tao et al., 2018; Ai et al., 2009; Kovacs et al., 2005; Rajapandi et al., 2000). GR is also reported to physically associate with HDAC6 in the nucleus (Govindan, 2010; Rimando et al., 2016), however, a mechanistic link between the two proteins has yet to be determined. We hypothesised that GCs inhibit cell migration by altering the stability of the microtubule network via HDAC6, likely through an inhibitory interaction facilitated by interconnected substrate Hsp90.

We now show that GCs act rapidly, and in a non-transcriptional mechanism, to inhibit cell migration; modelled as a change in α-stable distribution parameters. Furthermore, GCs impair HDAC6 regulation microtubule dynamics to increase microtubule stability. We find that activated GR is in complex with cytoplasmic HDAC6 using FCCS, which results in a small proportion of HDAC6 being shuttled into the nucleus and away from its substrate lysine-40 (K40) residue on α-tubulin. This study provides further insight into the non-genomic action of GCs and explains the mechanism by which GCs inhibit cell migration, thereby impairing wound healing.

3.3. Methods

Cell culture

Human lung epithelial carcinoma (A549) and human cervical adenocarcinoma (HeLa) cells (ATCC, Teddington, UK) were cultured in high glucose (4500 mg/l) Dulbecco's modified Eagle's medium (DMEM; D6429, Sigma) with L-glutamine, sodium bicarbonate, sodium pyruvate and supplemented with 10% heat-inactivated foetal bovine serum (FBS; F9665, Invitrogen, Paisley, UK) or 10% charcoal-stripped foetal bovine serum (cFBS; #12676029, Invitrogen, Paisley, UK) at 37°C in 5% CO_2.

Antibodies and Reagents

Antibodies: Rabbit polyclonal GR (24050-1-AP) was purchased from ProteinTech. Monoclonal mouse phospho-Ezrin^{Thr567}/ Radixin^{Thr564}/ Moesin^{Thr558} (#3141), monoclonal rabbit phospho-Src^{Tyr416} (#6943), monoclonal rabbit GAPDH (#2118), monoclonal rabbit phospho-Akt^{Ser473} (#4060), and monoclonal rabbit acetyl-α-Tubulin^{Lys40} (#5335) were purchased from Cell Signaling Technology. Monoclonal mouse α-tubulin (T5168) was purchased from Sigma. Polyclonal rabbit αTAT1 (HPA046816) was purchased from Atlas Antibodies. Mouse IgG horse radish peroxidase (HRP)-linked whole antibody (NXA931) and rabbit IgG HRP-linked whole antibody (NA934) were purchased from GE Healthcare.

Plasmids: N1-HDAC6-eGFP and GRα-GFP were purchased from Addgene. HaloTag-HDAC6, HaloTag-GR (FHC10483), and pHaloTag vector were purchased from Promega. pBOS-H2B-GFP was purchased from BD Biosciences.

siRNA: AllStars Negative Control siRNA (SI03650318), GR siRNA (SI02654764), and αTAT1 siRNA (S104145162) were purchased from Qiagen.

Cell treatments: Rhodamine Phalloidin (R415) was purchased from Invitrogen. Dexamethasone (Dex, D4902), mifepristone (RU486, M8046), nicotinamide (N3376), tubacin (SML0065), TSA (T8552), fluticasone propionate (FP, F9428), hoechst 33342 (#14533), and dimethylsulfoxide

(DMSO, D2650) were purchased from Sigma. ITSA1 (CAS 200626-61-5) was purchased from Santa Cruz. HaloTag TMR Direct ligand (G2991) was purchased from Promega. GRT7 and GW870086X were developed by GlaxoSmithKline.

Chemotaxis Migration Assay

Chemotaxis migration assay was performed in 24-well Millicell hanging cell culture inserts (Millipore, MCEP24H48) with an 8µm polyethylene terephthalate membrane pore. A549 cells were pre-conditioned to 100nM dex or vehicle control (DMSO) for 48 hours (37°C/5% CO_2). Cells were suspended in serum-free DMEM and seeded into the upper chamber of the Transwell insert ($2.5x10^4$ cells/well). The lower chamber was filled with FBS to act as the chemoattractant. 100nM dex or vehicle control was added to the upper and lower compartments of the transwell. The cells are incubated for 24 hours (37°C/5% CO_2) to allow chemotaxis to occur. Following incubation, the cells were fixed in 4% paraformaldehyde (PFA) for 15 minutes at RT. Any cells that did not migrate were removed from the upper side of the membrane with a cotton swab. Cells are stained with crystal violet (5mg/ml in 2% ethanol) for 30 minutes at RT. The inserts were washed twice in dH_2O and excess stain was removed mechanically from the upper side of the membrane. The migrated cells were solubilised in 2% SDS overnight at room temperature and absorbance was read at 560nm using a Glomax plate reader (Promega).

Cell Stopper Migration Assay

Migration assay was performed using an Oris 96-well plate with Oris Cell Seeding Stoppers (Platypus Technologies, CMA1.101) according to the manufacturer's instructions. A549 cells were seeded in DMEM + 10% FBS ($1x10^5$ cells/well) into an Oris 96-well plate containing Oris Cell Seeding Stoppers and incubated for 18 hours (37°C/5% CO_2) to allow attachment. Following incubation, stoppers were removed, and cells washed with 1xPBS. The media was replaced with DMEM + 10% cFBS and cells were treated with 100nM dex or vehicle control (DMSO). The cells were incubated for 48 hours to allow migration into the detection zone to occur (37°C/5% CO_2). Reference wells had Oris Cell Seeding Stoppers left in place to act as the pre-migration controls (t=0). Cells were washed with

1xPBS to remove any debris/unattached cells, fixed in 4% PFA for 40 minutes at 4^0C, and stained with Hoeschst (2µg/ml; #14533; Sigma) for 5 minutes at room temperature to label DNA. Images were collected on an Axio Observer A1 (Axiovision) inverted microscope using a 2.5x/0.07 Plan-Apochromat objective and captured using a Axio Cam HRc (Axiovision) through MetaVue Software (Molecular Devices). Specific band pass filter sets for DAPI were used to prevent bleed through from one channel to the next. Images were processed and quantification of migration was achieved using ImageJ (http://rsb.info.nih.gov/ij) (Schneider et al., 2012). Images were converted to binary format and coverage of the detection zone, using pre-migration controls for reference, was determined. Migration was quantified as the percentage of the detection zone covered with cells.

Scratch Wound Healing Assay

A549 cells were seeded in DMEM + 10% cFBS ($2x10^4$ cells/well) into a 96-well ImageLock plate (Essen Bioscience, #4379) and allowed to adhere for 24 hours (37°C/5% CO_2). Simultaneous, uniform scratch wounds were induced in each well with the WoundMaker tool (Essen Bioscience) and wells were washed twice in DMEM + 10% cFBS to remove debris. Cell migration into the wound was acquired immediately following administration of a dose response of dex, RU486, and hydrocortisone (0.1nM, 1nM, 10nM, 100nM, 1µM, 10µM) along with the vehicle control (DMSO). Images were taken at 30-minute intervals over 24 hours (37°C/5% CO2) on an Incucyte Zoom Live-Cell Analysis system using a 10x/0.3 Plan Fluor OFN25 (DIC L/N1) objective in brightfield. Cell migration was analysed and quantified using Incucyte Zoom software.

Live-Cell Brightfield Migration

A549 cells were seeded in DMEM + 10% cFBS ($5x10^4$ cells/well) into a glass-bottomed 24-well plate (Greiner, #82050-898) and allowed to adhere for 24 hours (37°C and 5% CO_2). Cell migration was monitored following treatment with 100nM dex, 100nM RU486, 100nM Tubacin, 100nM 086X, 3nM GRT7, or vehicle control (DMSO) in real-time (37°C/5% CO_2). Images were captured over 24 hours at intervals of 10 minutes on a Leica TCS SP5 AOBS inverted confocal using a 20x/0.5 Plan Fuotar

objective in brightfield. Cells were tracked using a wavelet plugin on IMARIS Pro Plus software (MediaCybernetics) developed by Dr Egor Zindy (University of Manchester, UK).

Live-cell Immunofluorescent Migration

A549 or HeLa cells were seeded onto glass-bottomed 24-well plates (#662892; Greiner) at 25,000 cells per well in CSM and left to adhere overnight. Cells were transiently transfected as described in the results and live-cell imaging was performed using an Eclipse Ti inverted microscope (Nikon). Images were acquired with a 20x/0.45 SPlan Fluar objective or 40x/0.6 SPlan Fluor objective as required. Nikon filter sets for GFP and mCherry and a pE-300 LED (CoolLED) fluorescent light source were used to visualise GFP- or rhodamine-tagged proteins. Cells were maintained at 37°C/5% CO_2 throughout imaging. Images were collected using a Retiga R6 (Q-Imaging) camera and images compiled into time-lapse movies using ImageJ software.

Quantitative RT-PCR

A human cell motility RT^2 Profiler PCR array (384-well plate) was used to assay gene expression changes following glucocorticoid treatment (PAHS-128Z; Qiagen). Cells were treated as required, then lysed and RNA extracted using an RNeasy kit (#74104; Qiagen). RNA was reverse transcribed and cDNA samples were added to the reaction plate and real-time PCR acquired using an ABI qPCR machine (Applied Biosystems, CA, USA). Data was analysed by RT^2 profiler PCR array data analysis software (Qiagen). Gene expression was normalised to the housekeeping gene β-actin.

Immunoblot analysis

Cells were treated as described in the results and lysed on ice for 30 minutes with modified RIPA buffer (50mM Tris-HCl, pH7.4, 1% NP-40, 0.25% sodium deoxycholate, 150mM NaCl, 1mM EDTA) supplemented with protease inhibitor (#04693124001, Roche) and phosphatase inhibitor cocktails (P5726; P0044; Sigma). Cell lysates were scraped into 1.5mL Eppendorf tubes, cleared by centrifugation at 14000xg for 10

minutes at 4°C. Supernatants were collected and protein concentration determined by Bradford assay #23236; ThermoFisher Scientific). Lysates were resuspended to 1mg/mL in 1x Laemmli buffer (0.125M Tris-HCl, pH6.8, 0.1% SDS, 20% glycerol, 0.2% β-mercaptoethanol, 0.001% bromophenol blue) and boiled at 95°C for 10 minutes. Lysates were electrophoresed on Tris-Glycine (4-20%) Mini-PROTEAN TGX precast polyacrylamide protein gels (15-well, 15µL per lane) (#4561096, BioRad, Hertfordshire, UK) using 1x Tris/Glycine running buffer (#1610732; BioRad) and run at 130V for 60 minutes at room temperature. Gels were transferred onto nitrocellulose membranes using transfer buffer (192mM glycine, 25mM Tris Base, 20% methanol) and run at 90V for 60 minutes at 4°C. Membranes were blocked in blocking buffer (2% skimmed milk, 150µM NaCl, 0.1% Tween-20) for 2 hours at room temperature and incubated with relevant primary antibodies diluted in blocking buffer overnight at 4°C. Membranes were washed 3x in wash buffer (0.3% milk, 48mM Tris-HCl, 24.8mM Tris Base, 0.1% Tween-20) for 10 minutes and incubated with relevant horse-radish peroxidase (HRP)-tagged secondary antibodies diluted (1:5000) in wash buffer for 1 hour at room temperature. Membranes were washed 3x in wash buffer and exposed to enhanced chemiluminescence (ECL) Clarity reagent (#1705060; BioRad) for 2 minutes. Protein bands were visualised using BioMax MR photographic film (#V8572786; GE Healthcare).

HaloTag pulldown assay

A549 cells were seeded onto 15cm^2 dishes at 300,000 cells per mL in CSM and left to incubate for 24 hours at 37°C/5% CO_2. Cells were transiently transfected with either HaloTag-GR (10µg) or HaloTag-HDAC6 (10µg) and left to incubate for 24 hours. Cells were treated with vehicle (DMSO) or dex (100nM) for 1 hour and washed 2x with ice-cold 1xPBS. Cells were gently scraped into conical tubes and centrifuged at 2000xg for 10 minutes at 4°C. Supernatant was discarded and cell pellets were stored overnight at -80°C prior to lysis. Before cell lysis, HaloTag resin (G1912; Promega) was mixed to obtain uniform suspension and 200µL resin was dispensed into 1.5mL Eppendorf tubes per treatment condition. Tubes were centrifuged at 800xg for 1 minute, supernatant discarded, and resuspended in 800µL resin equilibration buffer (100mM Tris-HCl, 150mM NaCl, 0.005% IGEPAL CA-630). Tubes were centrifuged at 800xg for 2

minutes and supernatant discarded. Resin was washed an additional 3x in equilibration buffer. Cell pellets were thawed on ice and resuspended in 300µL lysis buffer (50mM Tris-HCl pH7.5, 150mM NaCl, 1% Triton X-100, 0.1% sodium deoxycholate) supplemented with 6µL of 50x protease inhibitor cocktail (800µ/mL benzamidine HCl, 500µg/mL phenanthroline, 500µg/mL aprotinin, 500µg/mL leupeptin, 500µg/mL pepstatin A, 50mM PMSF). Cells were passed 5x through a 25G needle to complete lysis and centrifuged at 14000xg for 5 minutes at 4°C. Cleared lysates (300µL) were transferred to new 1.5mL tubes and diluted in 700µL 1xTBS (100mM Tris-HCl pH7.5 and 150mM NaCl). 1mL diluted lysates were mixed with the washed HaloTag resin and left to incubate overnight on a tube rotator at 4°C. Tubes were centrifuged at 800xg for 2 minutes and supernatant discarded. Pellets were washed 4x in resin equilibration buffer. After the last wash, resin was resuspended in 50µL HaloTEV Protease (G6601; Promega) and incubated at room temperature for 1 hour with constant shaking. Tubes were centrifuged at 800xg for 2 minutes and eluates transferred to new 1.5mL tubes. Samples were processed for western blotting as described above.

Transfection

Transfections were performed with Fugene 6 reagent (E2691; Promega) used at a ratio of 3:1 volume/weight ratio with DNA. Fugene 6 was pre-mixed with RPMI media (serum-free) for 5 minutes prior to incubation with DNA for 15 minutes at room temperature. Transfections were performed over 24 hours at 37°C/5% CO_2.
Small interfering RNA (siRNA) transfections were performed with Lipofectamine RNAiMAX reagent (#13778150; ThermoFisher Scientific) as described in the manufacturer's instructions and performed over 48 hours at 37°C/5% CO_2.

Luciferase reporter gene assay

HeLa cells were seeded onto 10cm^2 dishes at 50,000 cells per well in CSM and left to adhere overnight. Cells were transiently transfected with luciferase tagged-mouse mammary tumour virus (MMTV-Luc; 2µg) or luciferase tagged-nuclear factor-κB response element (NRE-Luc; 2µg) using Fugene 6 reagent (3:1 volume/weight ratio with DNA) for 24

hours. Cells were re-seeded onto 24-well plates at 50,000 cells per well in CSM and left to adhere overnight at 37°C/5% CO_2. Cells were treated as specified in the results and 18 hours later each well was washed twice with 1xPBS. 100µL of Bright Glo lysis buffer (Promega, E2620) was added to each well and left to lyse on ice for 30 minutes. Cell lysates were transferred to a white, flat-bottomed 96-well plate and luciferase absorbance was read using a luminometer (Glomax, Promega). 10x 1-second reads were taken of each well and the average relative light unit (RLU) determined. Background wells were included that only contained lysis buffer. IC_{50} and EC_{50} values were extrapolated from the resulting dose response curves using non-linear regression analysis in GraphPad Prism software, with the following equation:

Y=Bottom + (Top-Bottom) / (1+10^((LogIC50-X) *HillSlope))

Where X: log of dose or concentration; Y: Response; Top and Bottom: Plateaus; $LogIC_{50}$ interchangeable with $LogEC_{50}$; HillSlope: Slope factor or Hill slope, unitless.

Fixed-Cell Immunofluorescent Imaging

A549 cells were seeded in DMEM + 10% cFBS ($5x10^4$ cells per coverslip) and allowed to adhere for 24 hours (37°C/5% CO_2). Cells were treated with vehicle or dex (100nM) for 48 hours. Cells were fixed with 4 % PFA for 40 minutes at 4°C and blocked (0.1% Triton X-100, 1% FBS in PBS) for 1 hour at room temperature. Remaining incubations were performed at room temperature unless stated otherwise. Coverslips were incubated with primary antibody diluted in blocking buffer overnight at 4°C. After three 5-minute washes in PBS, coverslips were incubated with flourophore-conjugated secondary antibody for 2 hours. Cells were subsequently stained with rhodamine-phalloidin in PBS (2 µg/ml) for 15 minutes and then Hoeschst in PBS (2 µg/ml) for 5 minutes. Following four 5-minute washes in PBS, coverslips were mounted using Vectamount AQ (Vector Labs, H-5501). Images were acquired on a Delta Vision RT (Applied Precision, GE Healthcare) restoration microscope using either a 40X/0.85 Uplan Apo objective or a 60X/1.42 Plan Apo N objective and the Sedat Quad filter set (Chroma 86000v2, VT, USA). The images were collected using a Coolsnap HQ (Photometrics, AZ, USA) camera with a Z optical spacing of 0.5µm. Raw images were then deconvolved using the

Softworx software (GE Healthcare) and maximum intensity projections of these deconvolved images processed using Image J.

Live-Cell Immunofluorescent Imaging

GR Trafficking: A549 cells were seeded in DMEM containing cFBS ($2.5x10^4$cells/well) into a glass-bottomed 24-well plate (Greiner, #82050-898) and allowed to adhere for 24 hours at 37°C/5% CO_2. Each well was co-transfected (Fugene 6) with 0.25µg HaloTag-GR (Promega, FHC10483) and 0.25µg pBOS-H2B-GFP (BD Biosciences, Oxford, UK) and, 6 hours later, incubated for 16 hours with 0.25µL Halo ligand (HaloTag TMRDirect, G2991, Promega) to enable HaloTag visualisation. Alternately, wells were transfected with 0.5µg HaloTag-HDAC6 (Promega, Southampton, UK) and incubated for 16 hours with 0.25µL HaloTag TMR Direct ligand (Promega, G2991). Sub-cellular GR/HDAC6 trafficking was tracked in real-time at 37°C and 5% CO_2. Images were acquired on a Nikon TE2000 PFS microscope using a 20x Plan Apo objective and the Sedat filter set (Chroma 89000). The images were collected using a Coolsnap HQ (Photometrics, USA) camera and raw images were processed using ImageJ.

Fluorescence (cross)-correlation spectroscopy (FCCS): A549 cells were seeded onto glass-bottomed 35mm dishes (#627965; Greiner) at 25,000 cells per well in CSM and left to adhere overnight. Cells were transiently co-transfected with HaloTag-GR (500ng) and HDAC6-eGFP (500ng) using Fugene 6 reagent (3:1 v/w ratio with DNA) for 24 hours. 6 hours later, cells were treated with 100nM HaloTMR Direct ligand (G2991; Promega) overnight to visualise HaloTag-GR. The following morning, cells were washed once with CSM before being treated with GC. FCCS was performed using either a Zeiss LSM780 or Zeiss LSM880 with Confocor 3 mounted on an AxioObserver Z1 microscope with a 40x C-apochromat, 1.4 NA oil-immersion objective. Zen 2010B software was used for data collection and analysis. eGFP fluorescence was excited with 488nm laser light and emission collected between 500 and 530nm. Rhodamine was excited with 561nm laser light and emission collected between 580 and 630nm. 10x10 second runs were used for each experiment. Single-point FCCS measurements were taken within the cytoplasm and nucleus of individual cells.

Live-cell Microtubule Dynamics

Microtubule dynamics were monitored in A549 cells transiently transfected with 0.25µg of EB3-GFP and 0.75µg pcDNA3 using Fugene 6 reagent and treating with vehicle or dex (100nM) for 4 hours prior to imaging. Images were captured every 0.5 seconds for 1 minute using a 100x objective. The images were collected using a Cascade II EMCCD camera (Photometrics) with a Z optical spacing of 0.2µm. Raw images were then processed using Image J (Schneider et al., 2012).

Image Analysis

Live-cell immunofluorescent tracking: A549 cell movement was tracked using an ImageJ plugin, Mosaic, based on H2B-GFP expression. Tracking was performed following manufactures instructions. Co-ordinates of the tracks and the corresponding movies including tracks were exported, from which step length and total distance moved where calculated.

Mathematical analysis

Frequency distributions of step lengths against time were parameterised and fitted to alpha stable distribution using the *STBL: Alpha stable distributions* functions package for MATLAB (available at http://www.mathworks.com/MATLABcentral/fileexchange/37514). The functions package was used to calculate probability distribution functions (PDF) and cumulative distribution functions (CDF) of the empirical data and from the determined parameters. A standard resampling strategy was used to validate the parameters. Random sampling with replacement from the original data sets was performed to generate 100 subsets of 15,000 values. These subsets were then parameterised according to an alpha stable distribution to derive robust estimates of the standard deviations.

Live-cell brightfield tracking

A549 cell movement was tracked using Imaris 8.0 software (Media Cybernetics, ltd). Migration was tracked using an autoregressive motion algorithm from cells filtered by size (25 µm) and from tracks filtered by minimum movement speed (above 2.5 µm/minute) to discount stationary

debris. Cell migration was depicted as step length between each time point, which was determined using Pythagoras: SQRT of $a^2 + b^2 = c$, where a is the position along the x axis, b is the position along the y axis, and c is the step length.

EB3 tracking

A MATLAB-based software package, plusTipTracker (http://lccb.hms.harvard.edu/software.html) (Applegate *et al.*, 2011;Matov *et al.*, 2010), was used to determine microtubule (MT) dynamics from EB3-time lapse movies. Analysis was performed to determine the impact of dex on MT growth, shrinkage, and pausing events. All movies were analysed with the following parameter values, which were determined prior to analysis using the plusTipParamSweepGUI tool within plusTipTracker: maximum gap length, 10 frames; minimum track length, 3 frames; search radius range, 5–10 pixels; maximum forward angle, 20°; maximum backward angle, 10°; maximum shrinkage factor, 1; fluctuation radius, 1.5 pixel. The plusTipGetTracks tool was used to detect and track fluorescently-labelled MT plus end binding proteins (+TIPs). Overlay images showing the tracks for MT growth events for one of the three categories, speed, lifetime, and displacement, were generated with the plusTipSeeTracks tool. Raw data was collected from the gs_fs_bs_gl_fl_bl_gd_fd_bd.txt generated by the plusTipGetTracks tool and combined; histograms were created in GraphPad Prism.

Statistical analysis of cell movement data

Cumulative distance data for varying-length trajectories (~1000 cells in each experiment, measurements every 10 minutes up to 24 hours) for cells treated with GW8700O86X, dexamethasone, GRT7, and RU486 were used to perform statistical test on the median reduction in cumulative distance travelled against corresponding vehicle-treated cells.

For any pair, e.g., dexamethasone vs vehicle, and at each time point, two distributions of cumulative distances are compared using a non-parametric rank-sum test (using MATLAB), reporting significance (at $\alpha=0.0001$) of median reduction under treatment (e.g. dexamethasone)

w.r.t vehicle against the null hypothesis that medians are equal in both distributions.

3.4. Results

Glucocorticoid receptor agonists and antagonists inhibit cell migration

Dexamethasone (dex), a synthetic glucocorticoid receptor (GR) agonist, potently inhibits the migration of A549 cells (Fig 3.1A), causing a marked reduction in total displacement and median step length (Fig 3.1B). There is a significant increase in small step size and corresponding decrease in large step size typical of inhibited cell migration, revealing a shift in the cell walk properties (Fig 3.1C). Dex also inhibited A549 cell migration at the population level in wound healing and chemotaxis assays performed over 48 hours (Fig S3.1A-B). Cell migration is also significantly inhibited with the low potency GR agonist hydrocortisone and the GR antagonist RU486 (Fig S3.1C), and RU486 did not antagonise the inhibitory effect of dex (Fig S3.1D-E). RU486 is a competitive GR antagonist that binds and induces GR nuclear translocation, but then recruits corepressors including NCoR to block transcription (Fig S3.1C). This suggests that both dex and RU486 inhibit migration through a similar mechanism of action.

The overlapping actions of dex and RU486 on cell migration suggest a common mechanism of action, but one that requires the GR. We tested the requirement of the GR, using siRNA (Fig 3.1F-G), which confirmed the need for GR. Complementation assays using siRNA-resistant HaloTag-GR further confirmed specific requirement for the GR (Fig 3.1H).

GCs also inhibit the migration of many other cell types. To test the broader applicability of our findings we used primary peritoneal macrophages from $GR^{f/f}$ and LysM-cre$GR^{f/f}$ mice (Fig S3.1E). These cells show remarkable inhibition to GC, but this inhibitory effect is completely lost in the GR null cells.

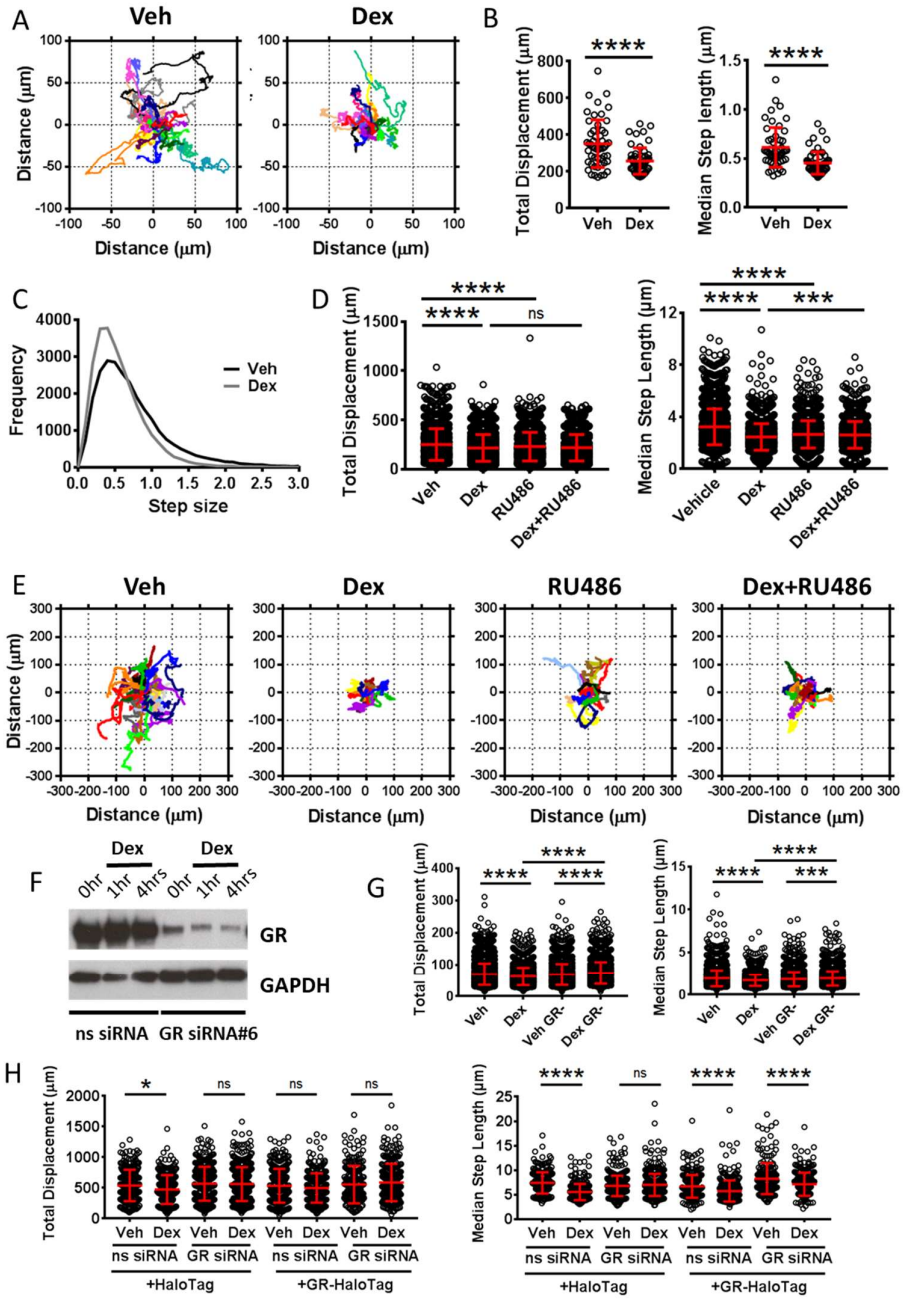

Figure 3.1: Glucocorticoid receptor agonists and antagonists inhibit cell migration. (A) Rose plots of A549 cell displacement in response to 48 hours of vehicle and dexamethasone (dex) (100nM) treatment. (B) Total displacement and median step length of A549 cells in response to 48 hours of vehicle and dex (100nM) treatment. (C) Frequency distribution curves of A549 median step length in response to 48 hours of vehicle and dex (100nM) treatment. (D) Total displacement and median step length of A549 cells in response to 24 hours of vehicle, dex (100nM), RU486 (100nM), and dex+RU486 co-treatment. (E) Rose plots of A549 cell displacement in response to 24 hours of dex (100nM), RU486 (100nM), RU486 (100nM), and a dex+RU486 co-treatment. (F) GR and GAPDH protein expression in control (non-silencing siRNA-treated) and GR knockdown (GR siRNA#6-

treated) A549 cells and in response to 1 and 4 hours of vehicle and dex (100nM) treatment. (G) Total displacement and median step length of control and GR knockdown A549 cells in response to 6 hours of vehicle and dex (100nM) treatment. (H) Total displacement and median step length of control and GR knockdown A549 cells overexpressing pHaloTag or HaloTag-GR in response to 24 hours of vehicle or dex (100nM) treatment. Migration data represents quantification of at least two independent experiments (mean ± SD, one-way ANOVA, ****p<0.0001, ***p=0.0002).

Alpha stable distribution models A549 motion

An alpha stable distribution (or Lévy distribution) is a continuous probability distribution for a non-negative random variable. Cell walk properties have previously been characterised by alpha stable distribution, characterised by "superdiffusive" movement and composed of many short steps interspersed with longer "searching" movements (Harris et al., 2012). The distribution of step lengths in vehicle and dex treated conditions (Fig 3.1C) showed the distinctive walk pattern indicative of an alpha stable distribution, characterised by four parameters that describe the stability exponent (α), skewness (β), scale (γ), and location (δ) (Salas-Gonzalez et al., 2013; Burnecki et al., 2012). Glucocorticoid treatment reduces median step length, signified by a left-shift frequency distribution curve (measured by a reduction in δ parameter). Alpha stable parameters were derived using MATLAB, showing that A549 cell movement adopts an alpha stable distribution irrespective of glucocorticoid treatment (Fig S3.2A-B). These changes in parameters show that the movement of vehicle-treated A549 cells primarily consists of small steps occasionally interspersed with larger relocating or searching steps. Glucocorticoids alters these parameters inhibiting the low frequency, large displacement searching movements.

Synthetic, selective GR ligands exhibit similar effects to conventional GC

In view of the surprising equipotency of RU486 to inhibit cell migration, the study was extended to further non-steroidal GR ligands with unique pharmacologies (Trebble et al., 2013; Schiller et al., 2014), and we selected a panel based on high affinity and specificity (Fig 3.2A). For example, GRT7 extends into the meta channel of the GR LBD driving slower kinetics of activation, but more potent transcriptional induction (Fig 3.2.B-C) (Trebble et al., 2013). GW870086X (086X), is a selective

GR modulator (SeGRM), deficient in transactivation function (Fig 3.2D). All the GR ligands tested similarly reduced A549 cell displacement (Fig 3.2E), affecting both total displacement and median step length and cell walk properties were similarly inhibited (Fig 3.2F-G, Fig S3.2C-F, Fig S3.3E-F). As with dex, RU486 did not co-treatment antagonise the inhibition of cell migration with GRT7 or O86X. Additional analysis was conducted using the high potency, steroidal GR agonist fluticasone propionate (FP), with similar effects on movement (Fig S3.3A-C) and alpha stable distribution parameter changes confirming altered walk properties (Fig S3.3C-F).

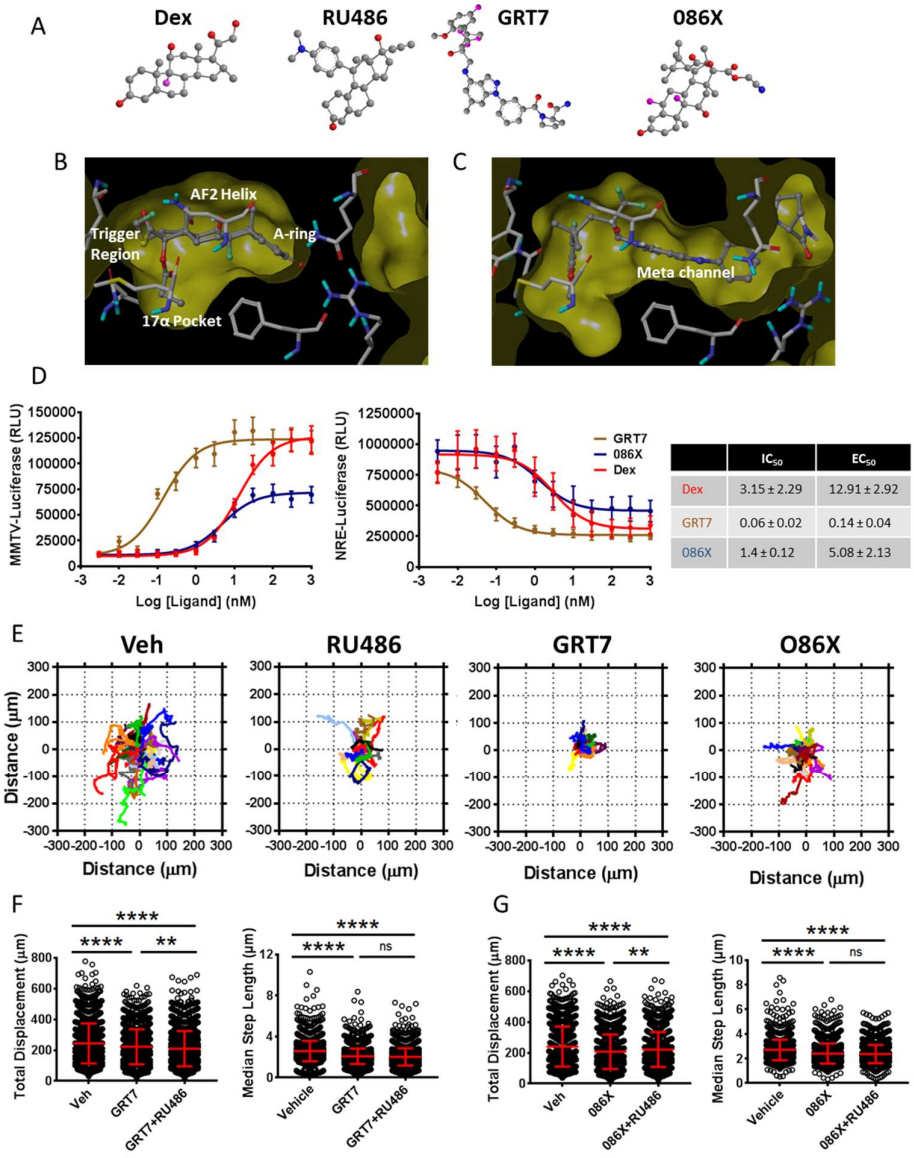

Figure legend on the next page.

Figure 3.2: Selective glucocorticoids also inhibit cell migration. (A) 3D chemical structures of dex, RU486, GRT7, and GW870086X (086X). (B) Crystal structures of the GR ligand-binding domain (LBD) bound to dex with trigger region annotated. (C) Crystal structure of the GR LBD bound to GRT7 annotated with regions altered by ligand-binding. (D) Transcriptional activation of the luciferase-tagged mouse mammary tumour virus (MMTV) and repression of the NFκB-response element (NRE) promoters in response to dex, GRT7, and 086X and accompanying table of IC_{50} and EC_{50} values. (E) Rose plots of A549 cell displacement in response to 24 hours potency-matched vehicle, RU486 (100nM), GRT7 (3nM), and 086X (100nM). (F) Total displacement and median step length of A549 cells in response to 24 hours of vehicle, 086X (100nM), RU486 (100nM), and 086X+RU486 co-treatment. (G) Total displacement and median step length of A549 cells in response to 24 hours of vehicle, GRT7 (3nM), RU486 (100nM), and GRT7+RU486 co-treatment. Migration data represents quantification of three independent experiments (mean ± SD, one-way ANOVA, ****p<0.0001, **p=0.005). Luciferase reporter gene data is representative of three independent experiments (mean ± SEM).

GC inhibit migration independent of gene transcription

Through dynamic cell tracking, we noted that the GC effect was of rapid onset, an observation not identified previously using fixed end-point assays (Fig S3.1A-B). We used a non-parametric rank-sum test to determine the earliest time-point at which cell migration is significantly reduced following treatment with each GC and compared this to the dynamics of ligand-induced GR nuclear translocation (Fig 3.3A-C). Dex and RU486 both inhibit migration within 60 minutes of administration; and GRT7 which does not translocate until 3 hours post treatment also inhibits migration after 60 minutes. O86X, which induces the most rapid GR translocation only inhibits migration after 5 hours (indicated by the coloured arrows, Fig 3.3C). The kinetics of nuclear translocation were inverse to those for migration inhibition, with such a rapid onset of effect whilst the GR was still cytoplasmic suggested a non-transcriptional mechanism of action.

Actinomycin D (AMD) was used as an inhibitor of new gene transcription to confirm that the GC effect on cell migration occurs through a non-transcriptional mechanism of action (Cervantes-Gomez et al., 2009). AMD pre-treatment did not rescue the dex effect (Fig 3.3D) and did not independently affect cell movement. We also profiled changes in gene expression of a panel of genes known to control cell migration timed after the observation of the early effect on migration (Fig 3.3E). Although two genes (PLAUR and BCAR1) were down-regulated by a 4-hour incubation

with dex, this regulation was opposed by RU486, as expected for a conventional GR antagonist. This suggests that these two genes are not implicated in mediating the migration phenomenon under investigation.

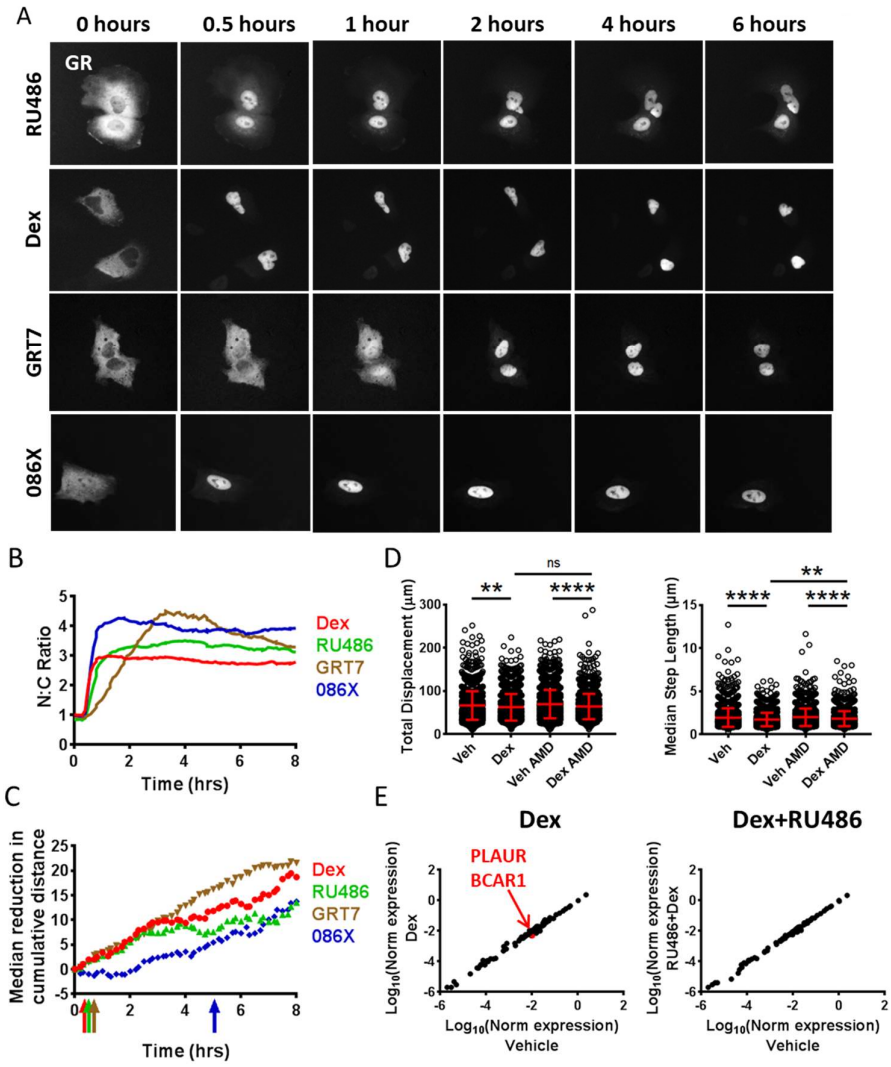

Figure 3.3: Ligand-specific regulation of migration kinetics. (A) Immunofluorescent widefield imaging of HaloTag-GR nuclear accumulation in A549 cells in response to 6 hours of dex (100nM), RU486 (100nM), GRT7 (3nM), and 086X (100nM) treatment. (B) Nuclear: cytoplasmic ratio of GR nuclear accumulation in response to potency-matched treatment of dex (100nM), RU486 (100nM), GRT7 (3nM), and 086X (100nM) over 8 hours. (C) Non-parametric rank-sum test of A549 cell migration (cumulative distance) signifying the earliest timepoint at which migration is statistically different in response to dex (100nM), RU486 (100nM), GRT7 (3nM), and 086X (100nM) compared to vehicle-treated controls. (D) Total displacement and median step length of A549 cells in response to 4 hours of vehicle or actinomycin D (AMD) pre-treatment (1µg/mL; 1 hour) and subsequent treatment with vehicle or dex (100nM). (E) RT^2 qPCR array of genes that regulate cell migration in response to 4 hours of dex (100nM), and a dex+RU486 (both 100nM) co-

treatment. Migration data represents quantification of two independent experiments (mean ± SD, one-way ANOVA, ****p<0.0001, **p=0.0227).

GC treatment rapidly stabilises microtubules

The rapid effect of dex on cell migration suggested cytoskeletal reorganization. Therefore, we screened the expression and activation status of a panel of cytoskeletal regulators (Fig 3.4A). Although changes in the phosphorylation of c-Src, Akt, and Ezrin/Radixin/Moesin (E/R/M) in response to dex were observed, these changes were only evident after 24 hours, long after the migration effects were seen (Fig 3.4B). However, we found a rapid increase (within 30 minutes) in the acetylation of α-tubulin, a marker of microtubule (MT) stability (Fig 3.4B). This was also seen after only 10 minutes dex treatment using immunofluorescence (Fig 3.4C).

To investigate further the actin and MT cytoskeletal networks we examined the effect of dex on MT dynamics using GFP-tagged MT plus-end (+TIP) binding protein, EB3 (Fig 3.4D). GC drives an increase in overall MT growth speed, consistent with stabilisation of microtubules (Fig 3.4E) (Applegate *et al.*, 2011; Matov *et al.*, 2010). There was a greater increase in medium- and high-speed microtubule growth in response to dex (Fig 3.4F) with concomitant reduction in low speed growth.

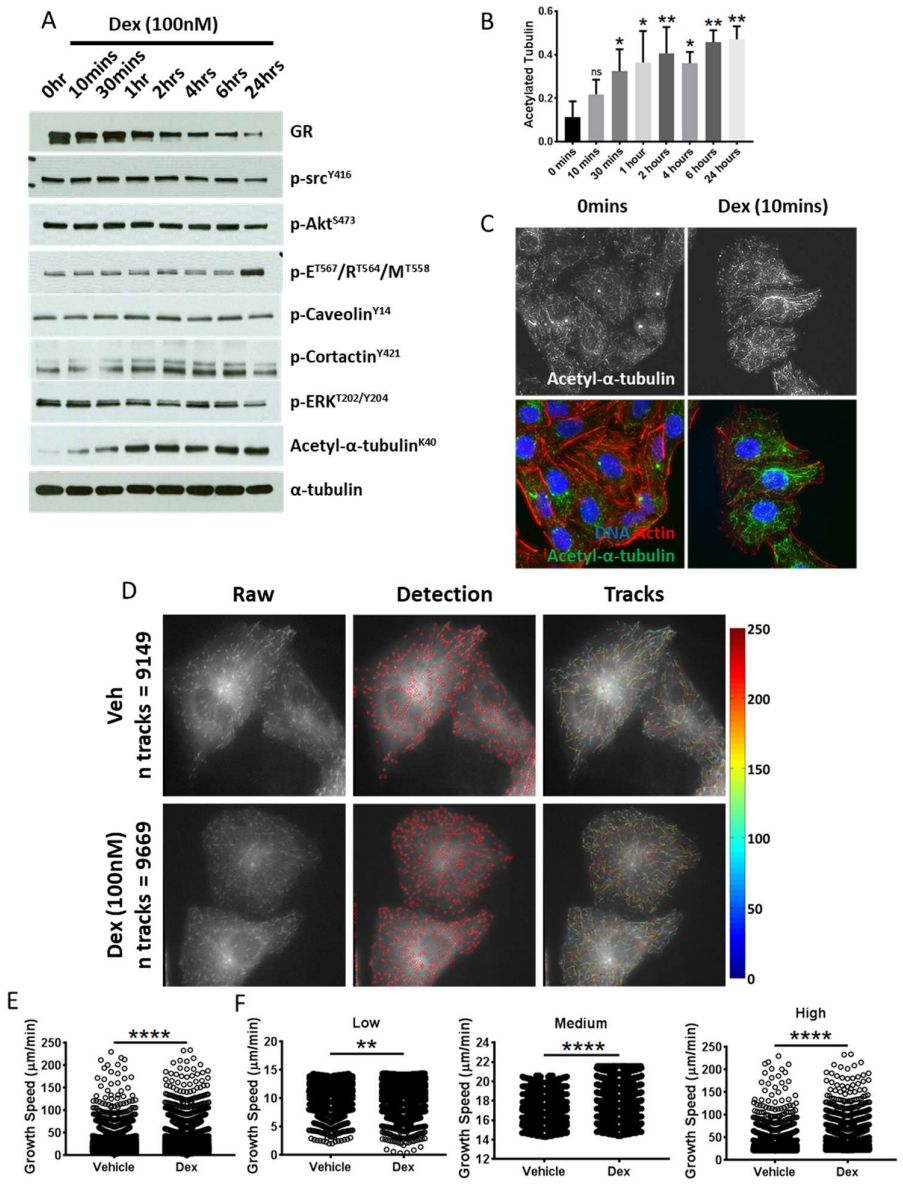

Figure 3.4: Glucocorticoids increase acetylation of α-tubulin to stabilise the microtubule network. (A) Total GR, phospho-Src^{Y416}, phospho-Akt^{S473}, phospho-Ezrin^{T567}/Radixin^{T564}/Moesin^{T558} (E/R/M), phospho-caveolin^{Y14}, phospho-cortactin^{Y421}, phospho-ERK$^{T202/Y204}$, acetyl-α-tubulin^{K40}, and total α-tubulin protein expression in response to dex (100nM) time series (0, 10 minutes, 30 minutes, 1 hour, 2 hours, 4 hours, 6 hours, and 24 hours). (B) Quantification of acetyl-α-tubulin western blot quantified over three independent experiments (mean ± SD, one-way ANOVA, *p=0.0228, **p=0.0025). (C) Immunofluorescent stain of acetyl-α-tubulin (green), F-actin (red), and DNA (blue) in A549 cells in response to 0 and 10 minutes of dex (100nM) treatment. (D) Raw images of EB3-GFP in A549 cells in response to 1 minute of vehicle and dex (100nM) treatment; detection by plusTipTracker (MATLAB) and microtubule growth speed tracks generated (colour-coded heat map). (E) Microtubule growth speed (μm/minute) in response to 1 minute of vehicle and dex (100nM) treatment. (F) Microtubule growth speed (μm/minute) in response to 1 minute of vehicle and dex (100nM) treatment, categorised into low-,

medium-, and high-speed growth. Number of EB3-GFP tracks analysed – vehicle (9149) and dex (9669) treated.

GC alters microtubule dynamics by inhibiting HDAC6

Acetylation of tubulin is tightly controlled by the α-tubulin acetyltransferase αTAT1 and the tubulin deacetylase HDAC6, making these two enzymes candidate effectors. We tested αTAT1 knockdown cells (Fig 3.5A), but found no effect on the GC-mediated inhibition of cell migration, suggesting an alternative mechanism of GR action (Fig 3.5B). Tubacin, a selective HDAC6 inhibitor, not only mimicked the inhibitory effect of dex (Fig 3.5C), but showed no additive effect in co-treatment protocols, suggesting convergent mechanism of action. Therefore, we analysed the effect of augmenting HDAC6 expression (Fig 3.5D), which increased both the displacement and median step length of cells and rendered cells resistant to GC (Fig 3.5E-G). Alpha stable distribution parameters changed in response to HDAC6 overexpression with cells adopting a higher proportion of large walk steps indicating increased cell migration relative to the controls, which was unchanged following administration of dex (Fig 3.5H). A pan-HDAC activator ITSA1 also reversed the GC migration phenotype (Fig 3.5I).

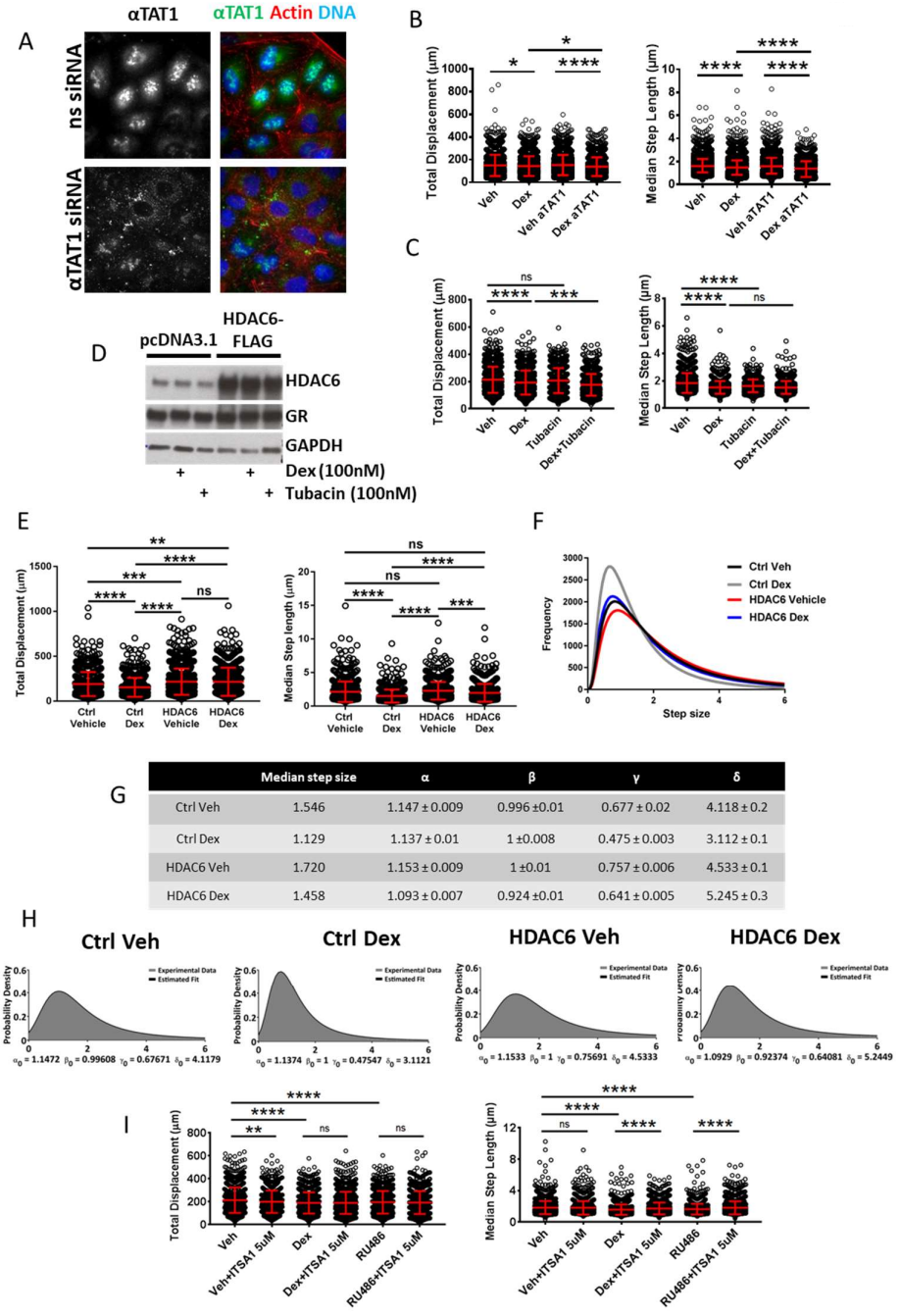

	Median step size	α	β	γ	δ
Ctrl Veh	1.546	1.147 ± 0.009	0.996 ±0.01	0.677 ± 0.02	4.118 ± 0.2
Ctrl Dex	1.129	1.137 ± 0.01	1 ±0.008	0.475 ± 0.003	3.112 ± 0.1
HDAC6 Veh	1.720	1.153 ± 0.009	1 ±0.01	0.757 ± 0.006	4.533 ± 0.1
HDAC6 Dex	1.458	1.093 ± 0.007	0.924 ±0.01	0.641 ± 0.005	5.245 ± 0.3

Figure 3.5: Glucocorticoids inhibit HDAC6 to regulate cell migration. (A) Immunofluorescent stain of αTAT1 (green), F-actin (red), and DNA (blue) in control and αTAT1 knockdown A549 cells. (B) Total displacement and median step length of control and αTAT1 knockdown A549 cells in response to 24 hours of vehicle and dex (100nM) treatment. (C) Total displacement and median step length of A549 cells in response to 24 hours of vehicle, dex (100nM), tubacin (100nM), and dex + tubacin co-treatment. (D) HDAC6 and GR protein expression in A549 cells transiently transfected with pcDNA3.1 (empty vector control) or HDAC6-FLAG treated ± 1 hour of dex (100nM) or tubacin (100nM). (E) Total displacement and median step length of control (H2B-GFP) and HDAC6 overexpressing (H2B-GFP + HDAC6-FLAG) A549 cells in response to 24 hours of vehicle

and dex (100nM) treatment. (F) Frequency distribution curves of control and HDAC6 overexpressing A549 cells in response to vehicle and dex (100nM) treatment. (G) Estimated alpha stable distribution parameters of control and HDAC6 overexpressing A549 cells in response to vehicle and dex (100nM) treatment. (H) Probability density function (PDF) of observed data and estimated parameters in response to vehicle and dex (100nM) treatment. (I) Total displacement and median step length of A549 cells in response to 24 hours vehicle, dex (100nM), RU486 (100nM), ITSA1 (5μM) + vehicle co-treatment, ITSA1 (5μM) + dex co-treatment, and ITSA1 (5μM) + RU486 co-treatment. Migration data represent quantification of at least three independent experiments (mean ± SD, one-way ANOVA, ****p<0.0001, ***p=0.0009).

GR and HDAC6 form a complex in the cytoplasm

There was no evidence of altered HDAC6 sub-cellular trafficking in response to dex with the enzyme remaining predominantly cytoplasmic (Fig S3.4A). Co-immunoprecipitation studies also failed to identify GR and HDAC6 in complex together (Fig S3.4B), despite previous reports of co-binding and interactive function on gene repression in the nucleus (Rimando et al., 2016; Govindan, 2010). However, we did detect a change in HDAC6 interactions with components of the cytoskeleton and saw increased association with actin in response to GC (Fig S3.4C).

To study the GR-HDAC6 interaction in further detail, we employed real-time fluorescence cross-correlation spectroscopy (FCCS) able to discriminate between cellular compartments (marked by crosses, Fig 3.6A). To investigate GR-HDAC6 interactions, as its more sensitive, and permits cell compartment localisation (marked by crosses, Fig 3.6A). We identify an increase in cytoplasmic interaction between GR and HDAC6 after dex treatment (Fig 3.6B), and measurable nuclear interaction post-dex (not present in vehicle treated controls), suggesting a change in HDAC6-GR interaction, particularly in the cytoplasm, and after GR ligand activation (Fig 3.6C-H).

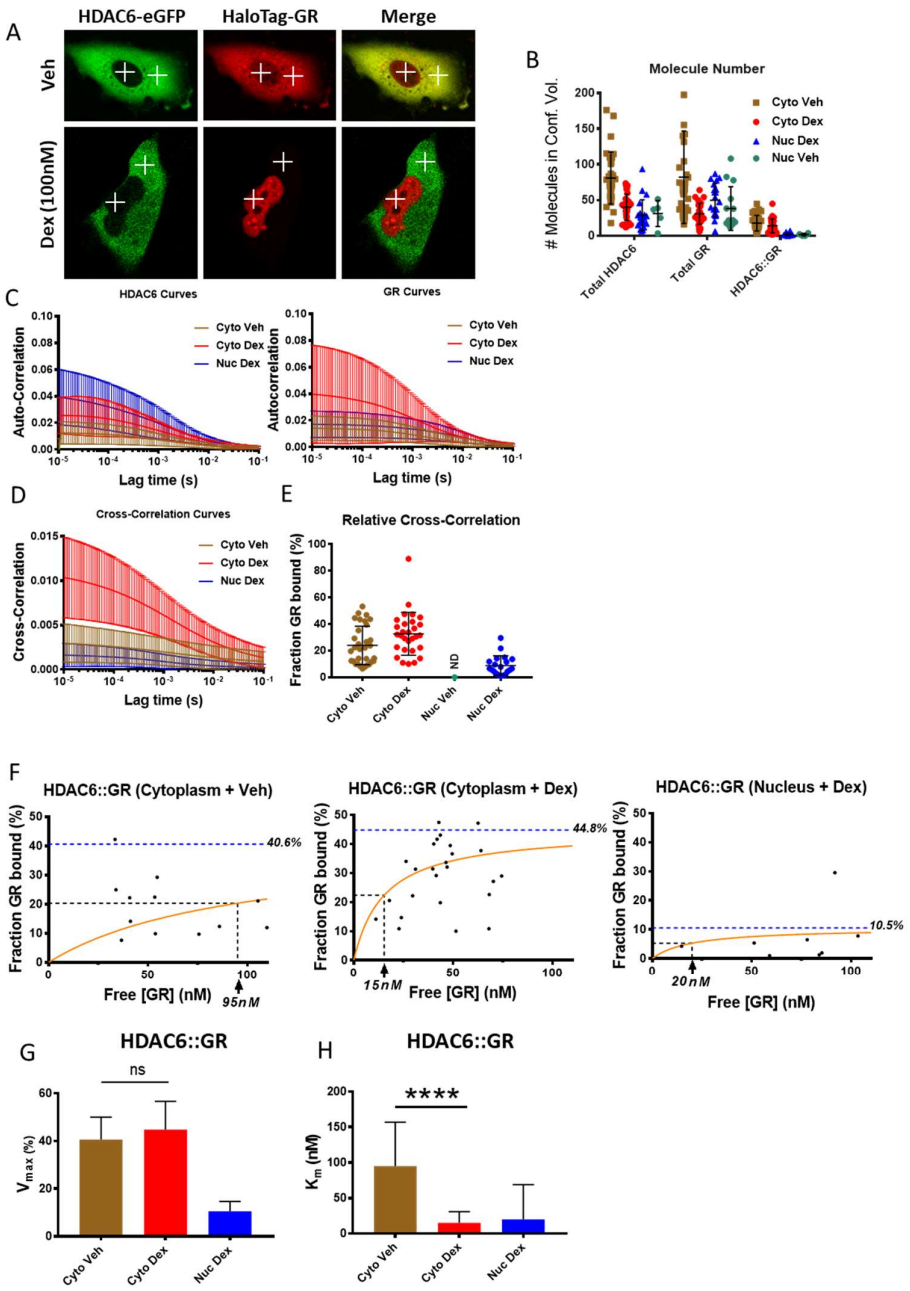

Figure 3.6: GR and HDAC6 interaction. (A) Confocal images of A549 cells co-transfected with HDAC6-eGFP and HaloTag-GR ± dex (100nM) for 1 hour. Confocal volumes designated for fluorescence cross-correlation spectroscopy (FCCS) measurements included as cross points (cytoplasm and nucleus). (B) Number of GR and HDAC6 molecules in response to vehicle and dex (100nM) within the cytoplasm and nucleus. (C) Autocorrelation curves of HDAC6 and GR in response to vehicle and dex (100nM) within the cytoplasm and nucleus. (D) Cross-correlation curves of HDAC6-GR interaction in response to vehicle and dex (100nM) within the cytoplasm and nucleus. (E) Relative cross-correlation of the fraction of GR bound to HDAC6 (%) in response to vehicle and dex (100nM) within the cytoplasm and nucleus. (F) Michaelis-Menten kinetics of the HDAC6-GR interaction in response to vehicle and dex (100nM) within the cytoplasm and nucleus. V_{max} (blue) and K_m (black) demonstrate

the strength of HDAC6-GR interaction. (G) V_{max} of HDAC6-GR interaction in response to vehicle and dex (100nM) within the cytoplasm and nucleus. (H) K_m of HDAC6-GR interaction in response to vehicle and dex (100nM) within the cytoplasm and nucleus. FCCS data represent quantification of three independent experiments from >30 cells. V_{max} and K_m displayed as mean ± SD (****p<0.0001).

3.5. Discussion

Although therapeutic GCs are widely used, their diverse actions limit long-term safety. Multiple candidate mechanisms of action have been advanced, with the major focus being how the same activated receptor can both repress and activate different genes in a cell-type specific context. Gene repression has classically been a focus of study, as this pathway appears to mediate the beneficial anti-inflammatory and immune suppressive actions of GCs. To this end, new partial agonist GR ligands have been developed and tested in the clinic. Such selective GR modulators (SeGRMs) differentiate GR function mainly by affecting the ligand-bound GR conformation, and thereby recruitment of co-modulators. However, GR can also affect other cellular processes through a non-transcriptional pathway, for example mitotic spindle function (Matthews et al., 2011). One major and consistent effect of GC treatment is loss of tissue integrity, and impaired wound healing. In part, this results from reduced epithelial, macrophage, and fibroblast migration (McDougall et al., 2006; Hardman et al., 2005). This programme has not received much attention but may serve as a model to understand the distinct actions of GCs. Therefore, we used an epithelial cell model to measure migratory responses to GC.

Our initial studies sought to mathematically model the walk properties of cells under basal conditions, to provide a solid baseline for GC comparison. Our cell walk characteristics fitted an alpha stable distribution, and the impact of GC altered the parameters in such a way that longer steps were selectively reduced in favour of shorter steps, thereby impairing the searching behaviour of cells. This real-time, individual cell tracking permitted the kinetics of response to be measured, and here the surprising finding was the very rapid onset of action with significant deviation from control cells within 40 minutes of treatment. This rapid onset of action was similarly seen with the GR antagonist RU486 and with

further non-steroidal ligands. That RU486 failed to oppose the agonist effects raised a question of specificity, which was addressed in siRNA studies in epithelial cells, and by replicating the migration assay in macrophages, which permitted genetic loss of GR to be tested. The rapid onset of effect, and paradoxical full agonist phenotype seen with RU486, suggested an unconventional mechanism of action, which was supported by showing that no new mRNA synthesis is required. We also employed selective GR ligands with well-characterised differences in GR nuclear translocation kinetics. Here we showed that rapid nuclear translocation did not associate with rapid inhibition of migration, but rather a GR ligand with a markedly slow GR translocation rate was still able to affect cell migration, even while predominantly residing within the cytoplasm. This is consequently a well-documented model of a truly non-genomic mechanism of GR action.

In pursuit of targets of the ligand-activated GR we turned to the cytoskeleton and found rapid induction of tubulin acetylation within 10 minutes of GC exposure. This was the earliest identified change in response to GC that preceded the inhibition of cell migration, with other changes requiring many hours of GC. Tubulin acetylation, a marker of microtubule stability (Hubbert et al., 2002; Boggs et al., 2015; Zhang et al., 2003), is tightly controlled by the dichotomous actions of the α-tubulin acetyltransferase-1 (α-TAT1) and the deacetylase HDAC6 (Castro-Castro et al., 2012; Liu et al., 2012). HDAC6 is localised predominantly in the cytoplasm where it directly interacts with microtubules and catalyses tubulin deacetylation along the length of the microtubule track (Asthana et al., 2013; Miyake et al., 2016). Moreover, HDAC6 has shown to prefer deacetylation of tubulin dimers over polymerized microtubules (Skultetyova et al., 2017).

Our studies identify a previous unrecognised mechanism of GR action with involvement of a protein-protein interaction circuit targeting HDAC6. We were able to show the HDAC6 dependence of the GC loss of long-step length migration and the rapid cellular response, coupled with a lack of requirement for new gene transcription pointed to a direct mechanism of action with a pathway connecting activated GR and the HDAC6 protein. We were not able to show HDAC6-GR interaction by co-immunoprecipitation, but FCCS studies identified a fraction of the

cytoplasmic HDAC6 pool as interacting with GR, with resultant changes in movement kinetics, implying a change in molecular complex formation. The unique cytoplasmic preference for GR amongst the nuclear receptors may explain its capacity to interact with cytoplasmic enzymes such as HDAC6. Our data support a GR-driven change in HDAC6 behaviour as the mechanism explaining rapid-kinetic loss of cell movement in response to GC exposure.

Defective cell migration in response to GC has widespread consequences including defective tissue repair, and loss of barrier function. Identification of a new mechanism of GC action has implications for attempts to design novel GR ligands, with reduced off-target effects, but also the screening for potent GR ligands capable to engaging this pathway to treat exuberant wound-healing, such as keloid.

The identification of a coherent non-genomic GR mechanism of action leading to a clinically relevant cell migratory phenotype offers new insight into the diversity of GC action. This pathway underlines the difficulty in developing specific anti-inflammatory GR ligands, exemplified by identical action of GR antagonists and agonists on cell migration. The reduced walk properties of epithelial cells are also observed in macrophages, providing a new insight into the anti-inflammatory and immune suppressive functions of GCs, which have largely been focused on chemokine production, adhesion molecule expression, cell survival, and enzyme production. Taken together we elucidate a newly discovered non-genomic pathway of GC action affecting cell migration, with proximal impacts on tissue integrity, repair, and innate immune function.

3.6. Acknowledgements

Special thanks to Peter March, Roger Meadows, and Steven Marsden for their help with the microscopy. Stephen Kershaw is supported by an MRC studentship. Bioimaging Facility microscopes used in this study were purchased with grants from the BBSRC, Wellcome Trust, and the University of Manchester Strategic Fund.

3.7. Supplementary Figures

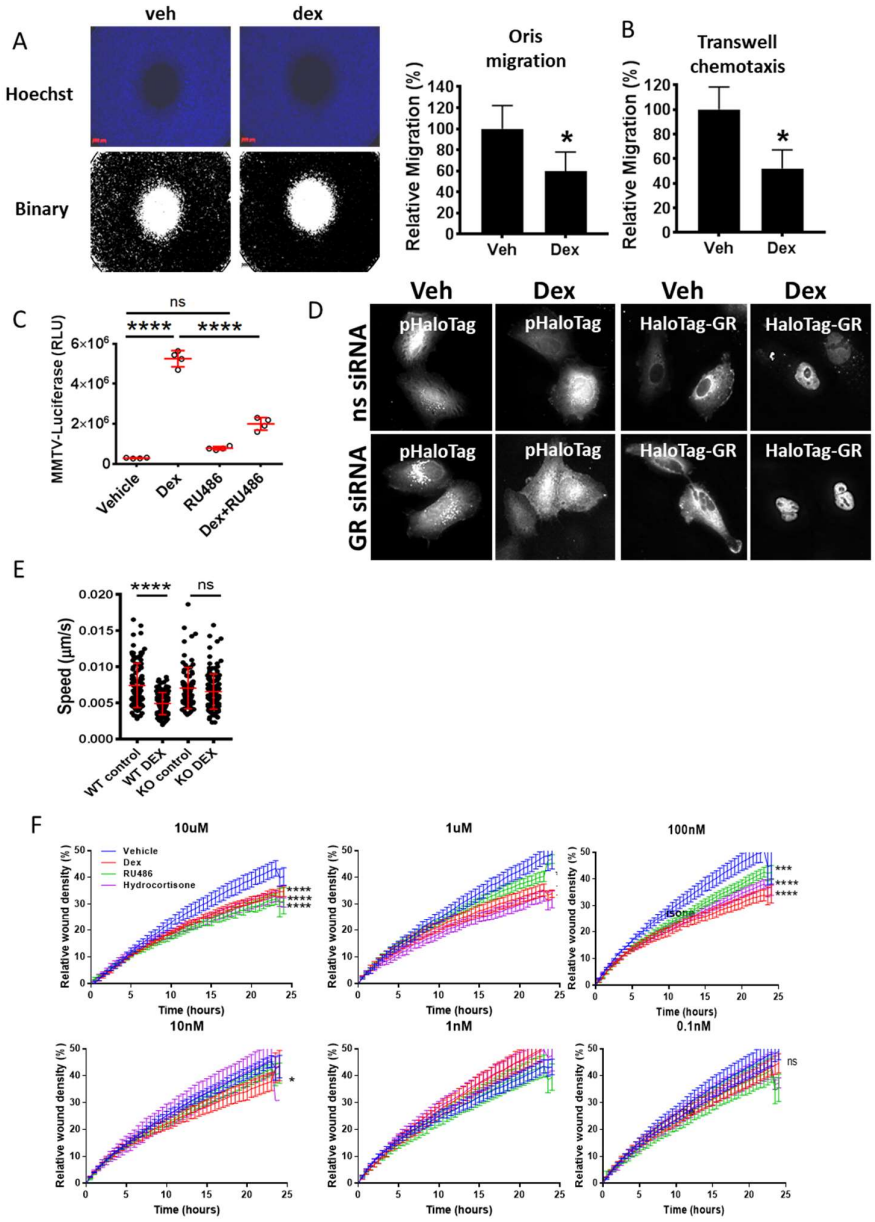

Figure S3.1: Glucocorticoids impair migration at a population level and reduce the motility of individual cells. (A) A549 cell migration in the Oris migration assay in response to 48 hours vehicle and dex (100nM) treatment quantified as relative migration (%) of A549 cells in response to 48 hours vehicle or dex (100nM) treatment. (B) Relative migration (%) of A549 cells using transwell chemotaxis migration assay in response to 48 hours vehicle or dex (100nM) treatment. (C) Transcriptional activation of the MMTV-luciferase promoter in response to 24 hours vehicle, dex (100nM), RU486 (100nM), and dex+RU486 treatment. (D) Confocal image of HaloTag-GR rescue in GR knockdown cells (using GR siRNA #11) in response to 1-hour vehicle or dex (100nM) treatment. (E) Speed (µm/s) of PECs from wild-type control and GR null mice in response to 24 hours vehicle or dex (100nM) treatment.

(F) Relative wound density (%) of A549 cells in response to 24 hours vehicle, dex, RU486, and hydrocortisone dose response (0.1nM, 1nM, 10nM, 100nM, 1μM, and 10μM) in a scratch wound healing assay. Oris and Transwell assay graphs represent quantification of at least 3 independent experiments (mean ± SD, *p<0.05, independent t-test). Migration data represents quantification of at least two independent experiments from >1000 cells (mean ± SD, ****p<0.0001). Scratch assay data represent quantification of at least two independent experiments (mean ± SD, *p<0.05 two-way ANOVA).

A

	Median step size	α	β	γ	δ
Veh	0.575	1.4935 ± 0.01	1	0.2475 ± 0.002	0.8091 ± 0.006
Dex	0.440	1.6537 ± 0.01	1	0.1899 ± 0.001	0.5541 ± 0.003

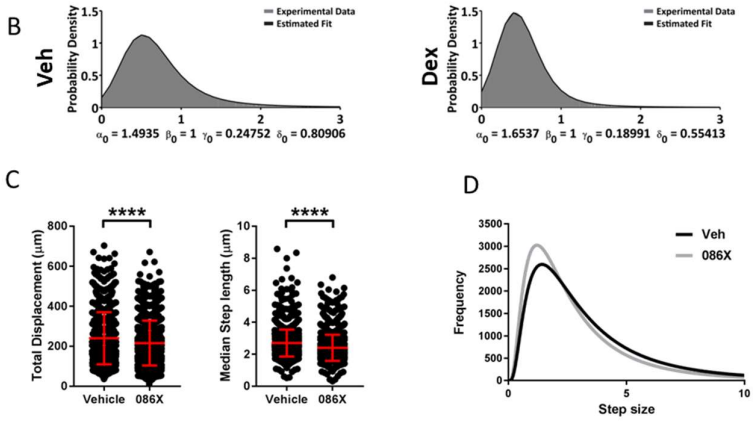

E

	Median step size	α	β	γ	δ
Vehicle	2.484	1.326 ± 0.01	1	1.057 ± 0.008	4.085 ± 0.06
086X	2.116	1.209 ± 0.009	1	0.898 ± 0.007	4.420 ± 0.1

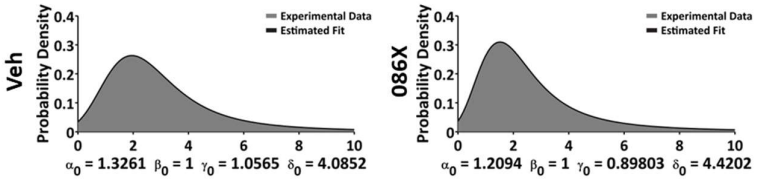

Figure S3.2: Changes in total net displacement following treatment of A549 cells with either conventional steroidal or selective ligands. (A) Estimated alpha stable distribution parameters of A549 cell migration in response to 48 hours vehicle and dex (100nM). (B) Probability density function (PDF) of observed data and estimated parameters in response to 48 hours vehicle and dex (100nM) treatment. (C) Total displacement and median step length of A549 cells in response to 24 hours of vehicle and GW870086X (086X, 100nM) treatment. (D) Frequency distribution curves of A549 median step length in response to 24 hours of vehicle and 086X (100nM) treatment. (E) Estimated alpha stable distribution parameters of A549 cell migration in response to 24 hours of vehicle and 086X (100nM) treatment. (F) Probability density function (PDF) of observed data and estimated

parameters in response to 24 hours of vehicle and 086X (100nM) treatment. Data represents three independent experiments, tracking data points from >1350 cells.

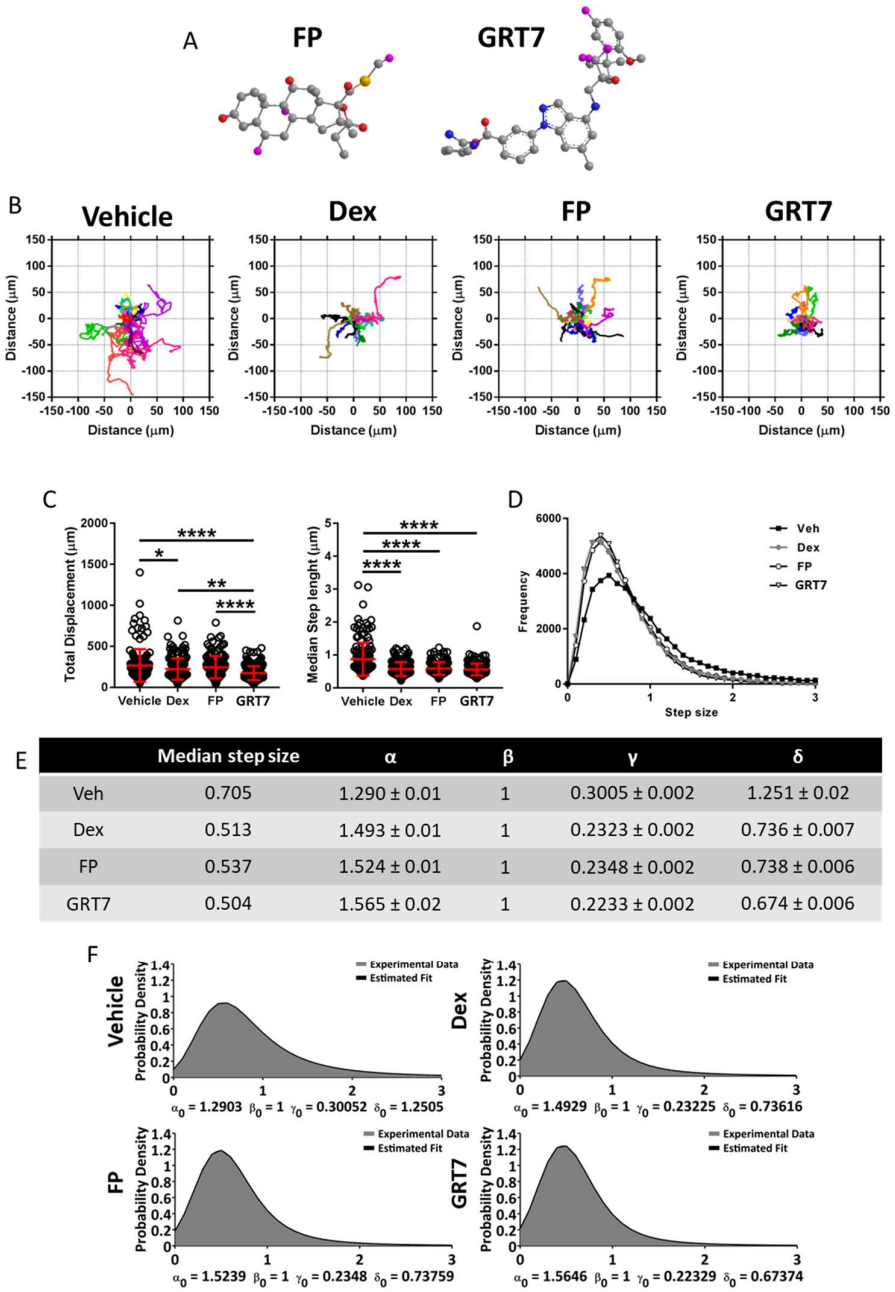

E

	Median step size	α	β	γ	δ
Veh	0.705	1.290 ± 0.01	1	0.3005 ± 0.002	1.251 ± 0.02
Dex	0.513	1.493 ± 0.01	1	0.2323 ± 0.002	0.736 ± 0.007
FP	0.537	1.524 ± 0.01	1	0.2348 ± 0.002	0.738 ± 0.006
GRT7	0.504	1.565 ± 0.02	1	0.2233 ± 0.002	0.674 ± 0.006

Figure S3.3: Comparison of the effects of steroidal and non-steroidal ligands on cell movement. (A) 3D chemical structures of fluticasone propionate (FP) and GRT7. (B) Rose plots of A549 cell displacement in response to 48 hours of vehicle, dex (100nM), FP (3nM), and GRT7 (3nM) treatment. (C) Total displacement and median step length of A549 cells in response to 48 hours of vehicle, dex (100nM), FP (3nM), and GRT7 (3nM) treatment. (D) Frequency distribution curves of A549 median step length in response to 48 hours of vehicle, dex (100nM), FP (3nM), and GRT7 (3nM) treatment. (E) Estimated alpha stable distribution parameters of A549 cell migration in response to 48 hours of vehicle, dex

(100nM), FP (3nM), and GRT7 (3nM) treatment. (F) PDF of observed data and estimated parameters in response to 48 hours of vehicle, dex (100nM), FP (3nM), and GRT7 (3nM) treatment. For observed data graphs represent >40,000 data points for each condition for >135 cells.

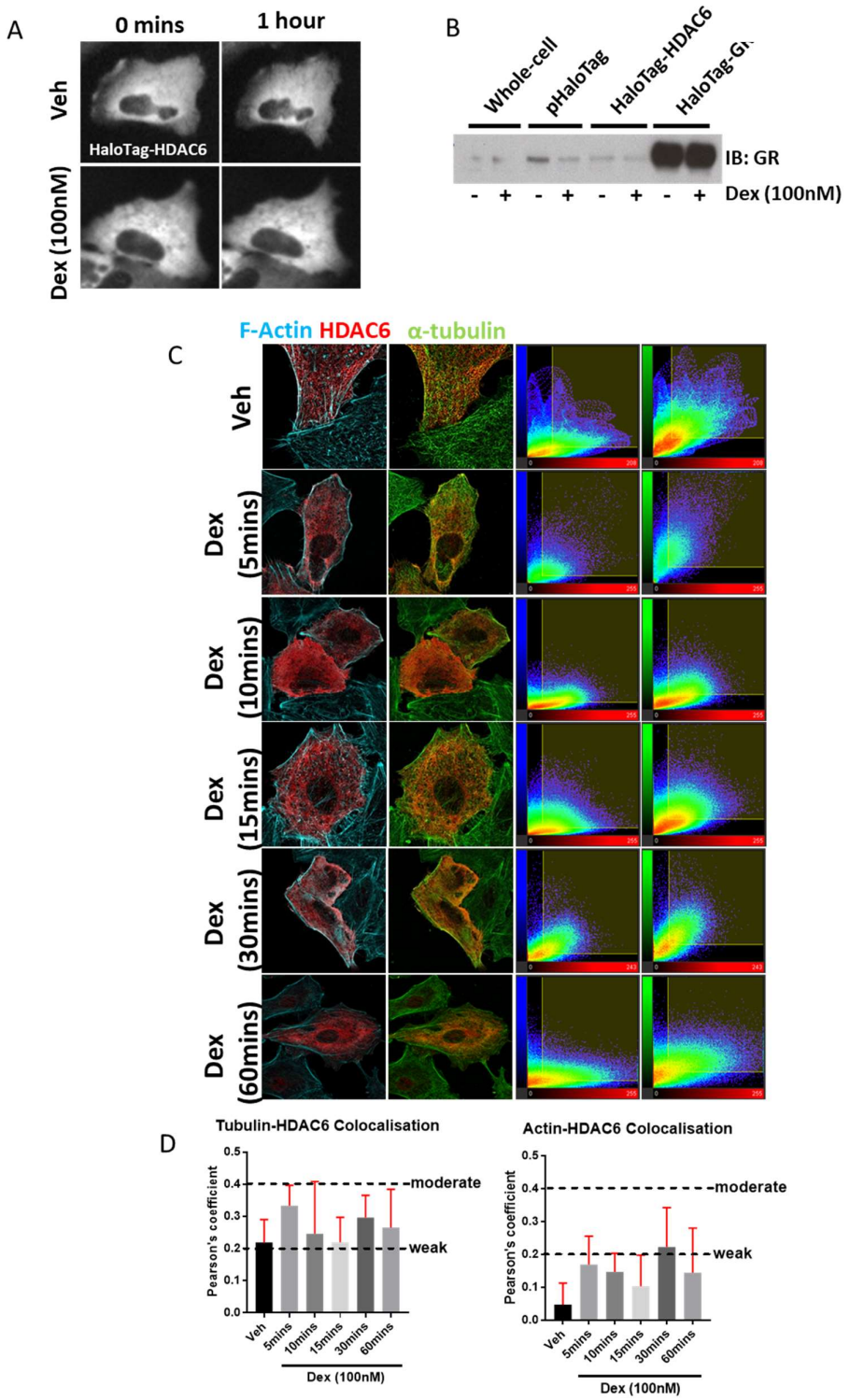

Figure S3.4: HDAC6-GR interaction and co-localisation with cytoskeletal architecture in response to glucocorticoid. (A) HaloTag-HDAC6 widefield immunofluorescence in A549 cells in response to 1hr vehicle and dex (100nM) treatment. (B) HaloTag pulldown from A549 cells transiently transfected with HaloTag-GR, HaloTag-HDAC6, or pHaloTag control and immunoblotted for GR and HDAC6 protein expression to demonstrate co-immunoprecipitation in response to 1 hour of dex (100nM) treatment. (C)

Confocal immunofluorescence of HDAC6 (red), F-actin (cyan), and α-tubulin (green) in A549 cells transiently transfected with HaloTag-HDAC6 and colocalisation analysis of HDAC6 v F-actin and HDAC6 v tubulin in response to dex (100nM) time series (5, 10, 15, 30, and 60 minutes). (D) Pearson's correlation coefficient of HDAC6-actin and HDAC6-tubulin colocalisation in response to dex (100nM) time series (0.2-0.4 as weak and >0.4 as moderate colocalisation).

Chapter 4: Non-Genomic Action of Glucocorticoids

Investigating the non-genomic effect of glucocorticoids on the cellular phosphoproteome

Stephen Kershaw[1], Pauline Pfänder[2], Toryn Poolman[1], Laura Matthews[3] & David Ray[1]

[1]Division of Diabetes, Endocrinology, and Gastroenterology, School of Biological Sciences, University of Manchester, Manchester, M19 3PT, [2]Institute of Comparative Molecular Endocrinology, Helmholtzstraße 8/1 89081 Ulm, [3]Nuclear Receptor Research Group, Faculty of Medicine and Health, University of Leeds, Leeds, LS2 9JT, UK

In preparation for submission to Scientific Reports (2018)

4.1. Abstract

Selective glucocorticoid receptor modulators (SeGRMs) are powerful tools in nuclear receptor research. SeGRMs can be used as tool compounds to differentiate glucocorticoid receptor (GR) biology based on conformational changes induced by ligand binding. We characterised a panel of tool compounds developed by GlaxoSmithKline (GSK) for potency and efficacy using luciferase-driven glucocorticoid response element promoter constructs, showing ligand-specific differences in GR transcriptional activity. Using live-cell imaging of fluorescent-labelled GR, we attribute differences in transcriptional potency to altered rates of GR nuclear accumulation initiated upon ligand binding. Rapid glucocorticoid effects (within 10 minutes) were tested using stable isotope labelling with amino acids in cell culture (SILAC)-based phosphoproteomics to characterise ligand-specific differences in GR non-genomic activity. Most differentially regulated phosphoproteins were shared amongst the tool compounds, with common proteins involved in chromatin remodelling and repression of RNA polymerase II, cytoskeletal organization, and induction of lipid raft-based endocytosis. Differentially-regulated phosphoproteins were validated by western blotting. This study demonstrates the importance of tool compounds in dissecting GR activity and further enhances our understanding of the non-genomic actions of glucocorticoids in cell biology.

4.2. Introduction

Synthetic glucocorticoids (GCs) are powerful anti-inflammatory agents used in the clinic to treat various inflammatory and autoimmune diseases (e.g. rheumatoid arthritis, asthma, COPD) (Lipworth and Menzies, 2005; Buttgereit and Burmester, 2016). However, long term GC therapy is compounded by the induction of severe side effects due to the pleiotropic actions of GCs on the ubiquitously expressed glucocorticoid receptor (GR). Such off-target effects include, but are not limited to, osteoporosis, impaired wound healing, hypertension, and hyperglycaemia (Vittorio and Werth, 2000; Moghadam-Kia and Werth, 2010; Ayroldi et al., 2014). Consequently, the pharmaceutical industries attempted to improve the therapeutic benefit of GCs by minimising off-target effects through the generation of "dissociated GCs" (Kuzmich et al., 2007; Ali et al., 2008; Razavi et al., 2014; Ripp et al., 2017; Miyoshi et al., 2016). The dissociated model is based on two distinct modes of transcriptional control; direct binding to GC response elements (GREs) followed by cofactor recruitment and transcriptional regulation (transactivation) and tethering to other DNA-bound transcription factors to inhibit their ability to regulate target genes (transrepression) (Dezitter et al., 2014; Schacke et al., 2004; Hudson et al., 2013).

Unfortunately, this model of GC action was too simplistic and failed to account for the transactivation of anti-inflammatory GREs including the glucocorticoid induced leucine zipper (GILZ) (Yang et al., 2017). Recent studies have also shown that GR directly regulates activation protein-1 (AP-1) recognition motifs without the need for tethering (Weikum et al., 2017). Furthermore, GCs elicit non-genomic effects that modulate kinase activity and the induction of parallel transcription factor signalling that regulates GR action over time. Nevertheless, of the compounds created with this model in mind, a select few have proven effective enough to enter clinical trials and demonstrate a reduced side effect profile. Of these, GW870086X (086X) appears to have promising application as a topical GC in the treatment of asthma, although its use is now restricted to topical application in the eye (Leaker et al., 2015; Stamer et al., 2013). Dissociated GCs can therefore be used as tool compounds to dissect GR activity and improve our understanding of GC molecular action. Ultimately this insight would help govern the design of

better GCs and minimise the negative side effects associated with prolonged GC therapy.

The aim of this study was to characterise the non-genomic action of tool compounds in an established human cell line by SILAC-based phosphoproteomics. Pharmacological properties of the tool compounds will be determined by luciferase reporter gene assay, while GR trafficking studies will ensure matched kinetics of GC response.

4.3. Methods

Materials

Dexamethasone (Dex; D1756), mifepristone (RU486; M8046), fluticasone propionate (FP; F9428) dimethyl sulfoxide (DMSO; #276855), phorbol 12-myristate 13-acetate (PMA; P8139), high glucose (4.5g/L) dulbecco's modified eagle's medium (DMEM) with L-glutamine, sodium pyruvate, and sodium bicarbonate (D6429) were purchased from Sigma. Heat-inactivated foetal bovine serum (FBS; F9665) and heat-inactivated charcoal-stripped foetal bovine serum (cFBS; #12676029) were purchased from Thermo Fisher Scientific (Life Technologies). HaloTag TMR Direct ligand (G852A) was purchased from Promega, UK. *Expression vectors*: pBOS-H2B-GFP (BD Bioscience), pHaloTag-GR (Promega), pMMTV-luciferase (AddGene), NRE-luciferase (AddGene).

Cell culture

Human lung epithelial carcinoma (A549) and human cervical cancer (HeLa) cells were cultured in a humidified environment (37°C, 5% CO_2) in high-glucose DMEM supplemented with 10% FBS or 10% cFBS for steroid-free conditions.

Reporter gene assay

HeLa cells were seeded at $5x10^4$ cells/mL in DMEM + cFBS (10%) into $10cm^2$ dishes and transiently transfected with 2µg mouse mammary tumour virus (MMTV) or NFκB response element (NRE) luciferase reporter genes using Fugene 6 (Promega; E2691) at a ratio of 3:1 (v/w) with DNA. 24 hours after transfection, cells were trypsinised and re-seeded in DMEM + cFBS (10%) into 24-well plates and left to adhere

overnight (37°C, 5% CO_2). Cells were treated as specified in the results and 18 hours later each well was washed twice with 1xPBS. Bright Glo (Promega, E2620) lysis buffer was added to each well according to the manufacturer's instructions. Cell lysates were read using a luminometer (Glomax, Promega). Ten 1-second reads were taken per well and the average RLU determined. IC_{50} and EC_{50} values were extrapolated from the resulting dose response curves using non-linear regression analysis in GraphPad Prism software, with the following equation:

Y=Bottom + (Top-Bottom)/(1+10^((LogIC50-X) * HillSlope))

Where X: log of dose or concentration; Y: Response; Top and Bottom: Plateaus; $LogIC_{50}$ interchangeable with $LogEC_{50}$; HillSlope: Slope factor or Hill slope, unitless.

GR trafficking

HeLa cells were seeded at $5x10^4$ cells/mL in DMEM + cFBS (10%) into glass-bottomed 24-well plates and left to adhere overnight (37°C, 5% CO_2). Cells were transiently co-transfected with 250ng HaloTag-GR and 250ng H2B-GFP using Fugene 6 (Promega; E2691) at a ratio of 3:1 (v/w) with DNA. 8 hours after transfection cells were labelled with HaloTag TMR Direct ligand (100nM, G2991, Promega) overnight (37°C, 5% CO_2). 24 hours after transfection, cells were washed once with DMEM + cFBS (10%) and live-cell imaging performed on a Pathway Bioimager 855 (BD) with laser autofocus and 10x/0.3 Uplan FLN objective. Images were collected every 5 minutes over 6 hours using the FITC and TRITC filter sets to visualise H2B-GFP and HaloTag-GR respectively. GR trafficking was captured in response to potency-matched drug treatment.

Stable isotope labelling with amino acids in cell culture (SILAC)

A549 cells were subjected to stable isotope labelling with amino acids in cell culture (SILAC) to generate "light", "medium", and "heavy" labelled cell lines. "Light" cells were labelled with L-arginine (Arg^0) and L-lysine (Lys^0), "medium" cells with L-arginine-U-$^{13}C_6$ (Arg^6) and L-lysine-$^2H_4$ (Lys^4), and "heavy" cells with L-arginine-U-$^{13}C_6$-$^{15}N_4$ (Arg^{10}), and L-lysine-U-$^{13}C_6$-$^{15}N_2$ (Lys^8). Three separate SILAC media were prepared per cell line (DMEM for SILAC; #88364; ThermoFisher Scientific) supplemented

with 10% dialyzed foetal bovine serum (#26400044; ThermoFisher Scientific) and appropriate amino acids. Cells were grown in the appropriate SILAC media for 10x doublings and L-arginine incorporation was tested in each cell line before further testing (>98%).

SILAC-based phosphoproteomics

SILAC-labelled cells were grown to sufficient quantities in 15cm^2 dishes and serum starved by washing twice in serum-free SILAC DMEM (SFM) and left overnight in SFM. "Light" cells were treated with vehicle (DMSO) control. "Medium" cells were treated with dex (100nM). "Heavy" cells were treated with GRT7 (3nM) or GW870086X (100nM). All ligands were made up in SFM. Cells were washed 3x in ice-cold 1xPBS and cells scraped into 1.5mL Eppendorf tubes, with cell pellets being collected by centrifugation at 2000xg for 10 minutes at 4°C and stored at -80°C. Cell pellets were re-suspended in 200µL guanidine hydrochloride lysis buffer (6M guanidine hydrochloride, 100mM Tris-HCl pH8.5, 10mM dithiothreitol [DTT], 40mM iodoacetamide – made up in MilliQ Ultrapure water) and heated at 95°C for 5 minutes, cooled on ice for 15 minutes, sonicated for 20-30 seconds at 30% amplification, and re-heated at 95°C for 5 minutes. Lysates were centrifuged at 3500xg for 30 minutes at 4°C, a 100µL aliquot transferred to a new 1.5mL Eppendorf tube, diluted 50% in MilliQ water, and precipitated by adding 4x volume of ice-cold (-20°C) 80% acetone and left overnight at -20°C. Precipitates were collected by centrifugation at 2000xg for 15 minutes at 4°C and washed 2x in -20°C 80% acetone, then air dried upside-down at room temperature for ~10 minutes (until acetone odor dissipated). Pellets were re-suspended in 500µL 2, 2, 2-trifluoroethanol (TFE) digestion buffer (10% TFE, 100mM ammonium bicarbonate) with sonication until a homogenous suspension was formed. Peptide concentrations were determined by Nanodrop, samples were diluted to equal concentration in TFE buffer, and samples stored at -80°C prior to processing. Peptides were processed using the filter-aided sample preparation (FASP) method (Hernandez-Valladares et al., 2016). Automated phosphopeptide enrichment was performed using a KingFisher Flex (ThermoFisher Scientific) magnetic particle-processing robot (Tape et al., 2014). TiO_2 (MR-TID002) and Ti-IMAC (MR-TIM002) magnetic microspheres were purchased from MagReSyn Biosciences.

Filter-aided sample preparation (FASP)

Microcon-20 columns were prepared and pre-washed with urea buffer (8M urea in 1M Tris-HCl) to check for leakages and flow-through discarded. 100µL sample was added per column and mixed with 100µL urea buffer to reduce SDS content in the samples. Tubes were centrifuged at 14000xg for 15 minutes and flow-through discarded. Samples were washed in another 200µL urea buffer. Samples were alkylated in 100µL of 50mM iodoacetamide (Sigma, 144-48-9), mixed at room temperature on a thermoshaker for 1 minute at 650RPM, and stored in the dark for 20 minutes at room temperature. Tubes were centrifuged and washed twice in urea buffer as stated above. Samples were washed three times in 100µL of 50mM NH_4CO_3 and centrifuged at 14000xg for 10 minutes. Samples were digested in 1µg trypsin in 50mM NH_4CO_3 per 200µg sample, mixed at 650RPM for 1 minute (wrapped in parafilm) and left to incubate at 37°C overnight. Filter units were transferred to new collecting tubes and agitated for 1 minute at 650RPM to homogenise peptides. Tubes were centrifuged at 14000xg for 5 minutes and washed three times in 50µL of NH_4CO_3. Samples were treated with 50µL of 0.5M NaCl and centrifuged as above. Samples were transferred to low-bind tubes and peptide concentration determined by NanoDrop. Samples were frozen at -80°C overnight. Samples were acidified in 10% TFA to a final concentration of 0.5% TFA and desalted in 0.1% formic acid and 0.1% formic acid in 80% acetonitrile (ACN) as the binding and elution buffers respectively.

Digested samples were analysed by LC-MS/MS using an UltiMate® 3000 Rapid Separation LC (RSLC, Dionex Corporation, Sunnyvale, CA) coupled to a Q Exactive HF (Thermo Fisher Scientific, Waltham, MA) mass spectrometer. Peptide mixtures were separated using a multistep gradient from 95% A (0.1% FA in water) and 5% B (0.1% FA in acetonitrile) to 7% B at 1 min, 18% B at 58 min, 27% B in 72 min and 60% B at 74 min at 300 nL min^{-1}, using a 75 mm x 250 µm i.d. 1.7 □M CSH M-Class C18, analytical column (Waters). The top 8 precursors were selected for fragmentation automatically by data dependant analysis during each cycle.

LC-MS/MS

Quantification was performed using MaxQuant (Tyanova et al., 2016) and phosphoproteomics data was interpreted using Perseus software (Tyanova et al., 2016). SILAC ratios were determined by normalising against vehicle-treated controls (H/L; M/L). Identified phosphopeptides were filtered based on a $\log_2$ fold change >0.2 or <-0.2 to focus on those differentially-regulated by GC. In addition, SILAC ratios were filtered for contaminants and by localization probability <0.75. Linear motifs and site-specific sequences were added in Perseus using publicly available datasets from PhosphoSitePlus (https://www.phosphositeplus.org). Samples were grouped according to GC treatment and phosphopeptides were filtered based on valid values (minimum of 2 values per group).

Statistical analysis

Statistical tests were performed using GraphPad Prism 7 software, with data represented as mean ± SEM unless otherwise stated. Experiments were performed in triplicate unless stated otherwise in the results.

4.4. Results

Selective glucocorticoids exhibit unique transcriptional activity

Luciferase reporter gene assays were used to assess the transcriptional activity of a panel of selective GCs (GRT1-11 and GW8700086X) alongside conventional steroids (dexamethasone, fluticasone propionate, prednisolone). The pMMTV-GRE luciferase was used to test transactivation and the NRE-luciferase for transrepression by inhibiting the action of the pro-inflammatory cytokine NFκB. HeLa cells were transiently transfected with each expression vector and a dose response of each ligand was tested against both promoters (Fig 4.1A-B). NRE-luciferase-transfected HeLa cells were pre-treated for 1 hour with 5nM of phorbol 12-myristate 13-acetate (PMA) as an inflammatory stimulus to induce NFκB expression prior to treatment with GCs. Resulting dose response curves were subjected to non-linear regression analysis to determine IC_{50} and EC_{50} values for each ligand, showing distinct ligand-specific differences in transactivation and transrepression (Table S4.1). Interestingly, the

selective GR modulator 086X demonstrated reduced efficacy whilst retaining the same potency as dex at the NRE promoter (Fig 4.1B). Of note, GRT1 did not demonstrate transcriptional activity at the NRE-Luc promoter nor GRT2 at the MMTV-Luc promoter. In addition, GRT1, GRT3, and GRT5 induced minimal activity at the MMTV-Luc promoter. This suggests that conformational changes in GR structure adopted upon ligand binding have profound effects on GR activity. Elucidating the reason behind this relationship would provide a greater insight into the pathways selective GCs induce (or bypass) to prevent induction of off-target effects.

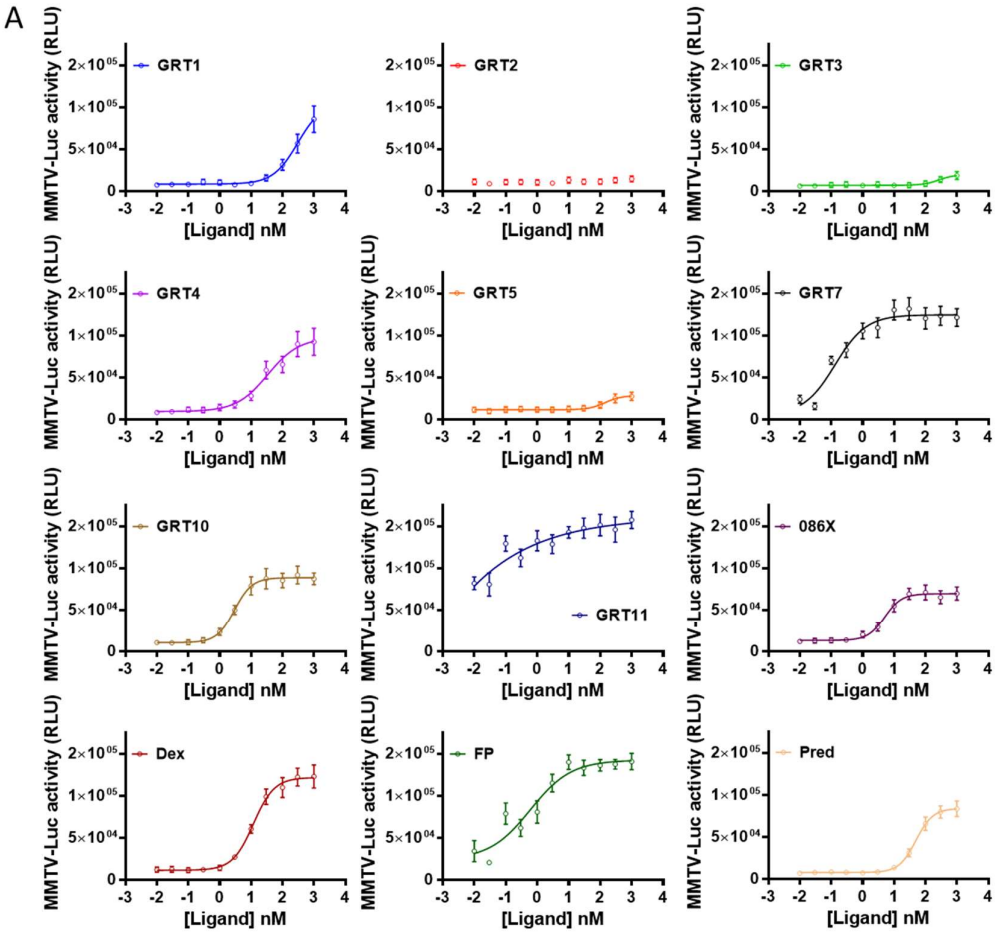

Figure legend on the next page.

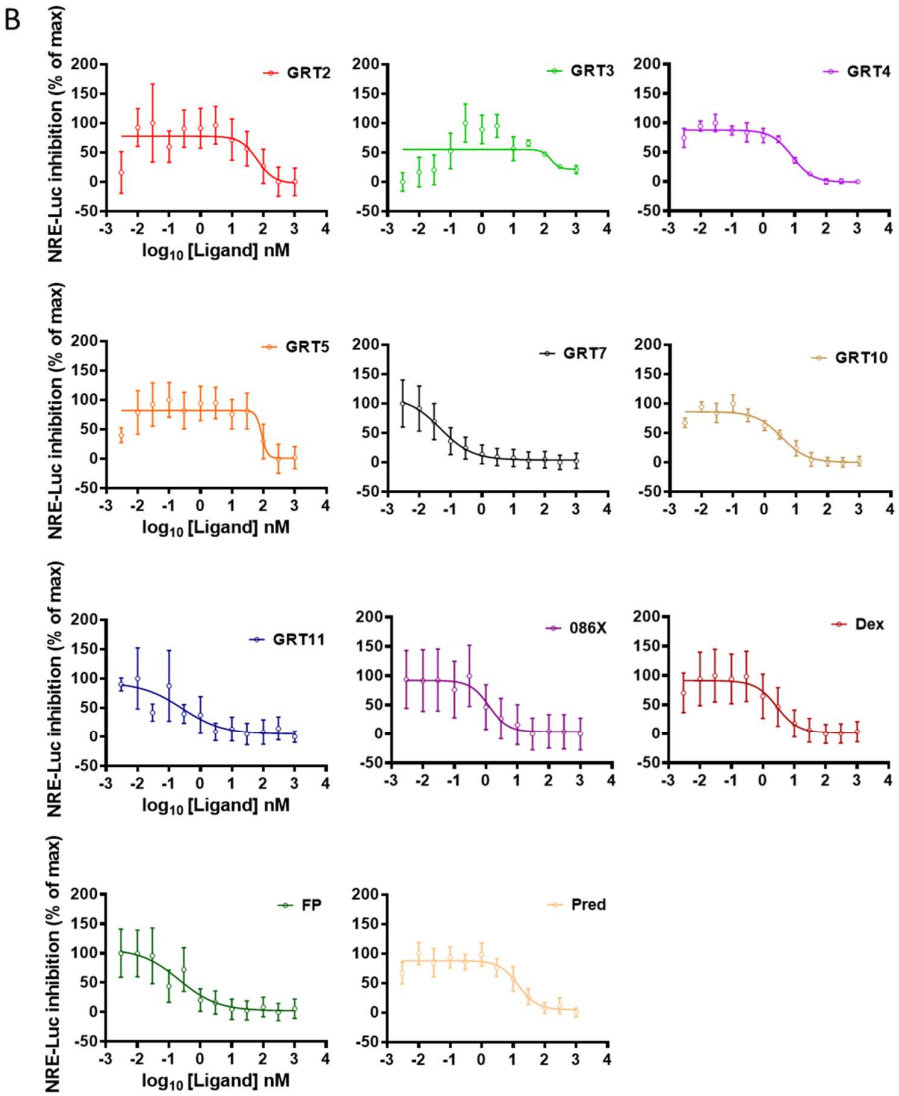

Figure 4.1. Tool compounds have varied effects on glucocorticoid-responsive luciferase promoter genes. (A) Luciferase reporter gene assay using HeLa cells transiently transfected with mouse mammary tumour virus (MMTV)-Luc reporter plasmid. Cells were transfected over 24 hours, re-seeded, and treated overnight with a dose-response of tool compounds (0.003nM, 0.001nM, 0.03nM, 0.01nM, 0.3nM, 0.1nM, 1nM, 3nM, 10nM, 30nM, 100nM, 300nM, 1μM). Cells were lysed using the Promega dual-luciferase assay kit and MMTV-Luc activity read on a 565nm plate reader as relative light units (RLU). (B) Luciferase reporter gene assay using HeLa cells transiently transfected with NFκB-response element (NRE)-Luc reporter plasmid. Cells were transfected over 24 hours, re-seeded, and pre-treated with 5nM PMA to induce NFκB activity. Cells were treated overnight with a dose-response of tool compounds (same as above). Cells were lysed as above, and NRE-Luc activity read on a 565nm plate reader (RLU). Graphs display an average of three independent experiments.

Ligand-specific differences in transcription due to altered rate of GR nuclear accumulation

Upon ligand binding, the GR undergoes a ligand-specific conformational change resulting in its accumulation within the nucleus. This nuclear translocation is facilitated by the dynein motor protein moving the GR along microtubule filaments. Recent evidence has shown this to involve regulation of microtubule dynamics through inhibition of HDAC6, the primary deacetylase for α-tubulin (lysine-40) (Kershaw *et al*., 2018, unpublished). The rate of GR nuclear accumulation thus has downstream effects on its activity within the nucleus and regulation of GR-target genes. GR trafficking was visualised by live-cell microscopy using HeLa cells transiently transfected with and a HaloTag-GR (labelled with a rhodamine-tagged Halo ligand) expression vector. Glucocorticoids were tested potency-matched at a saturating concentration (10x IC_{50}) to ensure appropriate GR transcriptional activity. Most ligands inducing total GR translocation after 30-60 minutes of administration. However, the potent non-steroidal GRT7 caused a significant delay in GR translocation with total accumulation occurring 4 hours after administration (Fig 4.2). This shows that glucocorticoid potency at glucocorticoid-responsive promoters is dependent on GR nuclear translocation, which dictates the time of GR nuclear occupancy and transcriptional activity.

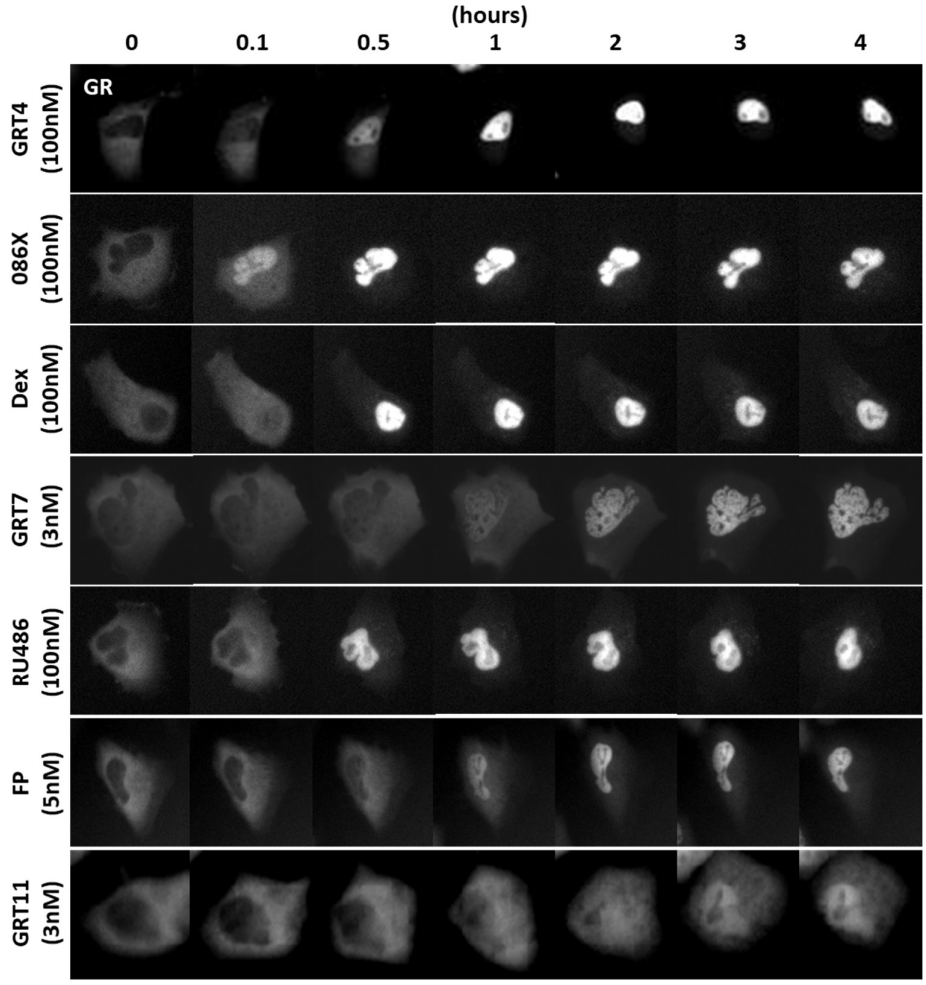

Figure 4.2. Potency-matched glucocorticoids induce differential rates of GR nuclear trafficking. Representative images of HeLa cells transiently transfected with HaloTag-GR and treated with potency-matched glucocorticoids treatment over 4 hours captured with live-cell widefield microscopy. Images are representative of two independent experiments.

SILAC-based phosphoproteomics of early GCs

The GR can interact with cytoplasmic proteins to initiate non-genomic effects, the full scope of which has yet to be fully determined. We investigated the early effect of GCs *in vitro* by comparing the phosphoproteome of A549 cells pre-treated with non-steroidal and conventional GR agonists. A rapid treatment of glucocorticoids was employed to elicit a non-genomic response in the GR. The activity of proteins induced by a short treatment with potency-matched glucocorticoids (10 minutes) was determined using triple-labelled SILAC-

based phosphoproteomics. This timepoint was chosen to ensure GR sub-cellular localisation was predominantly within the cytoplasm (Fig. 4.2). A549 cells were used as a more appropriate *in vitro* established cell line model over HeLa cells due to pre-existing RNA-seq and ChiP-seq datasets (Himes et al., 2014; Vockley et al., 2016). Glucocorticoid treatments were determined based on SILAC label, with medium (Arg^6/Lys^4)-labelled cells treated with dex (100nM) and heavy (Arg^{10}/Lys^8)-labelled cells treated with either GRT7 (3nM) or 086X (100nM). Light (Arg^0/Lys^0)-labelled cells were treated with vehicle control.

We identified 1870 unique phosphopeptides from triplicate samples, which were log_2-transformed [(log_2(H/L) or [(log_2(M/L)]. Of these, 24.9% were differentially-regulated by GCs (n=465) (Fig 4.1A).3110 phosphorylation events were identified in response to GC, with the majority of phosphorylations occurring at serine residues (n=2706; 87%), and threonine (n=390; 12.54%) and tyrosine (n=14; 0.45%) in the minority (Fig 4.3B). Of the phosphosites regulated by GC, 38.42% were single phosphorylation (n=1195), 49.16% were double phosphorylation (n=1529), and 12.41% were triply phosphorylated (n=386) (Fig 4.3C). Sample correlation plots indicate a good degree of positive correlation, between replicate samples (Fig S4.2A-B). Hierarchical clustering analysis shows that individual GC treatments cluster together, although there appears to be a degree of similarity across all three replicates (Fig S4.3). This suggests that the differentially regulated phosphopeptides we observed are engaged by all GCs to a similar extent. However, we also observe subtle ligand-specific differences in phosphorylation frequency amongst the shared GC-regulated phosphopeptides, albeit to a lesser frequency. This likely reflecting changes in GR conformation induced by ligand binding (Fig 4.3D). Such changes do not appear to affect the total number of phosphorylated proteins, meaning that the interaction between the GR and target proteins is unperturbed.

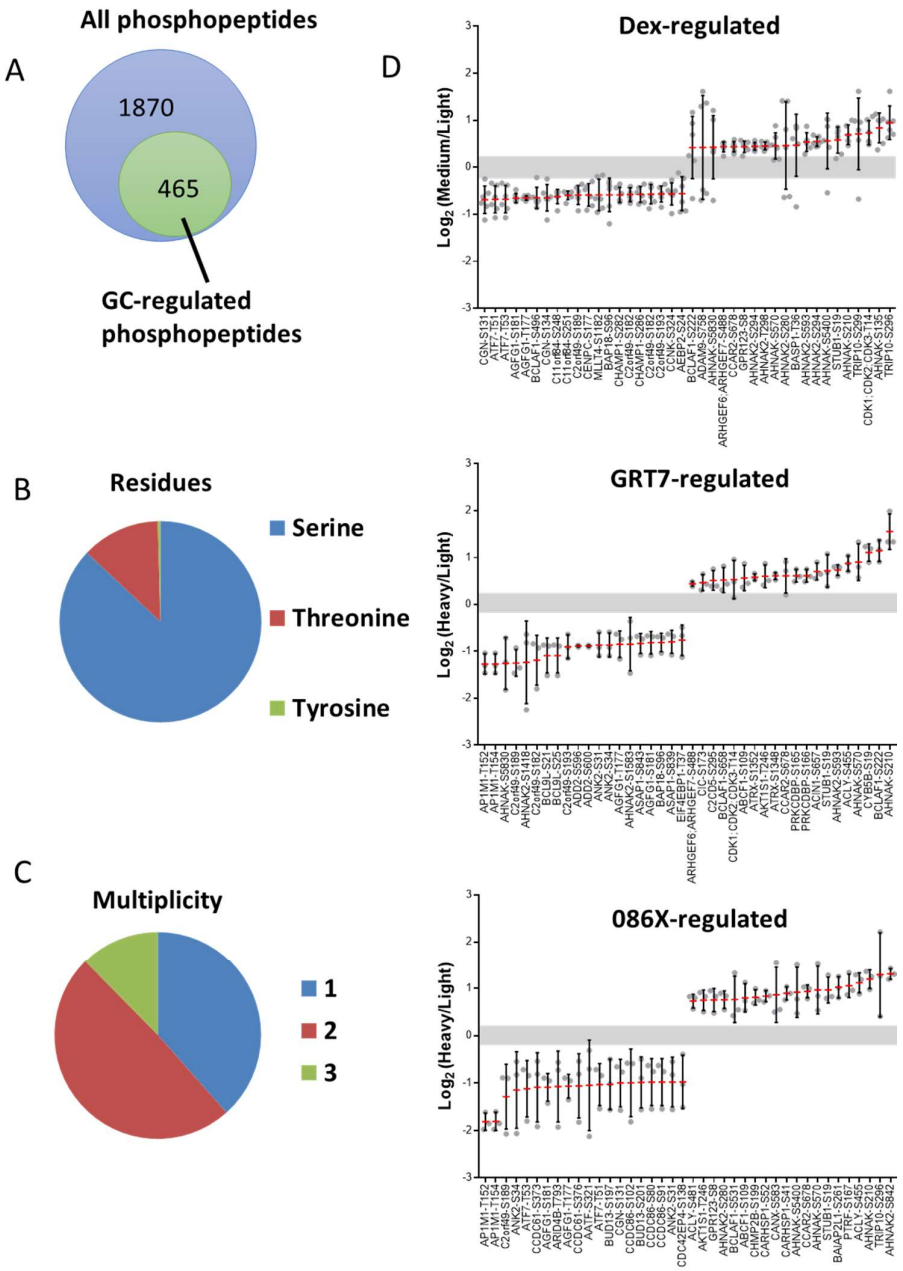

Figure 4.3. Differentially-regulated phosphoproteins by 10 minutes of GC. (A) Venn diagram displaying the distribution of identified phosphoproteins in response to dex (100nM), GRT7 (3nM), 086X (100nM), or vehicle control. (B) Pie chart of phosphorylated residues in response to GC; serine (blue), threonine (red), and tyrosine (green). (C) Pie chart of the number of peptide phosphorylations in response to GC; 1 (blue), 2 (red), or 3 (green). (D) Examples of phosphorylated proteins and associated phosphosites up- or down-regulated by GCs. Grey lines indicate the $\log_2$ ratio cut-off <0.2 and <-0.2. Data is displayed as median ± SD and representative of triplicate samples.

Pathway analysis was performed using gene ontology (GO) enrichment-based clustering to characterise the protein-protein interaction network (Fig 4.4A), cellular components, and enriched motifs of GC-regulated phosphopeptides (Fig 4.4B-C). Most differentially regulated phosphoproteins were similar between the ligands. The targets of these phosphoproteins can be separated into three sub-cellular compartments – nucleus, cytoplasm, and plasma membrane.

PPIHub network visualised key nodes of protein-protein interactions in response to GC, with ribosomal s6 kinase (RSK) linking to the highest number of other proteins (Fig 4.4A). Cellular component gene ontology analysis highlighted the cyclin-dependent kinase network (CDK12-CDK13-CKY), which phosphorylates and suppresses RNA polymerase II transcription machinery (Liang et al., 2015; Li et al., 2016) (Fig S4.4). Additional regulators of RNA polymerase II included AFF4, BAZ23, CCAR2, and CHD8, all of which inhibits RNA polymerase II activity (Kuzmina et al., 2014; Magni et al., 2015; Rodriguez-Paredes et al., 2009). Phosphorylation of RNA polymerase II C-terminal domain was significantly up-regulated by GC using Enrichr, suggesting a strong response to GC occurs within the nucleus even before nuclear translocation of the GR (Fig 4.4C).

Chromatin modifying proteins were also differentially regulated by glucocorticoids, including CHAF1B, BRD3, CHD3, and CHD9 (Volk and Crispino, 2015; Wai et al., 2018; Smith et al., 2018; Salomon-Kent et al., 2015). This suggests that additional mechanisms are activated by the GR with genome-wide consequences. This indirect mode of action may explain some of the diversity of GC actions and the regulation of gene expression despite the lack of GR recruitment to related chromatin.

Plasma membrane proteins were also identified, including caveolin-1 and its associated lipid raft proteins cavin-1, cavin-2, and cavin-3. Proteins involved in pinocytosis and membrane invagination were amongst the most enriched components, highlighting a strong response in the plasma membrane to GC. Phosphorylation of caveolin-1 by GCs has already been demonstrated, with downstream induction of GSK3β and regulation of cell cycle progression (Matthews et al., 2008). Additionally, lipid rafts and caveolin-1 are required for the endocytosis of a variety of plasma membrane proteins and ligand-inducible receptors, including Nox2, IL-

1βR, Rab5, beta1 integrins, and the muscle repair protein dysferlin (Oakley et al., 2009; Hagiwara et al., 2009; Shi and Sottile, 2008; Hernandez-Deviez et al., 2008). The G-protein-coupled receptor GPR123 was also identified as a commonly phosphorylated protein by all glucocorticoids. Interestingly, GPR123 is a member of the transmembrane GPCRs which induce intracellular signalling cascades upon ligand binding to the extracellular receptor surface, although GPR123 is an orphan receptor with relatively unexplored biology. Another GPCR, GPR30, is more characterised and binds extracellular oestrogen to initiate rapid intracellular oestrogen-dependent kinase activation and transcriptional activity (Gonzalez de Valdivia et al., 2017; Noel et al., 2009; Prossnitz et al., 2008). Consequently, it would be interesting to investigate the role of GPR123 as a transmembrane glucocorticoid receptor and whether GPR123 binds extracellular glucocorticoids to elicit GR-dependent genomic and non-genomic actions. Taken together, this may describe the mechanism of GC transmembrane entry which has classically been attributed to diffusion across the lipid bilayer.

Motif enrichment analysis highlighted key nodes regulated by GC, including GSK3, ERK1, ERK2, PKA, PKC, and the 14-3-3 domain binding motif (Fig S4.5). These enzymes function downstream of the epidermal growth factor receptor (EGFR) and other G-protein-coupled receptors (GPCRs) to initiate their respective intracellular signalling cascades. This coincides with the Enrichr Wikipathways analysis highlighting EGFR signalling and GPCR signalling as the pathways most significantly regulated by GC (Fig 4.4B). This suggests that the GR may interact with these plasma membrane-bound receptors, or at least their downstream effectors, to modulate cellular signalling pathways.

Actin filament capping, which occurs at the free barbed ends, is a major determining factor of actin elongation and thus actin dynamics (Kuhlman, 2005). Here we see a strong response to actin capping in response to GC (Fig 4.4C), which is likely achieved through down-regulation of cofilin-1 at serine-3, an actin depolymerizing factor that controls actin filament turnover (Ressad et al., 1999). Therefore, GCs may rapidly stabilise the actin network by inhibiting the activity of cofilin-1 (Sumi et al., 1999). Moreover, we show reduced phosphorylation of CAP1 at serine-308 and serine-310, which complexes with cofilin-1 and actin to regulate actin

capping (Zhou et al., 2014). The stabilisation of actin in response to GC mirrors the stabilisation of microtubules demonstrated in the earlier results chapter. This suggests that GCs rapidly alter the dynamics of both cytoskeletal components, likely to facilitate its entry into the nucleus in response to ligand binding.

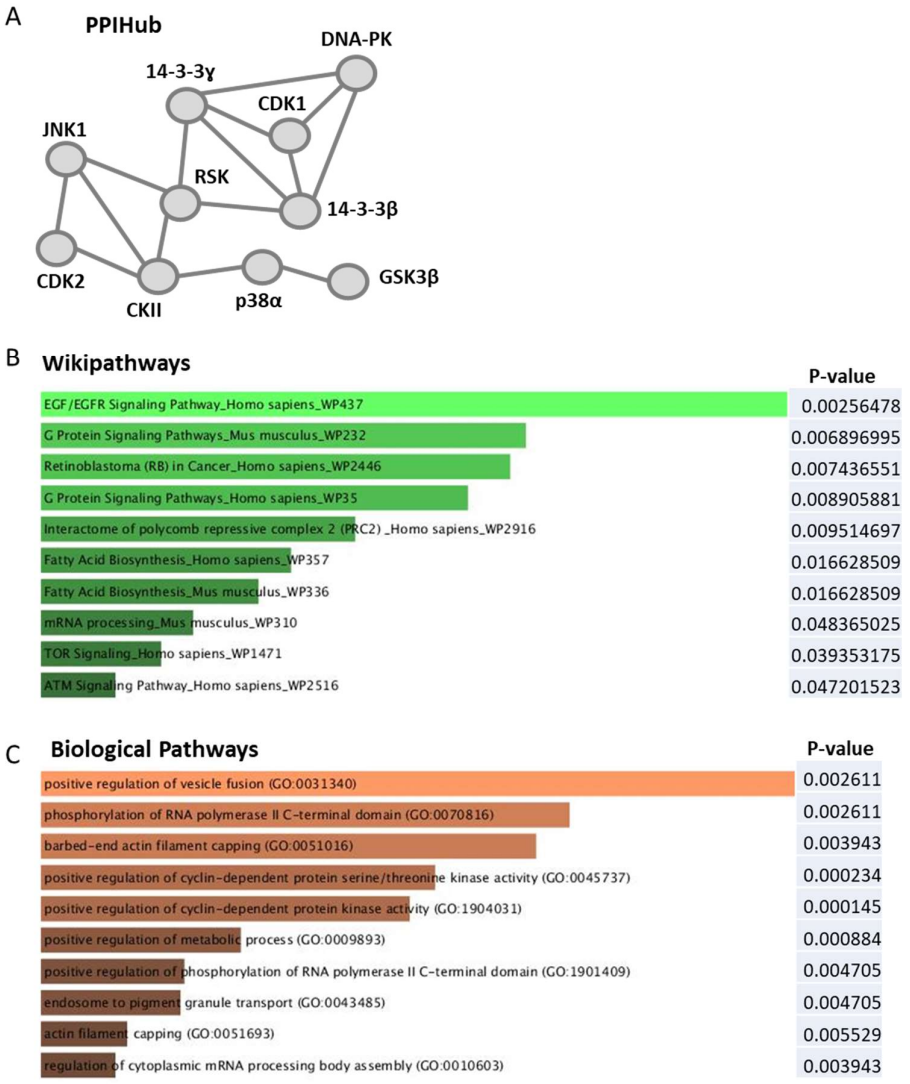

Figure 4.4. Pathway analysis of rapid glucocorticoid SILAC phosphoproteome. (A) Protein-protein interaction network of GC-regulated phosphopeptides shared amongst all three GR agonists, generated using STRING (B) SILAC phosphoproteomics data

Validation of GC-regulated phosphopeptides

Validation of select phosphoproteins was done using immunoblotting of both phosphorylation and total protein expression levels in pre-treated

A549 cells (Fig 4.5). These targets were chosen based on sub-cellular distribution (plasma membrane, cytoplasm, or nucleus) to provide a comprehensive validation of GR activity. A brief time course of dex was used to mirror the conditions used for the SILAC phosphoproteomics analysis. We observed a time-dependent increase in the phosphorylation of 14-3-3 binding motif, cdc2, caveolin-1, and the GR at two commonly regulated sites. Dephosphorylation of the largest RNA polymerase II subunit (RpB1) at serine-2 and PRAS40 was also observed in a time-dependent manner. Regulation of protein phosphorylation occurred rapidly after GC administration, suggesting that the activated GR is engaging with a select group of cytoplasmic proteins prior to nuclear translocation (non-genomic) and affecting their activity.

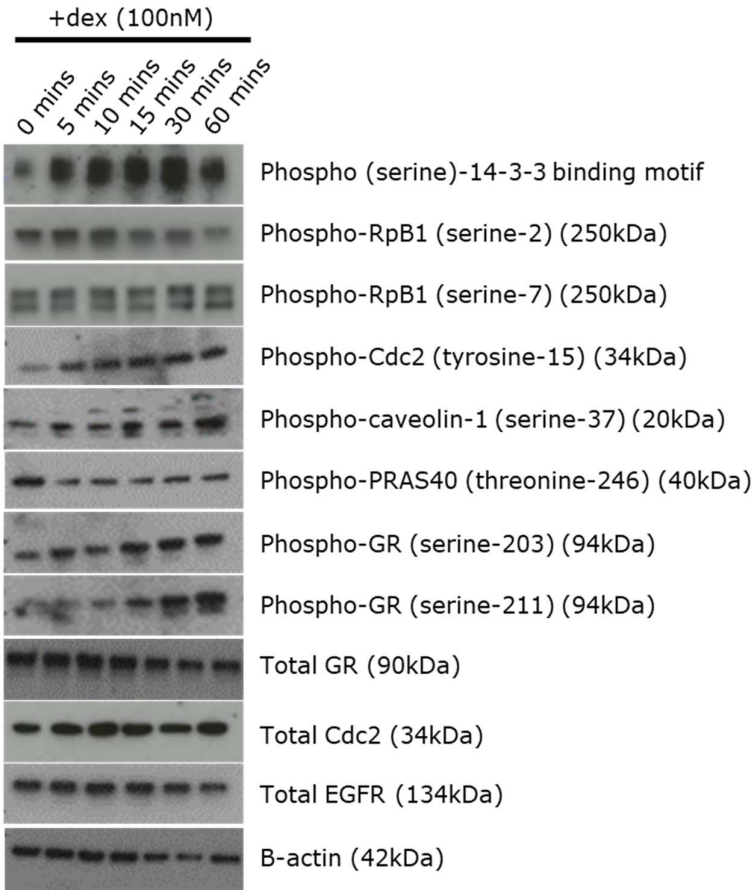

Fig 4.5. SILAC hit validation in response to GC. Panel of protein phosphorylation and total protein expression (with corresponding molecular weights) in response to 1 hour of dexamethasone (100nM) treatment. B-actin was used as a loading control.

4.5. Discussion

Selective GR modulators (SeGRMs) were initially developed as an alternative to conventional steroids, including dexamethasone and fluticasone propionate, to minimise the harmful side effects associated with high-dose, prolonged steroid therapy. These SeGRMs were created using the "dissociated model" of glucocorticoid action which divided GR transcriptional activity to transactivation (promoting off-target effects) by directly binding GC-responsive promoters and transrepression of pro-inflammatory transcription factors by tethering (anti-inflammatory action) (Belvisi et al., 2001). The simplicity of this model failed to account for the anti-inflammatory genes directly regulated by the GR and the activation of parallel transcription factor pathways that can modify GR output over time. Consequently, many of the SeGRMs were unsuccessful save for GW870086X which shows promise as an inhaled anti-inflammatory to treat mild to moderate asthma (Leaker et al., 2015). The SeGRMs can be used as tool compounds to delineate GR activity at target promoters and cytoplasmic proteins (kinases, acetylases, etc).

HeLa cells were chosen as the appropriate *in vitro* model for characterising tool compound pharmacology and pharmacokinetics due to the ease of transfection and pre-established work associated with glucocorticoids (Dvorak et al., 2006; Dvorak et al., 2005; Hoschutzky and Pongs, 1985). Differential induction and repression of GR target genes were demonstrated through MMTV- and NRE-luciferase reporter gene assays respectively, represented as differences in both potency and efficacy. This was explained by ligand-specific differences in GR nuclear accumulation, dictating the sub-cellular localisation of the GR between the cytoplasm (non-genomic action) and nucleus (genomic action).

The GC-regulated phosphoproteome contained proteins required for plasma membrane endocytosis, cytoskeletal reorganization, mobilisation of internal calcium stores, remodelling of chromatin, and transcription factors that regulate gene expression.
In summary, we have identified a non-genomic response to GC in A549 cells that occurs within 10 minutes of treatment. These findings extend the action of GCs beyond the nucleus and paint a more active picture of the GR in the cytoplasm. The engagement of multiple intracellular

signalling cascades may also yield additional GC-regulated phosphopeptides given a longer GC exposure. It may be that GCs bind to a transmembrane orphan receptor, GPR123, to induce endocytosis and transfer of steroid from extracellular matrix to the intracellular space. Here the GCs bind to cognate GR which rapidly interacts with components of the cytoplasm closest to its sub-cellular distribution when in an unliganded state. With time, the GR translocates to the nucleus, requiring reorganisation and stabilisation of the microtubule network, ending with nuclear entry.

By modulating the CDK12-CDK13 hub, the GR may be controlling the action of downstream RNA polymerase II required for the initiation of gene transcription. We hypothesis that the GR primes the nucleus prior to entry, inhibiting the action of RNA polymerase II and facilitating an open chromatin conformation at select GC response elements (GREs), allowing the GR to directly bind DNA or tether to other DNA-bound transcription factors. Further analysis into the early nuclear response to GC will need to be explored to verify this hypothesis but may yield greater insight into the early cellular response to GC in other sub-cellular locations.

4.6. Acknowledgements

Special thanks to Peter March, Roger Meadows, and Steven Marsden for their help with the microscopy. Stephen Kershaw is supported by an MRC studentship. Bioimaging Facility microscopes used in this study were purchased with grants from the BBSRC, Wellcome Trust, and the University of Manchester Strategic Fund.

4.7. Supplementary Figures

Ligands	IC_{50}	EC_{50}
GRT1	N/A	304.5nM
GRT2	63.86nM	N/A
GRT3	154.5nM	266.6nM
GRT4	8.13nM	33.73nM
GRT5	87.84nM	141nM
GRT7	0.05nM	0.13nM
GRT10	3.44nM	2.92nM
GRT11	0.26nM	$1.2x10^{-7}$nM
086X	1.27nM	5nM
Dex	2.8nM	11.78nM
FP	0.21nM	0.61nM
Pred	14.54nM	49.28nM

Figure S4.1: Tool compound potencies. IC_{50} and EC_{50} values of glucocorticoids derived from non-linear regression analysis of luciferase promoter-driven reporter constructs. Values were averaged from three independent experiments.

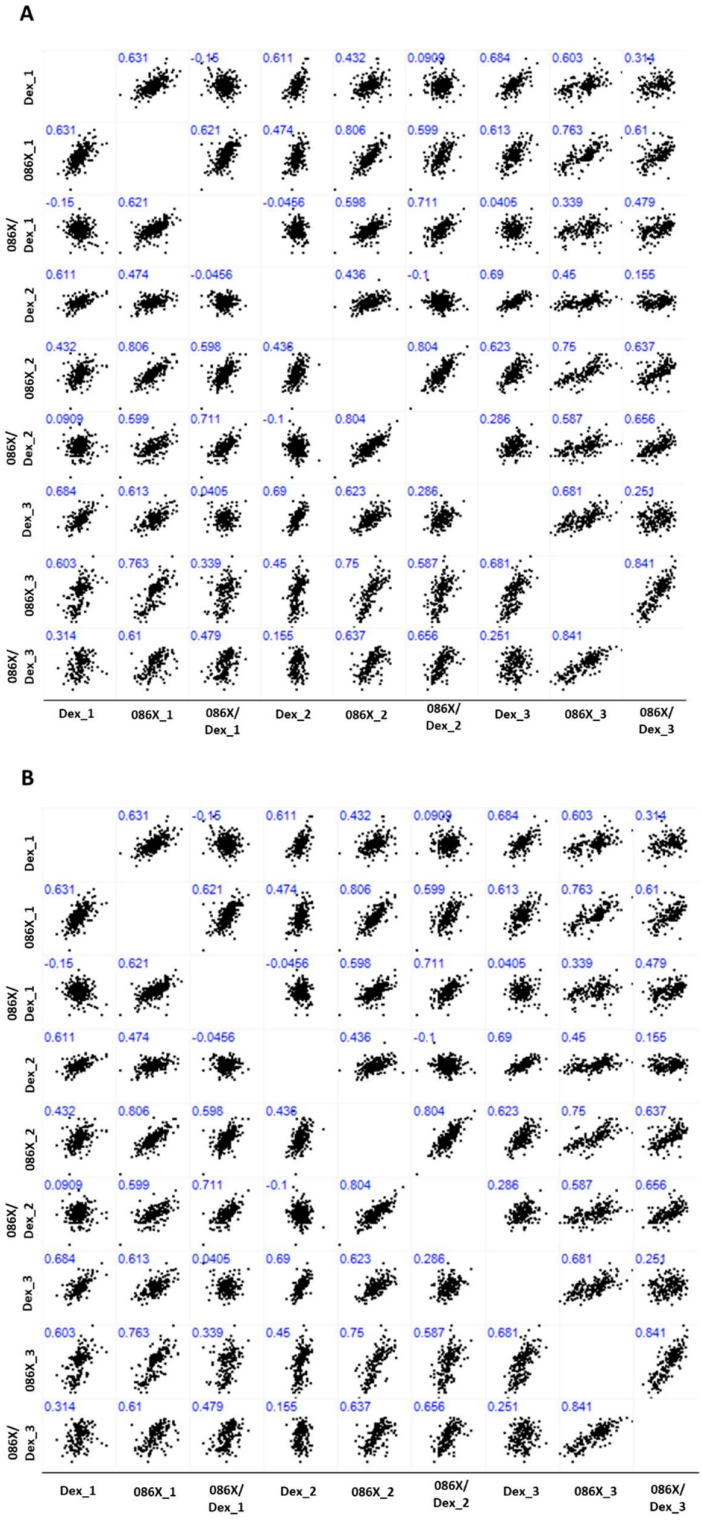

Figure S4.2. Multiscatter plots of differentially regulated phosphopeptides.
Correlation plots of each individual sample with associated Pearson's correlation coefficients highlighted in blue.

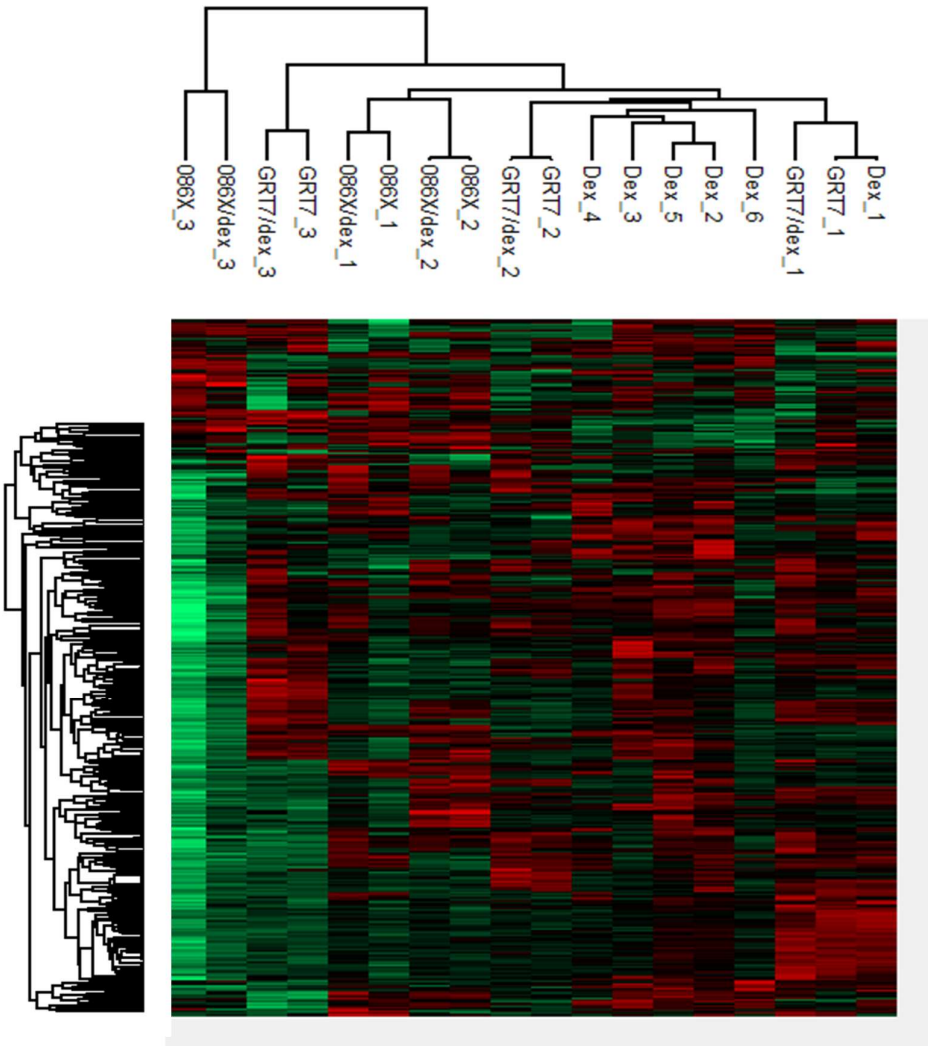

Figure S4.3. Hierarchical clustering of GC-regulated phosphopeptides. Heat map representation of the clustered matrix. Hierarchical clustering was performed using the default settings in Perseus software. Samples were tested in triplicate (indicated by _1, _2, or_3 respectively). Dexamethasone was tested alongside GRT7 and 086X separately, with dex_1, dex_2, dex_3 tested alongside the GRT7-treated samples, and dex_4, dex_5, and dex_6 tested alongside 086X-treated samples.

GO cellular component complete	Fold Enrichment	FDR
cyclin K-CDK13 complex (GO:0002945)	> 100	1.28E-02
cyclin K-CDK12 complex (GO:0002944)	> 100	1.25E-02
macropinosome (GO:0044354)	46.14	4.31E-02
pinosome (GO:0044352)	46.14	4.24E-02
nuclear pericentric heterochromatin (GO:0031618)	41.53	4.99E-03
pericentric heterochromatin (GO:0005721)	27.69	1.41E-03
nuclear cyclin-dependent protein kinase holoenzyme complex (GO:0019908)	25.96	1.30E-02
costamere (GO:0043034)	21.86	1.82E-02
condensed nuclear chromosome, centromeric region (GO:0000780)	17.3	3.03E-02
carboxy-terminal domain protein kinase complex (GO:0032806)	17.3	2.98E-02
cyclin-dependent protein kinase holoenzyme complex (GO:0000307)	15.97	2.35E-04
Flemming body (GO:0090543)	14.83	4.22E-02
heterochromatin (GO:0000792)	11.22	1.44E-03
plasma membrane raft (GO:0044853)	9.59	8.01E-04
caveola (GO:0005901)	8.76	1.38E-02
serine/threonine protein kinase complex (GO:1902554)	8.39	5.22E-03
protein kinase complex (GO:1902911)	6.92	1.29E-02
nuclear speck (GO:0016607)	6.37	1.14E-07
cortical cytoskeleton (GO:0030863)	6.29	4.28E-02
membrane region (GO:0098589)	5.64	7.25E-05
membrane microdomain (GO:0098857)	5.39	2.41E-04
membrane raft (GO:0045121)	5.39	2.33E-04
chromosome, centromeric region (GO:0000775)	5	2.23E-02
nuclear body (GO:0016604)	4.58	4.58E-08
chromatin (GO:0000785)	4.56	2.69E-05

Figure S4.4. Cellular compartment ontology. Top 25 cellular compartment gene ontology terms derived from SILAC phosphoproteomics, organised by fold enrichment and false discovery rate (FDR) for all GC-regulated phosphopeptides.

	Dex	GRt7	086x
GSK3, **Erk1, Erk2**, CDK5	807	463	437
WW domain binding domain	798	455	383
Casein kinase II	758	437	455
GPCR kinase I	657	383	368
PKA kinase	570	324	301
PKC kinase	518	296	260
MAPKAPK2	283	178	153
14-3-3 domain binding motif	219	131	126
DNA-dependent kinase substrate motif	216	97	123
Growth associated histone H1	187	113	101
Casein kinase I	180	107	102
Beta-adrenergic receptor motif	174	105	100
CDK1,2,4,6	153	95	95
Cdc2	153	95	95
Plk1 PBD domain binding	133	82	63
MDC1 BRCT domain binding	133	82	66
CDK	126	77	84
Akt kinase substrate motif	91	54	57
MAPKAPK1	90	57	42
Pyruvate dehydrogenase kinase substrate	53	30	36
Chk1	46	28	24
PKC-epsilon kinase	40	26	19
BARD1 BRCT kinase substrate motif	38	26	24
ZIP kinase substrate	31	28	14
AMPKI motif	30	21	19

Figure S4.5. Enriched GC-regulated motifs. Top 25 enriched motifs derived from SILAC phosphoproteomics data, separated by GC treatment and organised by frequency of enriched motifs.

Chapter 5: General discussion and future work

5.1. Overview

Glucocorticoids are powerful anti-inflammatory and immunosuppressive drugs that exert their cellular effects through the glucocorticoid receptor. Upon ligand binding, the GR undergoes a series of conformational changes and interacts with cytoplasmic proteins to mediate non-genomic effects (within minutes). The GR then translocates along microtubules to enter the nucleus and regulate gene expression (over hours) by binding target DNA sequences directly as a dimer (transactivation) or by tethering to other DNA-bound transcription factors (transrepression). The pleiotropic action of glucocorticoids leads to off-target effects which limits their therapeutic benefit. This aim of this thesis was to characterise the non-genomic actions of the glucocorticoid receptor, a relatively undefined field of GR biology. Using a combination of pharmacology and cell biology techniques, I have shown that GR interacts with a variety of cytoplasmic proteins prior to its entry into the nucleus and regulation of gene transcription. Furthermore, I have identified a novel interaction between GR and the tubulin deacetylase HDAC6 which explains the inhibitory effect of glucocorticoids on cell motility, a commonly described off-target effect of high-dose, long-term glucocorticoid therapy.

5.2. Glucocorticoids inhibit HDAC6 to impair cell motility

Impaired wound healing is a common side effect of prolonged GC (Dahmana et al., 2018; Kadmiel et al., 2016; de Almeida et al., 2016). Although amelioration has been achieved by adrenalectomy, GR blockade, and MR agonism the underlying mechanism that impairs wound healing remained elusive (de Almeida et al., 2016; Bitar et al., 1999; Dahmana et al., 2018). A cardinal feature of GC action in all cell types studied is impairment of cell migration, and it is this change in migration that underlies many aspects of the impaired wound healing and tissue remodelling that accompany GC use.

The human lung epithelial cell line A549 was used as an *in vitro* model due to the pre-established literature of GC action (Huang et al., 2016; Sun et al., 2012; Salem et al., 2012). Cell stopper and scratch wound healing assays were used to determine the effect of GC on A549 cell

migration after 24 hours. However, these assays are restricted to populations of cells grown in confluent monolayers and GC exposure more than 24 hours (Kisanga et al., 2018; Fietz et al., 2017). By discounting the early actions of GCs in cells, the non-genomic effects occurring within the cytoplasm are being ignored and limits scope to the transcriptional response alone. Therefore, I adopted a real-time microscopy approach to study single-cell changes in GC exposure to correctly identify the kinetics of the GC response to cell migration.

Brightfield microscopy was coupled with wavelet analysis, an image transformation algorithm that selects objects (cells) according to morphology, noise and background subtraction. (Yoon et al., 2018; Buranachai et al., 2008). Wavelet analysis allowed the tracking of live cells without the need for nuclei or cellular staining that could impact GC action. Cell movement was quantified using automated tracking software (Imaris Pro) as x, y co-ordinates in time-lapse movies. The total displacement (μm) of cells from the point of origin was calculated as the difference in x, y from point B (end of the movie) to point A (GC administration) and used as a measure of cell migration. Additionally, step length (displacement, μm) was used as an indication of the walk properties of cells when plotted as a frequency distribution (Weber, 1984). Together, step length and total displacement modelled the real-time movement of A549 cells in response to GC.

A prompt response to GC is observed within 30-40 minutes of administration for dexamethasone and RU486, confirmed by statistical comparison of GC-treated vs vehicle control-treated cells. The glucocorticoid effect is dependent on the GR and occurs without the need of new gene transcription, as shown the lack of induction of genes involved in cell migration by RT^2-PCR and the persistence of the glucocorticoid effect even after pre-treatment with the transcription inhibitor actinomycin D.

I hypothesised that the glucocorticoid inhibition of migration was similarly rapid, most likely within the cytoplasm where the GR resides in a high-affinity ligand-binding state prior to ligand binding. Cytoskeletal remodelling is integral to proper cell migration and altering microtubule dynamics can affect cell shape, motility, and direction (Sun and Zaman, 2017; Mouneimne et al., 2012; Hakkinen et al., 2011). Live-cell imaging

of GFP-tagged EB3 was used as an indicator of microtubule network stability, the speed of microtubule plus-end growth denoting stabilisation of the microtubule network. Glucocorticoids rapidly increase the stabilisation of microtubules which results in the inhibition of cell migration. This is achieved through the rapid induction of α-tubulin acetylation (within 10 minutes), as shown by fixed-cell immunofluorescence and western blotting. The regulation of tubulin acetylation is tightly regulated by the catalytic actions of two enzymes, the tubulin acetyltransferase αTAT1 and the primary tubulin deacetylase HDAC6 (Castro-Castro et al., 2012; Miyake et al., 2016; Zhao et al., 2010). I tested the role of both enzymes in the glucocorticoid effect on cell migration by using the cell migration assays adopted earlier in the study. Initially I found that siRNA knockdown of αTAT1 did not affect the inhibitory effect of dexamethasone on cell migration. I used tubacin (a selective HDAC6 inhibitor) in the cell migration assay to show a similar inhibition of cell migration as dexamethasone, with a co-treatment of dexamethasone and tubacin having no additive effect on cell migration, suggesting that both compounds are working through the same mechanism to inhibit cell migration, i.e. inhibition of HDAC6. Down-regulation of HDAC6 is shown to inhibit cell migration through downstream hyperacetylation of microtubules, a mechanism we also identify in this study (Zhang et al., 2014; Li et al., 2013; Li et al., 2011). Overexpression of HDAC6-FLAG using transient transfection reversed the inhibitory effect of glucocorticoids on cell migration, further supporting the role of HDAC6 in the glucocorticoid effect. Cells were tracked by co-transfecting equivalent quantities of GFP-tagged histone 2B (H2B-GFP) and HDAC6-FLAG and overexpression of HDAC6 quantified by western blot. This method of tracking was used due to unavailability of the GFP-tagged HDAC6 construct at the time of the initial experiment, although repeating the experiment using HDAC6-GFP in place of the dual plasmid co-expression would yield a similar result.

The next step was to demonstrate an interaction between the GR and HDAC6, with ligand activation inhibiting the deacetylase activity of HDAC6 at α-tubulin. I decided to use HaloTag immunoprecipitation to pull-down transiently transfected HaloTag-GR with HDAC6-eGFP or HaloTag-HDAC6 and GR-eGFP from A549 cells and use western blotting (co-IP) to determine whether GR and HDAC6 interacted in the absence or presence of dexamethasone. Unfortunately, such an interaction could

not be shown through co-IP, potentially due to the nature of the GR-HDAC6 interaction being weak or transient (Lee et al., 2013). However, another study has demonstrated an interaction between the GR and HDAC6 using antibody-based co-IP methods, suggesting that the HaloTag-pulldown method employed in this study was insufficient in precipitating the GR-HDAC6 complex (Rimando et al., 2016). Interestingly, this study showed that simultaneous inhibition of the GR and HDAC6 enhances expression of the osteoblast late marker osteocalcin (OCN) gene, suggesting that the GR-HDAC6 complex may mediate other negative side effects of GC therapy.

An alternate method of identifying weak protein interactions exists through fluorescence cross-correlation spectroscopy (FCCS), a quantitative imaging technique that utilises confocal microscopy in conjunction with fluorescently-labelled proteins to provide a real-time dynamic measurement of molecules in live cells (Bacia et al., 2006; Krieger et al., 2015). This technique has been applied in the characterising the dimerization of GR in the cytoplasm and nucleus (Tiwari et al., 2017).

FCCS detects the movement of fluorescently-labelled molecules as they pass through a small confocal volume (~1fL) and records movement as fluctuations in fluorescence intensity, which can be modelled to an autocorrelation curve following autocorrelation analysis. When the two fluorescent-labelled molecules move through the confocal volume together, a cross-correlation curve is generated signifying that the two molecules are in complex with one another. Considerations to be taken during FCCS include the use of low laser power during image acquisition and to select live, healthy cells for analysis. Since A549 cells are typically difficult to transiently transfect, a stably transfected cell line would have been ideal for homogenous expression of HaloTag-GR or HDAC6-eGFP. However due to time constraints this option was not available to me during my analysis and did not adversely affect the results gathered in this study.

I applied this technique in A549 cells transiently co-transfected with HaloTag-GR and HDAC6-eGFP treated with vehicle or dexamethasone. Simultaneous FCCS measurements were taken in the cytoplasm and nucleus of cells to model the compartmental shift of GR upon ligand

binding. Upon dexamethasone treatment there is a 10x fold reduction in the K_m of GR-HDAC6 cytoplasmic cross-correlation in comparison to the vehicle-treated controls. This shows that GR and HDAC6 interact within the cytoplasm in a ligand-dependent manner. Interestingly, a small proportion of HDAC6 (10%) appears to translocate into the nucleus after dexamethasone treatment, which suggests that the GR is trafficking HDAC6 in conjunction with its nuclear translocation. Considering the confocal volume employed in FCCS is ~1fL, additional proteins may be associated with the GR-HDAC6 complex, including components of the GR multi-protein complex (p23, Hsp90, immunophilins, etc). The interaction between GR and HDAC6 may be facilitated by Hsp90, a substrate for HDAC6 and key chaperone protein for GR (Kovacs et al., 2005). Hsp90 chaperone activity is highly dependent on the deacetylase activity of HDAC6, in which acetylation of Hsp90 induces dissociation with the co-chaperone p23 in the cytoplasmic GR multi-protein complex. HDAC6 therefore regulates the nuclear translocation, ligand binding capacity, and transcriptional activity of the GR (Kovacs et al., 2005; Kekatpure et al., 2009). Selective silencing of HDAC6 and Hsp90 inhibition are shown to the migration of squamous cells that overexpress HDAC6, which supports the existence of a HDAC6-Hsp90-GR multi-protein complex in regulating microtubule stability and cell motility (Tao et al., 2018).

5.3. Glucocorticoids rapidly alter the phosphoproteome

I began by investigating the pharmacology of a panel of non-steroidal glucocorticoids which were designed to mimic the anti-inflammatory action of conventional steroids (dexamethasone, fluticasone propionate) with a minimised side effect profile. These tool compounds are valuable in dissecting GR biology, specifically how changes in the receptor structure can alter its function. I identified ligand-specific differences in the transcriptional activity of the GR at glucocorticoid-responsive luciferase-tagged promoter genes, MMTV and NRE. These promoters were chosen due to their responsiveness to glucocorticoid treatment and use in other publications for compound profiling (John et al., 1989; Schumacher et al., 2003; Rao et al., 2011; Scheinman et al., 1995).

These differences were explained by altered kinetics of GR nuclear translocation demonstrated using real-time imaging of HaloTag-GR upon ligand binding within live cells. Using this information, a select number

of tool compounds were potency-matched according to their IC_{50} values. I then used phosphoproteomics analysis to identify the differentially regulated phosphoproteins between each ligand. SILAC was used over label-free phosphoproteomics methods to more easily quantify small differences in phosphorylated proteins regulated by each ligand. In addition, SILAC provided greater quantitative accuracy and lower experimental bias due to sample pooling. SILAC labelling allowed the three-way comparison between A549 cells treated with vehicle (light) and dexamethasone (medium) or GRT7/086X (heavy). A short ligand treatment (10 minutes) was chosen to ensure the non-genomic action of the GR were being activated with minimal activity at GC-responsive promoters in the nucleus confirmed by live-cell imaging of ligand-activated GR nuclear trafficking. Differentially-regulated phosphoproteins were shared amongst all three ligands (n=1436), with common proteins localised in the plasma membrane, cytoplasm, and nucleus. This suggests that activation of the GR elicits a rapid cellular response that is indiscriminate and further promotes GR activity, including endocytosis, reorganisation of the cytoskeletal architecture, and chromatin remodelling.

Although HDAC6 was not phosphorylated by 10 minutes of GC exposure, other cytoskeletal regulators such as cofilin-1 were differentially-regulated, suggesting that prolonged GC administration may elicit changes in additional associated proteins. Furthermore, GCs regulated key components of the GCPR and EGFR signalling pathways (GSK3β, ERK1/2, PKA, PKC), each of which can initiate parallel intracellular signalling cascades, the full scope of which would be of great interest to study further.

Taken together, both studies highlight the importance of the early GC response in cells and the need to account for non-genomic GR activity. We demonstrate the non-transcriptional inhibition of cell migration that is dependent on the GR which occurs within 30 minutes of GC administration. SILAC phosphoproteomics performed in cells treated with 10 minutes of GC indicate non-genomic regulation of other phosphoproteins.

5.4. Future work

Although I demonstrated that the GR is required for the glucocorticoid effect on cell migration using siRNA knockdown (90% efficiency), a small proportion of endogenous GR is still expressed in the total population. GR knockout using a CRISPR-Cas9 targeted system would ensure complete removal of endogenous GR and provide a more definitive answer for GR involvement. Additionally, one could use these GR-null cells to test the importance of GR modular domains in the glucocorticoid effect on cell migration (e.g. LDB, DBD, AF1). Site-directed mutagenesis of a fluorescent-tagged GR plasmid (HaloTag-GR) could be used to selectively delete these domains from the GR and determine whether direct DNA binding or ligand-binding or required to inhibit migration. This would also provide support for the proposed non-genomic glucocorticoid effect on migration and may also be used to identify the exact GR region required for inhibition of HDAC6 (repeating the FCCS with fluorescently-tagged GR mutants and the wild-type fluorescent HDAC6 to confirm an interaction persists after ligand binding).

Translating the findings into *in vivo* models of wound healing would enhance clinical relevance, especially in mice with silenced expression of HDAC6 in response to GC.

Although an initial validation of the SILAC phosphoproteomics was conducted by western blotting, a more in-depth analysis of the functional importance of glucocorticoids in repressing RNA polymerase II activity would be advantageous. Live-cell imaging of a fluorescently-tagged RNA polymerase II plasmid vector in response to glucocorticoid and quantifying the mobility of the protein (by FCCS or FRET for example). An advantage of using SILAC phosphoproteomics over a label-free method was easing the quantification of phosphorylated proteins in glucocorticoid vs vehicle treated cells. However, label-free phosphoproteomics might allow the unbiased analysis of a greater panel of glucocorticoids with different pharmacological properties, including the GR antagonist RU486 and other GR tool compounds. In addition, a label-free method would be useful for studying a time series of glucocorticoid activity, ranging from ligand activation of the receptor to entry into the nucleus. This would build a ligand- and time-specific picture of the phosphoproteome within cultured cells which would

showcase the true non-genomic action of the GR. RNA-sequencing can be used to provide a more thorough profile of SeGRM action when coupled with the pre-existing SILAC phosphoproteomics data. However, the quantitative analysis provided by triple-label SILAC was more appropriate for our experimental model in the first instance. The differential labelling of cells was used to compare the activities of three different glucocorticoid agonists which could be tested alongside one another.

Additional experiments should be conducted to confirm the rapid phosphorylation of RNA polymerase II is occurring devoid of GR occupancy within the nucleus. Repeating the SILAC phosphoproteomics using nuclear and cytoplasmic fractionation would better separate the sub-cellular compartments and delineate the phosphopeptides regulated by GCs.

5.5. Concluding Remarks

Glucocorticoids are critical endogenous hormones that are essential for development, glucose homeostasis, resolving inflammation, and the stress response. Therapeutic glucocorticoids are powerful anti-inflammatory and immunosuppressive agents that are widely used in the clinic. However, the pleiotropic expression of the glucocorticoid receptor permits the induction of off-target metabolic effects that severely hinder the therapeutic potential of glucocorticoids. In this thesis I have outlined the rationale for investigating glucocorticoid activity to better inform their non-genomic actions.

I have identified a novel interaction between the GR and the tubulin deacetylase HDAC6 that is integral for the inhibitory effect of glucocorticoids on cell migration. This ligand-dependent interaction inhibits the deacetylase activity of HDAC6 at microtubules, resulting in hyperacetylation and subsequent stabilisation of the microtubule network, leading to impaired cell movement. This mechanism occurs rapidly (within minutes of administration) and may explains how glucocorticoid therapy impairs wound healing as an off-target effect.

Additionally, I have characterised the rapid, non-genomic action of glucocorticoids by identifying phosphorylated proteins that are differentially regulated using SILAC-based phosphoproteomics.

Expanding glucocorticoid research to encompass non-genomic activity is important to establish a full profile of glucocorticoid action. This will inform better drug design and ultimately aid the development of glucocorticoids with a greater therapeutic benefit.

References

Abell, S., Zeimer, H., Chong, A. & MacIsaac, R. J. (2015) 'Prevalence of osteoporosis and the use of bone protective therapies in dermatology clinic patients on long-term glucocorticoids', *Australas J Dermatol,* 56(2), pp. 147-8.

Aguilar, D. C., Strom, J., Xu, B., Kappeler, K. & Chen, Q. M. (2013) 'Expression of glucocorticoid-induced leucine zipper (GILZ) in cardiomyocytes', *Cardiovasc Toxicol,* 13(2), pp. 91-9.

Ai, J., Wang, Y., Dar, J. A., Liu, J., Liu, L., Nelson, J. B. & Wang, Z. (2009) 'HDAC6 regulates androgen receptor hypersensitivity and nuclear localization via modulating Hsp90 acetylation in castration-resistant prostate cancer', *Mol Endocrinol,* 23(12), pp. 1963-72.

Akhshi, T. K., Wernike, D. & Piekny, A. (2014) 'Microtubules and actin crosstalk in cell migration and division', *Cytoskeleton (Hoboken),* 71(1), pp. 1-23.

Akner, G., Wikstrom, A. C., Stromstedt, P. E., Stockman, O., Gustafsson, J. A. & Wallin, M. (1995) 'Glucocorticoid receptor inhibits microtubule assembly in vitro', *Mol Cell Endocrinol,* 110(1-2), pp. 49-54.

Alangari, A. A. (2010) 'Genomic and non-genomic actions of glucocorticoids in asthma', *Ann Thorac Med,* 5(3), pp. 133-9.

Ali, A., Balkovec, J. M., Greenlee, M., Hammond, M. L., Rouen, G., Taylor, G., Einstein, M., Ge, L., Harris, G., Kelly, T. M., Mazur, P., Pandit, S., Santoro, J., Sitlani, A., Wang, C., Williamson, J., Forrest, M. J., Carballo-Jane, E., Luell, S., Lowitz, K. & Visco, D. (2008) 'Discovery of betamethasone 17alpha-carbamates as dissociated glucocorticoid receptor modulators in the rat', *Bioorg Med Chem,* 16(16), pp. 7535-42.

Asthana, J., Kapoor, S., Mohan, R. & Panda, D. (2013) 'Inhibition of HDAC6 deacetylase activity increases its binding with microtubules and suppresses microtubule dynamic instability in MCF-7 cells', *J Biol Chem,* 288(31), pp. 22516-26.

Avenant, C., Kotitschke, A. & Hapgood, J. P. (2010) 'Glucocorticoid receptor phosphorylation modulates transcription efficacy through GRIP-1 recruitment', *Biochemistry,* 49(5), pp. 972-85.

Ayroldi, E., Macchiarulo, A. & Riccardi, C. (2014) 'Targeting glucocorticoid side effects: selective glucocorticoid receptor modulator or glucocorticoid-induced leucine zipper? A perspective', *FASEB J,* 28(12), pp. 5055-70.

Bacia, K., Kim, S. A. & Schwille, P. (2006) 'Fluorescence cross-correlation spectroscopy in living cells', *Nat Methods,* 3(2), pp. 83-9.

Backman, P., Tehler, U. & Olsson, B. (2017) 'Predicting Exposure After Oral Inhalation of the Selective Glucocorticoid Receptor Modulator, AZD5423, Based on Dose, Deposition Pattern, and Mechanistic Modeling of Pulmonary Disposition', *J Aerosol Med Pulm Drug Deliv,* 30(2), pp. 108-117.

Baiula, M. & Spampinato, S. (2014) 'Mapracorat, a Novel Non-Steroidal Selective Glucocorticoid Receptor Agonist for the Treatment of Allergic Conjunctivitis', *Inflamm Allergy Drug Targets*.

Baiula, M., Sparta, A., Bedini, A., Carbonari, G., Bucolo, C., Ward, K. W., Zhang, J. Z., Govoni, P. & Spampinato, S. (2011) 'Eosinophil as a cellular target of the ocular anti-allergic action of mapracorat, a novel selective glucocorticoid receptor agonist', *Mol Vis,* 17, pp. 3208-23.

Ballegeer, M., Van Looveren, K., Timmermans, S., Eggermont, M., Vandevyver, S., Thery, F., Dendoncker, K., Souffriau, J., Vandewalle, J., Van Wyngene, L., De Rycke, R., Takahashi, N., Vandenabeele, P., Tuckermann, J., Reichardt, H. M., Impens, F., Beyaert, R., De Bosscher, K., Vandenbroucke, R. E. & Libert, C.

(2018) 'Glucocorticoid receptor dimers control intestinal STAT1 and TNF-induced inflammation in mice', *J Clin Invest,* 128(8), pp. 3265-3279.

Bareille, P., Hardes, K. & Donald, A. C. (2013) 'Efficacy and safety of once-daily GW870086 a novel selective glucocorticoid in mild-moderate asthmatics: a randomised, two-way crossover, controlled clinical trial', *J Asthma,* 50(10), pp. 1077-82.

Barnett, H. A., Coe, D. M., Cooper, T. W., Jack, T. I., Jones, H. T., Macdonald, S. J., McLay, I. M., Rayner, N., Sasse, R. Z., Shipley, T. J., Skone, P. A., Somers, G. I., Taylor, S., Uings, I. J., Woolven, J. M. & Weingarten, G. G. (2009) 'Aryl aminopyrazole benzamides as oral non-steroidal selective glucocorticoid receptor agonists', *Bioorg Med Chem Lett,* 19(1), pp. 158-62.

Baschant, U. & Tuckermann, J. (2010) 'The role of the glucocorticoid receptor in inflammation and immunity', *J Steroid Biochem Mol Biol,* 120(2-3), pp. 69-75.

Baumer, W., Rossbach, K. & Schmidt, B. H. (2017) 'The selective glucocorticoid receptor agonist mapracorat displays a favourable safety-efficacy ratio for the topical treatment of inflammatory skin diseases in dogs', *Vet Dermatol,* 28(1), pp. 46-e11.

Beaulieu, E. & Morand, E. F. (2011) 'Role of GILZ in immune regulation, glucocorticoid actions and rheumatoid arthritis', *Nat Rev Rheumatol,* 7(6), pp. 340-8.

Beck, L. S., DeGuzman, L., Lee, W. P., Xu, Y., Siegel, M. W. & Amento, E. P. (1993) 'One systemic administration of transforming growth factor-beta 1 reverses age- or glucocorticoid-impaired wound healing', *J Clin Invest,* 92(6), pp. 2841-9.

Bellavance, M. A. & Rivest, S. (2014) 'The HPA - Immune Axis and the Immunomodulatory Actions of Glucocorticoids in the Brain', *Front Immunol,* 5, pp. 136.

Belova, L., Sharma, S., Brickley, D. R., Nicolarsen, J. R., Patterson, C. & Conzen, S. D. (2006) 'Ubiquitin-proteasome degradation of serum- and glucocorticoid-regulated kinase-1 (SGK-1) is mediated by the chaperone-dependent E3 ligase CHIP', *Biochem J,* 400(2), pp. 235-44.

Belvedere, R., Bizzarro, V., Popolo, A., Dal Piaz, F., Vasaturo, M., Picardi, P., Parente, L. & Petrella, A. (2014) 'Role of intracellular and extracellular annexin A1 in migration and invasion of human pancreatic carcinoma cells', *BMC Cancer,* 14, pp. 961.

Belvisi, M. G., Wicks, S. L., Battram, C. H., Bottoms, S. E., Redford, J. E., Woodman, P., Brown, T. J., Webber, S. E. & Foster, M. L. (2001) 'Therapeutic benefit of a dissociated glucocorticoid and the relevance of in vitro separation of transrepression from transactivation activity', *J Immunol,* 166(3), pp. 1975-82.

Bertorelli, G., Bocchino, V. & Olivieri, D. (1998) 'Heat shock protein interactions with the glucocorticoid receptor', *Pulm Pharmacol Ther,* 11(1), pp. 7-12.

Biggadike, K. (2011) 'Fluticasone furoate/fluticasone propionate - different drugs with different properties', *Clin Respir J,* 5(3), pp. 183-4.

Biggadike, K., Bledsoe, R. K., Coe, D. M., Cooper, T. W., House, D., Iannone, M. A., Macdonald, S. J., Madauss, K. P., McLay, I. M., Shipley, T. J., Taylor, S. J., Tran, T. B., Uings, I. J., Weller, V. & Williams, S. P. (2009) 'Design and x-ray crystal structures of high-potency nonsteroidal glucocorticoid agonists exploiting a novel binding site on the receptor', *Proc Natl Acad Sci U S A,* 106(43), pp. 18114-9.

Bijsmans, I. T., Guercini, C., Ramos Pittol, J. M., Omta, W., Milona, A., Lelieveld, D., Egan, D. A., Pellicciari, R., Gioiello, A. & van Mil, S. W. (2015) 'The glucocorticoid mometasone furoate is a novel FXR ligand that decreases inflammatory but not metabolic gene expression', *Sci Rep,* 5, pp. 14086.

Bitar, M. S., Farook, T., Wahid, S. & Francis, I. M. (1999) 'Glucocorticoid-dependent impairment of wound healing in experimental diabetes: amelioration by adrenalectomy and RU 486', *J Surg Res,* 82(2), pp. 234-43.

Bledsoe, R. K., Montana, V. G., Stanley, T. B., Delves, C. J., Apolito, C. J., McKee, D. D., Consler, T. G., Parks, D. J., Stewart, E. L., Willson, T. M., Lambert, M. H., Moore, J. T., Pearce, K. H. & Xu, H. E. (2002) 'Crystal structure of the glucocorticoid receptor ligand binding domain reveals a novel mode of receptor dimerization and coactivator recognition', *Cell,* 110(1), pp. 93-105.

Bledsoe, R. K., Stewart, E. L. & Pearce, K. H. (2004) 'Structure and function of the glucocorticoid receptor ligand binding domain', *Vitam Horm,* 68, pp. 49-91.

Boggs, A. E., Vitolo, M. I., Whipple, R. A., Charpentier, M. S., Goloubeva, O. G., Ioffe, O. B., Tuttle, K. C., Slovic, J., Lu, Y., Mills, G. B. & Martin, S. S. (2015) 'alpha-Tubulin acetylation elevated in metastatic and basal-like breast cancer cells promotes microtentacle formation, adhesion, and invasive migration', *Cancer Res,* 75(1), pp. 203-15.

Boldizsar, F., Talaber, G., Szabo, M., Bartis, D., Palinkas, L., Nemeth, P. & Berki, T. (2010) 'Emerging pathways of non-genomic glucocorticoid (GC) signalling in T cells', *Immunobiology,* 215(7), pp. 521-6.

Bornelov, S., Reynolds, N., Xenophontos, M., Gharbi, S., Johnstone, E., Floyd, R., Ralser, M., Signolet, J., Loos, R., Dietmann, S., Bertone, P. & Hendrich, B. (2018) 'The Nucleosome Remodeling and Deacetylation Complex Modulates Chromatin Structure at Sites of Active Transcription to Fine-Tune Gene Expression', *Mol Cell,* 71(1), pp. 56-72 e4.

Bruna, A., Nicolas, M., Munoz, A., Kyriakis, J. M. & Caelles, C. (2003) 'Glucocorticoid receptor-JNK interaction mediates inhibition of the JNK pathway by glucocorticoids', *EMBO J,* 22(22), pp. 6035-44.

Buranachai, C., Kamiyama, D., Chiba, A., Williams, B. D. & Clegg, R. M. (2008) 'Rapid frequency-domain FLIM spinning disk confocal microscope: lifetime resolution, image improvement and wavelet analysis', *J Fluoresc,* 18(5), pp. 929-42.

Burnecki, K., Wylomanska, A., Beletskii, A., Gonchar, V. & Chechkin, A. (2012) 'Recognition of stable distribution with Levy index alpha close to 2', *Phys Rev E Stat Nonlin Soft Matter Phys,* 85(5 Pt 2), pp. 056711.

Buttgereit, F. & Burmester, G. R. (2016) 'Rheumatoid arthritis: Glucocorticoid therapy and body composition', *Nat Rev Rheumatol,* 12(8), pp. 444-5.

Buttgereit, F. & Scheffold, A. (2002) 'Rapid glucocorticoid effects on immune cells', *Steroids,* 67(6), pp. 529-34.

Carolina, E., Kato, T., Khanh, V. C., Moriguchi, K., Yamashita, T., Takeuchi, K., Hamada, H. & Ohneda, O. (2018) 'Glucocorticoid Impaired the Wound Healing Ability of Endothelial Progenitor Cells by Reducing the Expression of CXCR4 in the PGE2 Pathway', *Front Med (Lausanne),* 5, pp. 276.

Castro-Castro, A., Janke, C., Montagnac, G., Paul-Gilloteaux, P. & Chavrier, P. (2012) 'ATAT1/MEC-17 acetyltransferase and HDAC6 deacetylase control a balance of acetylation of alpha-tubulin and cortactin and regulate MT1-MMP trafficking and breast tumor cell invasion', *Eur J Cell Biol,* 91(11-12), pp. 950-60.

Cervantes-Gomez, F., Nimmanapalli, R. & Gandhi, V. (2009) 'Transcription inhibition of heat shock proteins: a strategy for combination of 17-allylamino-17-demethoxygeldanamycin and actinomycin d', *Cancer Res,* 69(9), pp. 3947-54.

Chapman, K. E., Coutinho, A., Gray, M., Gilmour, J. S., Savill, J. S. & Seckl, J. R. (2006) 'Local amplification of glucocorticoids by 11beta-hydroxysteroid dehydrogenase type 1 and its role in the inflammatory response', *Ann N Y Acad Sci,* 1088, pp. 265-73.

Chapman, K. E. & Seckl, J. R. (2008) '11beta-HSD1, inflammation, metabolic disease and age-related cognitive (dys)function', *Neurochem Res,* 33(4), pp. 624-36.

Charmandari, E., Chrousos, G. P., Lambrou, G. I., Pavlaki, A., Koide, H., Ng, S. S. & Kino, T. (2011) 'Peripheral CLOCK regulates target-tissue glucocorticoid receptor transcriptional activity in a circadian fashion in man', *PLoS One,* 6(9), pp. e25612.

Chen, W., Dang, T., Blind, R. D., Wang, Z., Cavasotto, C. N., Hittelman, A. B., Rogatsky, I., Logan, S. K. & Garabedian, M. J. (2008) 'Glucocorticoid receptor phosphorylation differentially affects target gene expression', *Mol Endocrinol,* 22(8), pp. 1754-66.

Chen, W., Rogatsky, I. & Garabedian, M. J. (2006) 'MED14 and MED1 differentially regulate target-specific gene activation by the glucocorticoid receptor', *Mol Endocrinol,* 20(3), pp. 560-72.

Chien, E. J., Hsu, C. H., Chang, V. H., Lin, E. P., Kuo, T. P., Chien, C. H. & Lin, H. Y. (2016) 'In human T cells mifepristone antagonizes glucocorticoid non-genomic rapid responses in terms of Na(+)/H(+)-exchange 1 activity, but not ezrin/radixin/moesin phosphorylation', *Steroids,* 111, pp. 29-36.

Chivers, J. E., Cambridge, L. M., Catley, M. C., Mak, J. C., Donnelly, L. E., Barnes, P. J. & Newton, R. (2004) 'Differential effects of RU486 reveal distinct mechanisms for glucocorticoid repression of prostaglandin E release', *Eur J Biochem,* 271(20), pp. 4042-52.

Conway-Campbell, B. L., George, C. L., Pooley, J. R., Knight, D. M., Norman, M. R., Hager, G. L. & Lightman, S. L. (2011) 'The HSP90 molecular chaperone cycle regulates cyclical transcriptional dynamics of the glucocorticoid receptor and its coregulatory

molecules CBP/p300 during ultradian ligand treatment', *Mol Endocrinol,* 25(6), pp. 944-54.

Cosio, B. G., Torrego, A. & Adcock, I. M. (2005) '[Molecular mechanisms of glucocorticoids]', *Arch Bronconeumol,* 41(1), pp. 34-41.

Crim, C., Pierre, L. N. & Daley-Yates, P. T. (2001) 'A review of the pharmacology and pharmacokinetics of inhaled fluticasone propionate and mometasone furoate', *Clin Ther,* 23(9), pp. 1339-54.

Croxtall, J. D., Choudhury, Q. & Flower, R. J. (2000) 'Glucocorticoids act within minutes to inhibit recruitment of signalling factors to activated EGF receptors through a receptor-dependent, transcription-independent mechanism', *Br J Pharmacol,* 130(2), pp. 289-98.

Cruz-Topete, D. & Cidlowski, J. A. (2015) 'One hormone, two actions: anti- and pro-inflammatory effects of glucocorticoids', *Neuroimmunomodulation,* 22(1-2), pp. 20-32.

Dahmana, N., Mugnier, T., Gabriel, D., Kaltsatos, V., Bertaim, T., Behar-Cohen, F., Gurny, R. & Kalia, Y. N. (2018) 'Topical Administration of Spironolactone-Loaded Nanomicelles Prevents Glucocorticoid-Induced Delayed Corneal Wound Healing in Rabbits', *Mol Pharm,* 15(3), pp. 1192-1202.

Daley-Yates, P. T. (2015) 'Inhaled corticosteroids: potency, dose equivalence and therapeutic index', *Br J Clin Pharmacol,* 80(3), pp. 372-80.

de Almeida, T. F., de Castro Pires, T. & Monte-Alto-Costa, A. (2016) 'Blockade of glucocorticoid receptors improves cutaneous wound healing in stressed mice', *Exp Biol Med (Maywood),* 241(4), pp. 353-8.

Deakin, N. O. & Turner, C. E. (2014) 'Paxillin inhibits HDAC6 to regulate microtubule acetylation, Golgi structure, and polarized migration', *J Cell Biol,* 206(3), pp. 395-413.

Dean, D. A., Urban, G., Aragon, I. V., Swingle, M., Miller, B., Rusconi, S., Bueno, M., Dean, N. M. & Honkanen, R. E. (2001) 'Serine/threonine protein phosphatase 5 (PP5) participates in the regulation of glucocorticoid receptor nucleocytoplasmic shuttling', *BMC Cell Biol,* 2, pp. 6.

DeFea, K. A. (2013) 'Arrestins in actin reorganization and cell migration', *Prog Mol Biol Transl Sci,* 118, pp. 205-22.

Deng, Q., Riquelme, D., Trinh, L., Low, M. J., Tomic, M., Stojilkovic, S. & Aguilera, G. (2015) 'Rapid Glucocorticoid Feedback Inhibition of ACTH Secretion Involves Ligand-Dependent Membrane Association of Glucocorticoid Receptors', *Endocrinology,* 156(9), pp. 3215-27.

Derbyshire, E. J., Yang, Y. C., Li, S., Comin, G. A., Belloir, J. & Thorpe, P. E. (1996) 'Heparin-steroid conjugates lacking glucocorticoid or mineralocorticoid activities inhibit the proliferation of vascular endothelial cells', *Biochim Biophys Acta,* 1310(1), pp. 86-96.

Dezitter, X., Fagart, J., Taront, S., Fay, M., Masselot, B., Hetuin, D., Formstecher, P., Rafestin-Oblin, M. E. & Idziorek, T. (2014) 'A structural explanation of the effects of dissociated glucocorticoids on glucocorticoid receptor transactivation', *Mol Pharmacol,* 85(2), pp. 226-36.

Diaz-Gallardo, M. Y., Cote-Velez, A., Charli, J. L. & Joseph-Bravo, P. (2010) 'A rapid interference between glucocorticoids and cAMP-activated signalling in hypothalamic neurones prevents binding of phosphorylated cAMP response element binding protein and glucocorticoid receptor at the CRE-Like and composite GRE sites of thyrotrophin-releasing hormone gene promoter', *J Neuroendocrinol,* 22(4), pp. 282-93.

Dittmar, K. D., Demady, D. R., Stancato, L. F., Krishna, P. & Pratt, W. B. (1997) 'Folding of the glucocorticoid receptor by the heat shock protein (hsp) 90-based chaperone machinery. The role of p23 is to stabilize receptor.hsp90 heterocomplexes formed by hsp90.p60.hsp70', *J Biol Chem,* 272(34), pp. 21213-20.

Dokoumetzidis, A., Iliadis, A. & Macheras, P. (2002) 'Nonlinear dynamics in clinical pharmacology: the paradigm of cortisol secretion and suppression', *Br J Clin Pharmacol,* 54(1), pp. 21-9.

Dong, H., Carlton, M. E., Lerner, A. & Epstein, P. M. (2015) 'Effect of cAMP signaling on expression of glucocorticoid receptor, Bim and Bad in glucocorticoid-sensitive and resistant leukemic and multiple myeloma cells', *Front Pharmacol,* 6, pp. 230.

Donn, R., Payne, D. & Ray, D. (2007) 'Glucocorticoid receptor gene polymorphisms and susceptibility to rheumatoid arthritis', *Clin Endocrinol (Oxf),* 67(3), pp. 342-5.

Drebert, Z., MacAskill, M., Doughty-Shenton, D., De Bosscher, K., Bracke, M., Hadoke, P. W. F. & Beck, I. M. (2017) 'Colon cancer-derived myofibroblasts increase endothelial cell migration by glucocorticoid-sensitive secretion of a pro-migratory factor', *Vascul Pharmacol,* 89, pp. 19-30.

Druker, J., Liberman, A. C., Antunica-Noguerol, M., Gerez, J., Paez-Pereda, M., Rein, T., Iniguez-Lluhi, J. A., Holsboer, F. & Arzt, E. (2013) 'RSUME enhances glucocorticoid receptor SUMOylation and transcriptional activity', *Mol Cell Biol,* 33(11), pp. 2116-27.

Du, J., Cheng, B., Zhu, X. & Ling, C. (2011) 'Ginsenoside Rg1, a novel glucocorticoid receptor agonist of plant origin, maintains glucocorticoid efficacy with reduced side effects', *J Immunol,* 187(2), pp. 942-50.

Duma, D., Jewell, C. M. & Cidlowski, J. A. (2006) 'Multiple glucocorticoid receptor isoforms and mechanisms of post-translational modification', *J Steroid Biochem Mol Biol,* 102(1-5), pp. 11-21.

Dvorak, Z., Modriansky, M., Ulrichova, J. & Maurel, P. (2004) 'Speculations on the role of the microtubule network in glucocorticoid receptor signaling', *Cell Biol Toxicol,* 20(6), pp. 333-43.

Dvorak, Z., Modriansky, M., Ulrichova, J., Maurel, P., Vilarem, M. J. & Pascussi, J. M. (2005) 'Disruption of microtubules leads to glucocorticoid receptor degradation in HeLa cell line', *Cell Signal,* 17(2), pp. 187-96.

Dvorak, Z., Vrzal, R., Maurel, P. & Ulrichova, J. (2006) 'Differential effects of selected natural compounds with anti-inflammatory activity on the glucocorticoid receptor and NF-kappaB in HeLa cells', *Chem Biol Interact,* 159(2), pp. 117-28.

Ebong, I. O., Beilsten-Edmands, V., Patel, N. A., Morgner, N. & Robinson, C. V. (2016) 'The interchange of immunophilins leads to parallel pathways and different intermediates in the assembly of Hsp90 glucocorticoid receptor complexes', *Cell Discov,* 2, pp. 16002.

Echeverria, P. C., Mazaira, G., Erlejman, A., Gomez-Sanchez, C., Piwien Pilipuk, G. & Galigniana, M. D. (2009) 'Nuclear import of the glucocorticoid receptor-hsp90 complex through the nuclear pore complex is mediated by its interaction with Nup62 and importin beta', *Mol Cell Biol,* 29(17), pp. 4788-97.

Esposito, E., Bruscoli, S., Mazzon, E., Paterniti, I., Coppo, M., Velardi, E., Cuzzocrea, S. & Riccardi, C. (2012) 'Glucocorticoid-induced leucine zipper (GILZ) over-expression in T lymphocytes inhibits inflammation and tissue damage in spinal cord injury', *Neurotherapeutics,* 9(1), pp. 210-25.

Fietz, E. R., Keenan, C. R., Lopez-Campos, G., Tu, Y., Johnstone, C. N., Harris, T. & Stewart, A. G. (2017) 'Glucocorticoid resistance of migration and gene expression in a daughter MDA-MB-231 breast

tumour cell line selected for high metastatic potential', *Sci Rep,* 7, pp. 43774.

Fitzsimons, C. P., Ahmed, S., Wittevrongel, C. F., Schouten, T. G., Dijkmans, T. F., Scheenen, W. J., Schaaf, M. J., de Kloet, E. R. & Vreugdenhil, E. (2008) 'The microtubule-associated protein doublecortin-like regulates the transport of the glucocorticoid receptor in neuronal progenitor cells', *Mol Endocrinol,* 22(2), pp. 248-62.

Freel, E. M. & Connell, J. M. (2004) 'Mechanisms of hypertension: the expanding role of aldosterone', *J Am Soc Nephrol,* 15(8), pp. 1993-2001.

Fruchter, O., Kino, T., Zoumakis, E., Alesci, S., De Martino, M., Chrousos, G. & Hochberg, Z. (2005) 'The human glucocorticoid receptor (GR) isoform {beta} differentially suppresses GR{alpha}-induced transactivation stimulated by synthetic glucocorticoids', *J Clin Endocrinol Metab,* 90(6), pp. 3505-9.

Galigniana, M. D., Harrell, J. M., Housley, P. R., Patterson, C., Fisher, S. K. & Pratt, W. B. (2004) 'Retrograde transport of the glucocorticoid receptor in neurites requires dynamic assembly of complexes with the protein chaperone hsp90 and is linked to the CHIP component of the machinery for proteasomal degradation', *Brain Res Mol Brain Res,* 123(1-2), pp. 27-36.

Galigniana, M. D., Radanyi, C., Renoir, J. M., Housley, P. R. & Pratt, W. B. (2001) 'Evidence that the peptidylprolyl isomerase domain of the hsp90-binding immunophilin FKBP52 is involved in both dynein interaction and glucocorticoid receptor movement to the nucleus', *J Biol Chem,* 276(18), pp. 14884-9.

Galliher-Beckley, A. J., Williams, J. G., Collins, J. B. & Cidlowski, J. A. (2008) 'Glycogen synthase kinase 3beta-mediated serine phosphorylation of the human glucocorticoid receptor redirects gene expression profiles', *Mol Cell Biol,* 28(24), pp. 7309-22.

Gametchu, B., Watson, C. S., Shih, C. C. & Dashew, B. (1991) 'Studies on the arrangement of glucocorticoid receptors in the plasma membrane of S-49 lymphoma cells', *Steroids,* 56(8), pp. 411-9.

Gauvreau, G. M., Boulet, L. P., Leigh, R., Cockcroft, D. W., Killian, K. J., Davis, B. E., Deschesnes, F., Watson, R. M., Swystun, V., Mardh, C. K., Wessman, P., Jorup, C., Aurivillius, M. & O'Byrne, P. M. (2015) 'A Nonsteroidal Glucocorticoid Receptor Agonist Inhibits Allergen-induced Late Asthmatic Responses', *Am J Respir Crit Care Med,* 191(2), pp. 161-7.

George, A. A., Schiltz, R. L. & Hager, G. L. (2009) 'Dynamic access of the glucocorticoid receptor to response elements in chromatin', *Int J Biochem Cell Biol,* 41(1), pp. 214-24.

George, S. P., Chen, H., Conrad, J. C. & Khurana, S. (2013) 'Regulation of directional cell migration by membrane-induced actin bundling', *J Cell Sci,* 126(Pt 1), pp. 312-26.

Gibbs, J., Ince, L., Matthews, L., Mei, J., Bell, T., Yang, N., Saer, B., Begley, N., Poolman, T., Pariollaud, M., Farrow, S., DeMayo, F., Hussell, T., Worthen, G. S., Ray, D. & Loudon, A. (2014) 'An epithelial circadian clock controls pulmonary inflammation and glucocorticoid action', *Nat Med,* 20(8), pp. 919-26.

Giguere, V., Hollenberg, S. M., Rosenfeld, M. G. & Evans, R. M. (1986) 'Functional domains of the human glucocorticoid receptor', *Cell,* 46(5), pp. 645-52.

Gonzalez-Robayna, I. J., Falender, A. E., Ochsner, S., Firestone, G. L. & Richards, J. S. (2000) 'Follicle-Stimulating hormone (FSH) stimulates phosphorylation and activation of protein kinase B (PKB/Akt) and serum and glucocorticoid-lnduced kinase (Sgk): evidence for A kinase-independent signaling by FSH in granulosa cells', *Mol Endocrinol,* 14(8), pp. 1283-300.

Gonzalez de Valdivia, E., Broselid, S., Kahn, R., Olde, B. & Leeb-Lundberg, L. M. F. (2017) 'G protein-coupled estrogen receptor 1

(GPER1)/GPR30 increases ERK1/2 activity through PDZ motif-dependent and -independent mechanisms', *J Biol Chem,* 292(24), pp. 9932-9943.

Gonzalez, M. V., Jimenez, B., Berciano, M. T., Gonzalez-Sancho, J. M., Caelles, C., Lafarga, M. & Munoz, A. (2000) 'Glucocorticoids antagonize AP-1 by inhibiting the Activation/phosphorylation of JNK without affecting its subcellular distribution', *J Cell Biol,* 150(5), pp. 1199-208.

Goodman, P. A., Medina-Martinez, O. & Fernandez-Mejia, C. (1996) 'Identification of the human insulin negative regulatory element as a negative glucocorticoid response element', *Mol Cell Endocrinol,* 120(2), pp. 139-46.

Goodwin, J. E., Feng, Y., Velazquez, H., Zhou, H. & Sessa, W. C. (2014) 'Loss of the endothelial glucocorticoid receptor prevents the therapeutic protection afforded by dexamethasone after LPS', *PLoS One,* 9(10), pp. e108126.

Goodwin, J. E. & Geller, D. S. (2012) 'Glucocorticoid-induced hypertension', *Pediatr Nephrol,* 27(7), pp. 1059-66.

Govindan, M. V. (2010) 'Recruitment of cAMP-response element-binding protein and histone deacetylase has opposite effects on glucocorticoid receptor gene transcription', *J Biol Chem,* 285(7), pp. 4489-510.

Grad, I. & Picard, D. (2007) 'The glucocorticoid responses are shaped by molecular chaperones', *Mol Cell Endocrinol,* 275(1-2), pp. 2-12.

Gratsias, Y., Moutsatsou, P., Chrysanthopoulou, G., Tsagarakis, S., Thalassinos, N. & Sekeris, C. E. (2000) 'Diurnal changes in glucocorticoid sensitivity in human peripheral blood samples', *Steroids,* 65(12), pp. 851-6.

Hagiwara, M., Shirai, Y., Nomura, R., Sasaki, M., Kobayashi, K., Tadokoro, T. & Yamamoto, Y. (2009) 'Caveolin-1 activates Rab5

and enhances endocytosis through direct interaction', *Biochem Biophys Res Commun,* 378(1), pp. 73-8.

Hakkinen, K. M., Harunaga, J. S., Doyle, A. D. & Yamada, K. M. (2011) 'Direct comparisons of the morphology, migration, cell adhesions, and actin cytoskeleton of fibroblasts in four different three-dimensional extracellular matrices', *Tissue Eng Part A,* 17(5-6), pp. 713-24.

Hardman, M. J., Waite, A., Zeef, L., Burow, M., Nakayama, T. & Ashcroft, G. S. (2005) 'Macrophage migration inhibitory factor: a central regulator of wound healing', *Am J Pathol,* 167(6), pp. 1561-74.

Hardy, R. S., Raza, K. & Cooper, M. S. (2014) 'Glucocorticoid metabolism in rheumatoid arthritis', *Ann N Y Acad Sci,* 1318, pp. 18-26.

Harris, T. H., Banigan, E. J., Christian, D. A., Konradt, C., Tait Wojno, E. D., Norose, K., Wilson, E. H., John, B., Weninger, W., Luster, A. D., Liu, A. J. & Hunter, C. A. (2012) 'Generalized Levy walks and the role of chemokines in migration of effector CD8+ T cells', *Nature,* 486(7404), pp. 545-8.

He, Y., Yi, W., Suino-Powell, K., Zhou, X. E., Tolbert, W. D., Tang, X., Yang, J., Yang, H., Shi, J., Hou, L., Jiang, H., Melcher, K. & Xu, H. E. (2014) 'Structures and mechanism for the design of highly potent glucocorticoids', *Cell Res,* 24(6), pp. 713-26.

Hernandez-Deviez, D. J., Howes, M. T., Laval, S. H., Bushby, K., Hancock, J. F. & Parton, R. G. (2008) 'Caveolin regulates endocytosis of the muscle repair protein, dysferlin', *J Biol Chem,* 283(10), pp. 6476-88.

Hernandez-Valladares, M., Aasebo, E., Mjaavatten, O., Vaudel, M., Bruserud, O., Berven, F. & Selheim, F. (2016) 'Reliable FASP-based procedures for optimal quantitative proteomic and

phosphoproteomic analysis on samples from acute myeloid leukemia patients', *Biol Proced Online,* 18, pp. 13.

Himes, B. E., Jiang, X., Wagner, P., Hu, R., Wang, Q., Klanderman, B., Whitaker, R. M., Duan, Q., Lasky-Su, J., Nikolos, C., Jester, W., Johnson, M., Panettieri, R. A., Jr., Tantisira, K. G., Weiss, S. T. & Lu, Q. (2014) 'RNA-Seq transcriptome profiling identifies CRISPLD2 as a glucocorticoid responsive gene that modulates cytokine function in airway smooth muscle cells', *PLoS One,* 9(6), pp. e99625.

Hinds, T. D., Stechschulte, L. A., Elkhairi, F. & Sanchez, E. R. (2014) 'Analysis of FK506, timcodar (VX-853) and FKBP51 and FKBP52 chaperones in control of glucocorticoid receptor activity and phosphorylation', *Pharmacol Res Perspect,* 2(6), pp. e00076.

Hirst, S. J. & Lee, T. H. (1998) 'Airway smooth muscle as a target of glucocorticoid action in the treatment of asthma', *Am J Respir Crit Care Med,* 158(5 Pt 3), pp. S201-6.

Hoffman, J. A., Trotter, K. W., Ward, J. M. & Archer, T. K. (2018) 'BRG1 governs glucocorticoid receptor interactions with chromatin and pioneer factors across the genome', *Elife,* 7.

Hollenberg, S. M., Weinberger, C., Ong, E. S., Cerelli, G., Oro, A., Lebo, R., Thompson, E. B., Rosenfeld, M. G. & Evans, R. M. (1985) 'Primary structure and expression of a functional human glucocorticoid receptor cDNA', *Nature,* 318(6047), pp. 635-41.

Hong, J. M., Teitelbaum, S. L., Kim, T. H., Ross, F. P., Kim, S. Y. & Kim, H. J. (2011) 'Calpain-6, a target molecule of glucocorticoids, regulates osteoclastic bone resorption via cytoskeletal organization and microtubule acetylation', *J Bone Miner Res,* 26(3), pp. 657-65.

Hoschutzky, H. & Pongs, O. (1985) 'Characterization of glucocorticoid receptor in HeLa-S3 cells', *Biochemistry,* 24(25), pp. 7348-56.

Hua, G., Paulen, L. & Chambon, P. (2016) 'GR SUMOylation and formation of an SUMO-SMRT/NCoR1-HDAC3 repressing complex is mandatory for GC-induced IR nGRE-mediated transrepression', *Proc Natl Acad Sci U S A,* 113(5), pp. E626-34.

Huang, G. X., Pan, X. Y., Jin, Y. D., Wang, Y., Song, X. L., Wang, C. H., Li, Y. D. & Lu, J. (2016) 'The mechanisms and significance of up-regulation of RhoB expression by hypoxia and glucocorticoid in rat lung and A549 cells', *J Cell Mol Med,* 20(7), pp. 1276-86.

Huang, G. X., Qi, M. F., Li, X. L., Tang, F. & Zhu, L. (2018) 'Involvement of upregulation of fibronectin in the proadhesive and prosurvival effects of glucocorticoid on melanoma cells', *Mol Med Rep,* 17(2), pp. 3380-3387.

Hubbert, C., Guardiola, A., Shao, R., Kawaguchi, Y., Ito, A., Nixon, A., Yoshida, M., Wang, X. F. & Yao, T. P. (2002) 'HDAC6 is a microtubule-associated deacetylase', *Nature,* 417(6887), pp. 455-8.

Hudson, W. H., Youn, C. & Ortlund, E. A. (2013) 'The structural basis of direct glucocorticoid-mediated transrepression', *Nat Struct Mol Biol,* 20(1), pp. 53-8.

Inaba, H. & Pui, C. H. (2010) 'Glucocorticoid use in acute lymphoblastic leukaemia', *Lancet Oncol,* 11(11), pp. 1096-106.

Ito, A., Takii, T., Matsumura, T. & Onozaki, K. (1999) 'Augmentation of type I IL-1 receptor expression and IL-1 signaling by IL-6 and glucocorticoid in murine hepatocytes', *J Immunol,* 162(7), pp. 4260-5.

Ito, K., Yamamura, S., Essilfie-Quaye, S., Cosio, B., Ito, M., Barnes, P. J. & Adcock, I. M. (2006) 'Histone deacetylase 2-mediated deacetylation of the glucocorticoid receptor enables NF-kappaB suppression', *J Exp Med,* 203(1), pp. 7-13.

Itoh, M., Adachi, M., Yasui, H., Takekawa, M., Tanaka, H. & Imai, K. (2002) 'Nuclear export of glucocorticoid receptor is enhanced by c-Jun N-terminal kinase-mediated phosphorylation', *Mol Endocrinol,* 16(10), pp. 2382-92.

Iwasaki, Y., Aoki, Y., Katahira, M., Oiso, Y. & Saito, H. (1997) 'Non-genomic mechanisms of glucocorticoid inhibition of adrenocorticotropin secretion: possible involvement of GTP-binding protein', *Biochem Biophys Res Commun,* 235(2), pp. 295-9.

Jenkins, B. D., Pullen, C. B. & Darimont, B. D. (2001) 'Novel glucocorticoid receptor coactivator effector mechanisms', *Trends Endocrinol Metab,* 12(3), pp. 122-6.

Jewell, C. M., Scoltock, A. B., Hamel, B. L., Yudt, M. R. & Cidlowski, J. A. (2012) 'Complex human glucocorticoid receptor dim mutations define glucocorticoid induced apoptotic resistance in bone cells', *Mol Endocrinol,* 26(2), pp. 244-56.

John, N. J., Bravo, D. A. & Firestone, G. L. (1989) 'Glucocorticoid responsiveness of mouse mammary tumor virus (MMTV) promoters in a down-transcription hepatoma tissue culture (HTC) variant', *Mol Cell Endocrinol,* 61(1), pp. 57-68.

Juanes, M. A., Bouguenina, H., Eskin, J. A., Jaiswal, R., Badache, A. & Goode, B. L. (2017) 'Adenomatous polyposis coli nucleates actin assembly to drive cell migration and microtubule-induced focal adhesion turnover', *J Cell Biol,* 216(9), pp. 2859-2875.

Kadmiel, M., Janoshazi, A., Xu, X. & Cidlowski, J. A. (2016) 'Glucocorticoid action in human corneal epithelial cells establishes roles for corticosteroids in wound healing and barrier function of the eye', *Exp Eye Res,* 152, pp. 10-33.

Kagoshima, M., Wilcke, T., Ito, K., Tsaprouni, L., Barnes, P. J., Punchard, N. & Adcock, I. M. (2001) 'Glucocorticoid-mediated

transrepression is regulated by histone acetylation and DNA methylation', *Eur J Pharmacol,* 429(1-3), pp. 327-34.

Karmakar, S., Jin, Y. & Nagaich, A. K. (2013) 'Interaction of glucocorticoid receptor (GR) with estrogen receptor (ER) alpha and activator protein 1 (AP1) in dexamethasone-mediated interference of ERalpha activity', *J Biol Chem,* 288(33), pp. 24020-34.

Kaverina, I. & Straube, A. (2011) 'Regulation of cell migration by dynamic microtubules', *Semin Cell Dev Biol,* 22(9), pp. 968-74.

Kekatpure, V. D., Dannenberg, A. J. & Subbaramaiah, K. (2009) 'HDAC6 modulates Hsp90 chaperone activity and regulates activation of aryl hydrocarbon receptor signaling', *J Biol Chem,* 284(12), pp. 7436-45.

Khan, M. O. & Lee, H. J. (2008) 'Synthesis and pharmacology of anti-inflammatory steroidal antedrugs', *Chem Rev,* 108(12), pp. 5131-45.

Khan, S. H., McLaughlin, W. A. & Kumar, R. (2017) 'Site-specific phosphorylation regulates the structure and function of an intrinsically disordered domain of the glucocorticoid receptor', *Sci Rep,* 7(1), pp. 15440.

Khan, Z. A., Barbin, Y. P., Farhangkhoee, H., Beier, N., Scholz, W. & Chakrabarti, S. (2005) 'Glucose-induced serum- and glucocorticoid-regulated kinase activation in oncofetal fibronectin expression', *Biochem Biophys Res Commun,* 329(1), pp. 275-80.

Ki, S. H., Cho, I. J., Choi, D. W. & Kim, S. G. (2005) 'Glucocorticoid receptor (GR)-associated SMRT binding to C/EBPbeta TAD and Nrf2 Neh4/5: role of SMRT recruited to GR in GSTA2 gene repression', *Mol Cell Biol,* 25(10), pp. 4150-65.

Kino, T. & Chrousos, G. P. (2011) 'Acetylation-mediated epigenetic regulation of glucocorticoid receptor activity: circadian rhythm-

associated alterations of glucocorticoid actions in target tissues', *Mol Cell Endocrinol,* 336(1-2), pp. 23-30.

Kino, T., Kopp, J. B. & Chrousos, G. P. (2000) 'Glucocorticoids suppress human immunodeficiency virus type-1 long terminal repeat activity in a cell type-specific, glucocorticoid receptor-mediated fashion: direct protective effects at variance with clinical phenomenology', *J Steroid Biochem Mol Biol,* 75(4-5), pp. 283-90.

Kino, T., Manoli, I., Kelkar, S., Wang, Y., Su, Y. A. & Chrousos, G. P. (2009) 'Glucocorticoid receptor (GR) beta has intrinsic, GRalpha-independent transcriptional activity', *Biochem Biophys Res Commun,* 381(4), pp. 671-5.

Kino, T., Tiulpakov, A., Ichijo, T., Chheng, L., Kozasa, T. & Chrousos, G. P. (2005) 'G protein beta interacts with the glucocorticoid receptor and suppresses its transcriptional activity in the nucleus', *J Cell Biol,* 169(6), pp. 885-96.

Kisanga, E. P., Tang, Z., Guller, S. & Whirledge, S. (2018) 'Glucocorticoid signaling regulates cell invasion and migration in the human first-trimester trophoblast cell line Sw.71', *Am J Reprod Immunol,* 80(1), pp. e12974.

Kleiman, A., Hubner, S., Rodriguez Parkitna, J. M., Neumann, A., Hofer, S., Weigand, M. A., Bauer, M., Schmid, W., Schutz, G., Libert, C., Reichardt, H. M. & Tuckermann, J. P. (2012) 'Glucocorticoid receptor dimerization is required for survival in septic shock via suppression of interleukin-1 in macrophages', *FASEB J,* 26(2), pp. 722-9.

Kovacs, J. J., Murphy, P. J., Gaillard, S., Zhao, X., Wu, J. T., Nicchitta, C. V., Yoshida, M., Toft, D. O., Pratt, W. B. & Yao, T. P. (2005) 'HDAC6 regulates Hsp90 acetylation and chaperone-dependent activation of glucocorticoid receptor', *Mol Cell,* 18(5), pp. 601-7.

Kramer, O. H., Mahboobi, S. & Sellmer, A. (2014) 'Drugging the HDAC6-HSP90 interplay in malignant cells', *Trends Pharmacol Sci,* 35(10), pp. 501-9.

Krause, D., Rau, R. & Braun, J. (2011) 'Glucocorticoid treatment in early rheumatoid arthritis', *Clin Exp Rheumatol,* 29(5 Suppl 68), pp. S121-5.

Krieger, J. W., Singh, A. P., Bag, N., Garbe, C. S., Saunders, T. E., Langowski, J. & Wohland, T. (2015) 'Imaging fluorescence (cross-) correlation spectroscopy in live cells and organisms', *Nat Protoc,* 10(12), pp. 1948-74.

Kuhlman, P. A. (2005) 'Dynamic changes in the length distribution of actin filaments during polymerization can be modulated by barbed end capping proteins', *Cell Motil Cytoskeleton,* 61(1), pp. 1-8.

Kumar, R. & Thompson, E. B. (2005) 'Gene regulation by the glucocorticoid receptor: structure:function relationship', *J Steroid Biochem Mol Biol,* 94(5), pp. 383-94.

Kumar, R. & Thompson, E. B. (2012) 'Folding of the glucocorticoid receptor N-terminal transactivation function: dynamics and regulation', *Mol Cell Endocrinol,* 348(2), pp. 450-6.

Kuna, P., Aurivillius, M., Jorup, C., Prothon, S., Taib, Z. & Edsbacker, S. (2017) 'Efficacy and Tolerability of an Inhaled Selective Glucocorticoid Receptor Modulator - AZD5423 - in Chronic Obstructive Pulmonary Disease Patients: Phase II Study Results', *Basic Clin Pharmacol Toxicol,* 121(4), pp. 279-289.

Kunkemoeller, B. & Kyriakides, T. R. (2017) 'Redox Signaling in Diabetic Wound Healing Regulates Extracellular Matrix Deposition', *Antioxid Redox Signal,* 27(12), pp. 823-838.

Kurihara, I., Shibata, H., Suzuki, T., Ando, T., Kobayashi, S., Hayashi, M., Saito, I. & Saruta, T. (2002) 'Expression and regulation of

nuclear receptor coactivators in glucocorticoid action', *Mol Cell Endocrinol,* 189(1-2), pp. 181-9.

Kuzmich, D., Kirrane, T., Proudfoot, J., Bekkali, Y., Zindell, R., Beck, L., Nelson, R., Shih, C. K., Kukulka, A. J., Paw, Z., Reilly, P., Deleon, R., Cardozo, M., Nabozny, G. & Thomson, D. (2007) 'Identification of dissociated non-steroidal glucocorticoid receptor agonists', *Bioorg Med Chem Lett,* 17(18), pp. 5025-31.

Kuzmina, A., Verstraete, N., Galker, S., Maatook, M., Bensaude, O. & Taube, R. (2014) 'A single point mutation in cyclin T1 eliminates binding to Hexim1, Cdk9 and RNA but not to AFF4 and enforces repression of HIV transcription', *Retrovirology,* 11, pp. 51.

Le Drean, Y., Mincheneau, N., Le Goff, P. & Michel, D. (2002) 'Potentiation of glucocorticoid receptor transcriptional activity by sumoylation', *Endocrinology,* 143(9), pp. 3482-9.

Leaker, B. R., O'Connor, B., Singh, D. & Barnes, P. J. (2015) 'The novel inhaled glucocorticoid receptor agonist GW870086X protects against adenosine-induced bronchoconstriction in asthma', *J Allergy Clin Immunol,* 136(2), pp. 501-2 e6.

Lecker, S. H., Goldberg, A. L. & Mitch, W. E. (2006) 'Protein degradation by the ubiquitin-proteasome pathway in normal and disease states', *J Am Soc Nephrol,* 17(7), pp. 1807-19.

Lee, H. W., Kyung, T., Yoo, J., Kim, T., Chung, C., Ryu, J. Y., Lee, H., Park, K., Lee, S., Jones, W. D., Lim, D. S., Hyeon, C., Heo, W. D. & Yoon, T. Y. (2013) 'Real-time single-molecule co-immunoprecipitation analyses reveal cancer-specific Ras signalling dynamics', *Nat Commun,* 4, pp. 1505.

Leis, H., Page, A., Ramirez, A., Bravo, A., Segrelles, C., Paramio, J., Barettino, D., Jorcano, J. L. & Perez, P. (2004) 'Glucocorticoid Receptor Counteracts Tumorigenic Activity of Akt in Skin through Interference with the Phosphatidylinositol 3-Kinase Signaling Pathway', *Mol Endocrinol,* 18(2), pp. 303-11.

Lewis-Tuffin, L. J. & Cidlowski, J. A. (2006) 'The physiology of human glucocorticoid receptor beta (hGRbeta) and glucocorticoid resistance', *Ann N Y Acad Sci,* 1069, pp. 1-9.

Li, D., Xie, S., Ren, Y., Huo, L., Gao, J., Cui, D., Liu, M. & Zhou, J. (2011) 'Microtubule-associated deacetylase HDAC6 promotes angiogenesis by regulating cell migration in an EB1-dependent manner', *Protein Cell,* 2(2), pp. 150-60.

Li, N., Tie, X. J., Liu, P. J., Zhang, Y., Ren, H. Z., Gao, X. & Xu, Z. Q. (2013) 'Effects of down-regulation of HDAC6 expression on proliferation, cell cycling and migration of esophageal squamous cell carcinoma cells and related molecular mechanisms', *Asian Pac J Cancer Prev,* 14(2), pp. 685-9.

Li, X., Chatterjee, N., Spirohn, K., Boutros, M. & Bohmann, D. (2016) 'Cdk12 Is A Gene-Selective RNA Polymerase II Kinase That Regulates a Subset of the Transcriptome, Including Nrf2 Target Genes', *Sci Rep,* 6, pp. 21455.

Liang, K., Gao, X., Gilmore, J. M., Florens, L., Washburn, M. P., Smith, E. & Shilatifard, A. (2015) 'Characterization of human cyclin-dependent kinase 12 (CDK12) and CDK13 complexes in C-terminal domain phosphorylation, gene transcription, and RNA processing', *Mol Cell Biol,* 35(6), pp. 928-38.

Lim, H. W., Uhlenhaut, N. H., Rauch, A., Weiner, J., Hubner, S., Hubner, N., Won, K. J., Lazar, M. A., Tuckermann, J. & Steger, D. J. (2015) 'Genomic redistribution of GR monomers and dimers mediates transcriptional response to exogenous glucocorticoid in vivo', *Genome Res,* 25(6), pp. 836-44.

Limbourg, F. P. & Liao, J. K. (2003) 'Nontranscriptional actions of the glucocorticoid receptor', *J Mol Med (Berl),* 81(3), pp. 168-74.

Lipworth, B. J. & Menzies, D. (2005) 'Systemic versus topical glucocorticoid therapy for acute asthma', *Am J Respir Crit Care Med,* 172(8), pp. 1055; author reply 1055.

Liu, J. & DeFranco, D. B. (2000) 'Protracted nuclear export of glucocorticoid receptor limits its turnover and does not require the exportin 1/CRM1-directed nuclear export pathway', *Mol Endocrinol,* 14(1), pp. 40-51.

Liu, L., Aleksandrowicz, E., Schonsiegel, F., Groner, D., Bauer, N., Nwaeburu, C. C., Zhao, Z., Gladkich, J., Hoppe-Tichy, T., Yefenof, E., Hackert, T., Strobel, O. & Herr, I. (2017) 'Dexamethasone mediates pancreatic cancer progression by glucocorticoid receptor, TGFbeta and JNK/AP-1', *Cell Death Dis,* 8(10), pp. e3064.

Liu, Y., Peng, L., Seto, E., Huang, S. & Qiu, Y. (2012) 'Modulation of histone deacetylase 6 (HDAC6) nuclear import and tubulin deacetylase activity through acetylation', *J Biol Chem,* 287(34), pp. 29168-74.

Longui, C. A. (2007) 'Glucocorticoid therapy: minimizing side effects', *J Pediatr (Rio J),* 83(5 Suppl), pp. S163-77.

Lu, N. Z. & Cidlowski, J. A. (2004) 'The origin and functions of multiple human glucocorticoid receptor isoforms', *Ann N Y Acad Sci,* 1024, pp. 102-23.

Lu, Z., Ricci, W. A., Schmitz, R. J. & Zhang, X. (2018) 'Identification of cis-regulatory elements by chromatin structure', *Curr Opin Plant Biol,* 42, pp. 90-94.

Lucki, N. C., Li, D. & Sewer, M. B. (2012) 'Sphingosine-1-phosphate rapidly increases cortisol biosynthesis and the expression of genes involved in cholesterol uptake and transport in H295R adrenocortical cells', *Mol Cell Endocrinol,* 348(1), pp. 165-75.

Lund, B., Storm, T. L., Lund, B., Melsen, F., Mosekilde, L., Andersen, R. B., Egmose, C. & Sorensen, O. H. (1985) 'Bone mineral loss, bone histomorphometry and vitamin D metabolism in patients with rheumatoid arthritis on long-term glucocorticoid treatment', *Clin Rheumatol,* 4(2), pp. 143-9.

Lundback, T., Cairns, C., Gustafsson, J. A., Carlstedt-Duke, J. & Hard, T. (1993) 'Thermodynamics of the glucocorticoid receptor-DNA interaction: binding of wild-type GR DBD to different response elements', *Biochemistry,* 32(19), pp. 5074-82.

Magni, M., Ruscica, V., Restelli, M., Fontanella, E., Buscemi, G. & Zannini, L. (2015) 'CCAR2/DBC1 is required for Chk2-dependent KAP1 phosphorylation and repair of DNA damage', *Oncotarget,* 6(19), pp. 17817-31.

Mammi, C., Marzolla, V., Armani, A., Feraco, A., Antelmi, A., Maslak, E., Chlopicki, S., Cinti, F., Hunt, H., Fabbri, A. & Caprio, M. (2016) 'A novel combined glucocorticoid-mineralocorticoid receptor selective modulator markedly prevents weight gain and fat mass expansion in mice fed a high-fat diet', *Int J Obes (Lond),* 40(6), pp. 964-72.

Matsubayashi, Y., Ebisuya, M., Honjoh, S. & Nishida, E. (2004) 'ERK activation propagates in epithelial cell sheets and regulates their migration during wound healing', *Curr Biol,* 14(8), pp. 731-5.

Matthews, L., Berry, A., Ohanian, V., Ohanian, J., Garside, H. & Ray, D. (2008) 'Caveolin mediates rapid glucocorticoid effects and couples glucocorticoid action to the antiproliferative program', *Mol Endocrinol,* 22(6), pp. 1320-30.

Matthews, L., Johnson, J., Berry, A., Trebble, P., Cookson, A., Spiller, D., Rivers, C., Norman, M., White, M. & Ray, D. (2011) 'Cell cycle phase regulates glucocorticoid receptor function', *PLoS One,* 6(7), pp. e22289.

Mayanagi, T., Morita, T., Hayashi, K., Fukumoto, K. & Sobue, K. (2008) 'Glucocorticoid receptor-mediated expression of caldesmon regulates cell migration via the reorganization of the actin cytoskeleton', *J Biol Chem,* 283(45), pp. 31183-96.

McDougall, S., Dallon, J., Sherratt, J. & Maini, P. (2006) 'Fibroblast migration and collagen deposition during dermal wound healing: mathematical modelling and clinical implications', *Philos Trans A Math Phys Eng Sci,* 364(1843), pp. 1385-405.

McMaster, A., Chambers, T., Meng, Q. J., Grundy, S., Loudon, A. S., Donn, R. & Ray, D. W. (2008) 'Real-time analysis of gene regulation by glucocorticoid hormones', *J Endocrinol,* 197(2), pp. 205-11.

Mehta, A. B., Nadkarni, N. J., Patil, S. P., Godse, K. V., Gautam, M. & Agarwal, S. (2016) 'Topical corticosteroids in dermatology', *Indian J Dermatol Venereol Leprol,* 82(4), pp. 371-8.

Melin, J., Prothon, S., Kloft, C., Cleton, A., Amilon, C., Jorup, C., Backman, P., Olsson, B. & Hamren, U. W. (2017) 'Pharmacokinetics of the Inhaled Selective Glucocorticoid Receptor Modulator AZD5423 Following Inhalation Using Different Devices', *AAPS J,* 19(3), pp. 865-874.

Memmel, S., Sisario, D., Zoller, C., Fiedler, V., Katzer, A., Heiden, R., Becker, N., Eing, L., Ferreira, F. L. R., Zimmermann, H., Sauer, M., Flentje, M., Sukhorukov, V. L. & Djuzenova, C. S. (2017) 'Migration pattern, actin cytoskeleton organization and response to PI3K-, mTOR-, and Hsp90-inhibition of glioblastoma cells with different invasive capacities', *Oncotarget,* 8(28), pp. 45298-45310.

Meyer, M., Lara, A., Hunt, H., Belanoff, J., de Kloet, E. R., Gonzalez Deniselle, M. C. & De Nicola, A. F. (2018) 'The Selective Glucocorticoid Receptor Modulator Cort 113176 Reduces Neurodegeneration and Neuroinflammation in Wobbler Mice Spinal Cord', *Neuroscience,* 384, pp. 384-396.

Min, J. S., Kim, J. C., Kim, J. A., Kang, I. & Ahn, J. K. (2018) 'SIRT2 reduces actin polymerization and cell migration through deacetylation and degradation of HSP90', *Biochim Biophys Acta Mol Cell Res,* 1865(9), pp. 1230-1238.

Miyake, Y., Keusch, J. J., Wang, L., Saito, M., Hess, D., Wang, X., Melancon, B. J., Helquist, P., Gut, H. & Matthias, P. (2016) 'Structural insights into HDAC6 tubulin deacetylation and its selective inhibition', *Nat Chem Biol,* 12(9), pp. 748-54.

Miyoshi, S., Hey-Hadavi, J., Nagaoka, M. & Tammara, B. (2016) 'Pharmacokinetics and food-effect of fosdagrocorat (PF-04171327), a dissociated agonist of the glucocorticoid receptor, in healthy adult Caucasian and Japanese subjects', *Int J Clin Pharmacol Ther,* 54(12), pp. 966-976.

Moghadam-Kia, S. & Werth, V. P. (2010) 'Prevention and treatment of systemic glucocorticoid side effects', *Int J Dermatol,* 49(3), pp. 239-48.

Moraitis, A. N., Giguere, V. & Thompson, C. C. (2002) 'Novel mechanism of nuclear receptor corepressor interaction dictated by activation function 2 helix determinants', *Mol Cell Biol,* 22(19), pp. 6831-41.

Morgan, D. J., Poolman, T. M., Williamson, A. J., Wang, Z., Clark, N. R., Ma'ayan, A., Whetton, A. D., Brass, A., Matthews, L. C. & Ray, D. W. (2016) 'Glucocorticoid receptor isoforms direct distinct mitochondrial programs to regulate ATP production', *Sci Rep,* 6, pp. 26419.

Mouneimne, G., Hansen, S. D., Selfors, L. M., Petrak, L., Hickey, M. M., Gallegos, L. L., Simpson, K. J., Lim, J., Gertler, F. B., Hartwig, J. H., Mullins, R. D. & Brugge, J. S. (2012) 'Differential remodeling of actin cytoskeleton architecture by profilin isoforms leads to distinct effects on cell migration and invasion', *Cancer Cell,* 22(5), pp. 615-30.

Mukudai, S., Hiwatashi, N., Bing, R., Garabedian, M. & Branski, R. C. (2018) 'Phosphorylation of the glucocorticoid receptor alters SMAD signaling in vocal fold fibroblasts', *Laryngoscope*.

Murakami, N., Fukuchi, S., Takeuchi, K., Hori, T., Shibamoto, S. & Ito, F. (1998) 'Antagonistic regulation of cell migration by epidermal growth factor and glucocorticoid in human gastric carcinoma cells', *J Cell Physiol,* 176(1), pp. 127-37.

Mylka, V., Deckers, J., Ratman, D., De Cauwer, L., Thommis, J., De Rycke, R., Impens, F., Libert, C., Tavernier, J., Vanden Berghe, W., Gevaert, K. & De Bosscher, K. (2018) 'The autophagy receptor SQSTM1/p62 mediates anti-inflammatory actions of the selective NR3C1/glucocorticoid receptor modulator compound A (CpdA) in macrophages', *Autophagy,* 14(12), pp. 2049-2064.

Niraula, A., Wang, Y., Godbout, J. P. & Sheridan, J. F. (2018) 'Corticosterone Production during Repeated Social Defeat Causes Monocyte Mobilization from the Bone Marrow, Glucocorticoid Resistance, and Neurovascular Adhesion Molecule Expression', *J Neurosci,* 38(9), pp. 2328-2340.

Noel, S. D., Keen, K. L., Baumann, D. I., Filardo, E. J. & Terasawa, E. (2009) 'Involvement of G protein-coupled receptor 30 (GPR30) in rapid action of estrogen in primate LHRH neurons', *Mol Endocrinol,* 23(3), pp. 349-59.

Oakley, F. D., Smith, R. L. & Engelhardt, J. F. (2009) 'Lipid rafts and caveolin-1 coordinate interleukin-1beta (IL-1beta)-dependent activation of NFkappaB by controlling endocytosis of Nox2 and IL-1beta receptor 1 from the plasma membrane', *J Biol Chem,* 284(48), pp. 33255-64.

Oakley, R. H. & Cidlowski, J. A. (2011) 'Cellular processing of the glucocorticoid receptor gene and protein: new mechanisms for generating tissue-specific actions of glucocorticoids', *J Biol Chem,* 286(5), pp. 3177-84.

Oehling, A. G., Akdis, C. A., Schapowal, A., Blaser, K., Schmitz, M. & Simon, H. U. (1997) 'Suppression of the immune system by oral glucocorticoid therapy in bronchial asthma', *Allergy,* 52(2), pp. 144-54.

Ogasawara, N., Poposki, J. A., Klingler, A. I., Tan, B. K., Weibman, A. R., Hulse, K. E., Stevens, W. W., Peters, A. T., Grammer, L. C., Schleimer, R. P., Welch, K. C., Smith, S. S., Conley, D. B., Raviv, J. R., Soroosh, P., Akbari, O., Himi, T., Kern, R. C. & Kato, A. (2018) 'IL-10, TGF-beta, and glucocorticoid prevent the production of type 2 cytokines in human group 2 innate lymphoid cells', *J Allergy Clin Immunol,* 141(3), pp. 1147-1151 e8.

Oh, K. S., Patel, H., Gottschalk, R. A., Lee, W. S., Baek, S., Fraser, I. D. C., Hager, G. L. & Sung, M. H. (2017) 'Anti-Inflammatory Chromatinscape Suggests Alternative Mechanisms of Glucocorticoid Receptor Action', *Immunity,* 47(2), pp. 298-309 e5.

Oppong, E., Hedde, P. N., Sekula-Neuner, S., Yang, L., Brinkmann, F., Dorlich, R. M., Hirtz, M., Fuchs, H., Nienhaus, G. U. & Cato, A. C. (2014) 'Localization and dynamics of glucocorticoid receptor at the plasma membrane of activated mast cells', *Small,* 10(10), pp. 1991-8.

Ou, X. M., Storring, J. M., Kushwaha, N. & Albert, P. R. (2001) 'Heterodimerization of mineralocorticoid and glucocorticoid receptors at a novel negative response element of the 5-HT1A receptor gene', *J Biol Chem,* 276(17), pp. 14299-307.

Paakinaho, V., Kaikkonen, S., Levonen, A. L. & Palvimo, J. J. (2014a) 'Electrophilic lipid mediator 15-deoxy-Delta12,14-prostaglandin j2 modifies glucocorticoid signaling via receptor SUMOylation', *Mol Cell Biol,* 34(17), pp. 3202-13.

Paakinaho, V., Kaikkonen, S., Makkonen, H., Benes, V. & Palvimo, J. J. (2014b) 'SUMOylation regulates the chromatin occupancy and

anti-proliferative gene programs of glucocorticoid receptor', *Nucleic Acids Res,* 42(3), pp. 1575-92.

Paakinaho, V., Makkonen, H., Jaaskelainen, T. & Palvimo, J. J. (2010) 'Glucocorticoid receptor activates poised FKBP51 locus through long-distance interactions', *Mol Endocrinol,* 24(3), pp. 511-25.

Paguio, A., Stecha, P., Wood, K. V. & Fan, F. (2010) 'Improved dual-luciferase reporter assays for nuclear receptors', *Curr Chem Genomics,* 4, pp. 43-9.

Pariante, C. M. (2009) 'Risk factors for development of depression and psychosis. Glucocorticoid receptors and pituitary implications for treatment with antidepressant and glucocorticoids', *Ann N Y Acad Sci,* 1179, pp. 144-52.

Patel, R., Williams-Dautovich, J. & Cummins, C. L. (2014) 'Minireview: new molecular mediators of glucocorticoid receptor activity in metabolic tissues', *Mol Endocrinol,* 28(7), pp. 999-1011.

Pawlak, M., Lefebvre, P. & Staels, B. (2012) 'General molecular biology and architecture of nuclear receptors', *Curr Top Med Chem,* 12(6), pp. 486-504.

Peng, R., Li, Z., Lin, Z., Wang, Y., Wang, W., Hu, B., Wang, X., Zhang, J., Wang, Y., Zhou, R., Lu, C., Shen, Y., Wang, J. & Shi, G. (2015) 'The HSP90 inhibitor 17-PAG effectively inhibits the proliferation and migration of androgen-independent prostate cancer cells', *Am J Cancer Res,* 5(10), pp. 3198-209.

Pfeiffer, J., Tarbashevich, K., Bandemer, J., Palm, T. & Raz, E. (2018) 'Rapid progression through the cell cycle ensures efficient migration of primordial germ cells - The role of Hsp90', *Dev Biol,* 436(2), pp. 84-93.

Piperno, G., LeDizet, M. & Chang, X. J. (1987) 'Microtubules containing acetylated alpha-tubulin in mammalian cells in culture', *J Cell Biol,* 104(2), pp. 289-302.

Pitaval, A., Senger, F., Letort, G., Gidrol, X., Guyon, L., Sillibourne, J. & Thery, M. (2017) 'Microtubule stabilization drives 3D centrosome migration to initiate primary ciliogenesis', *J Cell Biol,* 216(11), pp. 3713-3728.

Presman, D. M., Ganguly, S., Schiltz, R. L., Johnson, T. A., Karpova, T. S. & Hager, G. L. (2016) 'DNA binding triggers tetramerization of the glucocorticoid receptor in live cells', *Proc Natl Acad Sci U S A,* 113(29), pp. 8236-41.

Presman, D. M. & Hager, G. L. (2017) 'More than meets the dimer: What is the quaternary structure of the glucocorticoid receptor?', *Transcription,* 8(1), pp. 32-39.

Presman, D. M., Ogara, M. F., Stortz, M., Alvarez, L. D., Pooley, J. R., Schiltz, R. L., Grontved, L., Johnson, T. A., Mittelstadt, P. R., Ashwell, J. D., Ganesan, S., Burton, G., Levi, V., Hager, G. L. & Pecci, A. (2014) 'Live cell imaging unveils multiple domain requirements for in vivo dimerization of the glucocorticoid receptor', *PLoS Biol,* 12(3), pp. e1001813.

Prossnitz, E. R., Arterburn, J. B., Smith, H. O., Oprea, T. I., Sklar, L. A. & Hathaway, H. J. (2008) 'Estrogen signaling through the transmembrane G protein-coupled receptor GPR30', *Annu Rev Physiol,* 70, pp. 165-90.

Przybycien-Szymanska, M. M., Mott, N. N. & Pak, T. R. (2011) 'Alcohol dysregulates corticotropin-releasing-hormone (CRH) promoter activity by interfering with the negative glucocorticoid response element (nGRE)', *PLoS One,* 6(10), pp. e26647.

Rajapandi, T., Greene, L. E. & Eisenberg, E. (2000) 'The molecular chaperones Hsp90 and Hsc70 are both necessary and sufficient to activate hormone binding by glucocorticoid receptor', *J Biol Chem,* 275(29), pp. 22597-604.

Rao, N. A., McCalman, M. T., Moulos, P., Francoijs, K. J., Chatziioannou, A., Kolisis, F. N., Alexis, M. N., Mitsiou, D. J. & Stunnenberg, H. G. (2011) 'Coactivation of GR and NFKB alters the repertoire of their binding sites and target genes', *Genome Res,* 21(9), pp. 1404-16.

Rao, R., Fiskus, W., Yang, Y., Lee, P., Joshi, R., Fernandez, P., Mandawat, A., Atadja, P., Bradner, J. E. & Bhalla, K. (2008) 'HDAC6 inhibition enhances 17-AAG--mediated abrogation of hsp90 chaperone function in human leukemia cells', *Blood,* 112(5), pp. 1886-93.

Razavi, H., Riether, D., Harcken, C., Bentzien, J., Dinallo, R. M., Souza, D., Nelson, R. M., Kukulka, A., Fadra-Khan, T. N., Pack, E. J., Jr., Zuvela-Jelaska, L., Pelletier, J., Panzenbeck, M., Torcellini, C. A., Proudfoot, J. R., Nabozny, G. H. & Thomson, D. S. (2014) 'Discovery of a potent and dissociated non-steroidal glucocorticoid receptor agonist containing an alkyl carbinol pharmacophore', *Bioorg Med Chem Lett,* 24(8), pp. 1934-40.

Ressad, F., Didry, D., Egile, C., Pantaloni, D. & Carlier, M. F. (1999) 'Control of actin filament length and turnover by actin depolymerizing factor (ADF/cofilin) in the presence of capping proteins and ARP2/3 complex', *J Biol Chem,* 274(30), pp. 20970-6.

Ricci, E., Ronchetti, S., Pericolini, E., Gabrielli, E., Cari, L., Gentili, M., Roselletti, E., Migliorati, G., Vecchiarelli, A. & Riccardi, C. (2017) 'Role of the glucocorticoid-induced leucine zipper gene in dexamethasone-induced inhibition of mouse neutrophil migration via control of annexin A1 expression', *FASEB J,* 31(7), pp. 3054-3065.

Ridley, A. J., Schwartz, M. A., Burridge, K., Firtel, R. A., Ginsberg, M. H., Borisy, G., Parsons, J. T. & Horwitz, A. R. (2003) 'Cell migration: integrating signals from front to back', *Science,* 302(5651), pp. 1704-9.

Rimando, M. G., Wu, H. H., Liu, Y. A., Lee, C. W., Kuo, S. W., Lo, Y. P., Tseng, K. F., Liu, Y. S. & Lee, O. K. (2016) 'Glucocorticoid receptor and Histone deacetylase 6 mediate the differential effect of dexamethasone during osteogenesis of mesenchymal stromal cells (MSCs)', *Sci Rep,* 6, pp. 37371.

Ripp, S. L., Mukherjee, A., Eng, H., Stock, T., Fleishaker, D., Checchio, T. & Tammara, B. (2017) 'In Vitro and In Vivo Investigation of Potential for Complex CYP3A Interaction for PF-00251802 (Dagrocorat), a Novel Dissociated Agonist of the Glucocorticoid Receptor', *Clin Pharmacol Drug Dev*.

Rodriguez-Paredes, M., Ceballos-Chavez, M., Esteller, M., Garcia-Dominguez, M. & Reyes, J. C. (2009) 'The chromatin remodeling factor CHD8 interacts with elongating RNA polymerase II and controls expression of the cyclin E2 gene', *Nucleic Acids Res,* 37(8), pp. 2449-60.

Russcher, H., Dalm, V. A., de Jong, F. H., Brinkmann, A. O., Hofland, L. J., Lamberts, S. W. & Koper, J. W. (2007) 'Associations between promoter usage and alternative splicing of the glucocorticoid receptor gene', *J Mol Endocrinol,* 38(1-2), pp. 91-8.

Salas-Gonzalez, D., Gorriz, J. M., Ramirez, J., Schloegl, M., Lang, E. W. & Ortiz, A. (2013) 'Parameterization of the distribution of white and grey matter in MRI using the alpha-stable distribution', *Comput Biol Med,* 43(5), pp. 559-67.

Salem, S., Harris, T., Mok, J. S., Li, M. Y., Keenan, C. R., Schuliga, M. J. & Stewart, A. G. (2012) 'Transforming growth factor-beta impairs glucocorticoid activity in the A549 lung adenocarcinoma cell line', *Br J Pharmacol,* 166(7), pp. 2036-48.

Salomon-Kent, R., Marom, R., John, S., Dundr, M., Schiltz, L. R., Gutierrez, J., Workman, J., Benayahu, D. & Hager, G. L. (2015) 'New Face for Chromatin-Related Mesenchymal Modulator: n-CHD9 Localizes to Nucleoli and Interacts With Ribosomal Genes', *J Cell Physiol,* 230(9), pp. 2270-80.

Salter, M., Biggadike, K., Matthews, J. L., West, M. R., Haase, M. V., Farrow, S. N., Uings, I. J. & Gray, D. W. (2007) 'Pharmacological properties of the enhanced-affinity glucocorticoid fluticasone furoate in vitro and in an in vivo model of respiratory inflammatory disease', *Am J Physiol Lung Cell Mol Physiol,* 293(3), pp. L660-7.

Sanchez-Vega, B., Krett, N., Rosen, S. T. & Gandhi, V. (2006) 'Glucocorticoid receptor transcriptional isoforms and resistance in multiple myeloma cells', *Mol Cancer Ther,* 5(12), pp. 3062-70.

Savkur, R. S. & Burris, T. P. (2004) 'The coactivator LXXLL nuclear receptor recognition motif', *J Pept Res,* 63(3), pp. 207-12.

Schacke, H., Docke, W. D. & Asadullah, K. (2002) 'Mechanisms involved in the side effects of glucocorticoids', *Pharmacol Ther,* 96(1), pp. 23-43.

Schacke, H., Schottelius, A., Docke, W. D., Strehlke, P., Jaroch, S., Schmees, N., Rehwinkel, H., Hennekes, H. & Asadullah, K. (2004) 'Dissociation of transactivation from transrepression by a selective glucocorticoid receptor agonist leads to separation of therapeutic effects from side effects', *Proc Natl Acad Sci U S A,* 101(1), pp. 227-32.

Schakman, O., Kalista, S., Barbe, C., Loumaye, A. & Thissen, J. P. (2013) 'Glucocorticoid-induced skeletal muscle atrophy', *Int J Biochem Cell Biol,* 45(10), pp. 2163-72.

Scheinman, R. I., Gualberto, A., Jewell, C. M., Cidlowski, J. A. & Baldwin, A. S., Jr. (1995) 'Characterization of mechanisms involved in transrepression of NF-kappa B by activated glucocorticoid receptors', *Mol Cell Biol,* 15(2), pp. 943-53.

Schiller, B. J., Chodankar, R., Watson, L. C., Stallcup, M. R. & Yamamoto, K. R. (2014) 'Glucocorticoid receptor binds half sites

as a monomer and regulates specific target genes', *Genome Biol,* 15(7), pp. 418.

Schneider, C. A., Rasband, W. S. & Eliceiri, K. W. (2012) 'NIH Image to ImageJ: 25 years of image analysis', *Nat Methods,* 9(7), pp. 671-5.

Schneider, R. & Persson, S. (2015) 'Connecting two arrays: the emerging role of actin-microtubule cross-linking motor proteins', *Front Plant Sci,* 6, pp. 415.

Schumacher, S. B., Van den Hauwe, O., Van Peteghem, C. H. & Naegeli, H. (2003) 'Development of a dual luciferase reporter screening assay for the detection of synthetic glucocorticoids in animal tissues', *Analyst,* 128(12), pp. 1406-12.

Shao, W., Rosenauer, A., Mann, K., Chang, C. P., Rachez, C., Freedman, L. P. & Miller, W. H., Jr. (2000) 'Ligand-inducible interaction of the DRIP/TRAP coactivator complex with retinoid receptors in retinoic acid-sensitive and -resistant acute promyelocytic leukemia cells', *Blood,* 96(6), pp. 2233-9.

Shi, F. & Sottile, J. (2008) 'Caveolin-1-dependent beta1 integrin endocytosis is a critical regulator of fibronectin turnover', *J Cell Sci,* 121(Pt 14), pp. 2360-71.

Shi, X., Yao, Y., Wang, Y., Zhang, Y., Huang, Q., Zhou, J., Liu, M. & Li, D. (2015) 'Cep70 regulates microtubule stability by interacting with HDAC6', *FEBS Lett,* 589(15), pp. 1771-7.

Silverstein, A. M., Galigniana, M. D., Chen, M. S., Owens-Grillo, J. K., Chinkers, M. & Pratt, W. B. (1997) 'Protein phosphatase 5 is a major component of glucocorticoid receptor.hsp90 complexes with properties of an FK506-binding immunophilin', *J Biol Chem,* 272(26), pp. 16224-30.

Singh, R., Bassett, E., Chakravarti, A. & Parthun, M. R. (2018) 'Replication-dependent histone isoforms: a new source of

complexity in chromatin structure and function', *Nucleic Acids Res,* 46(17), pp. 8665-8678.

Skultetyova, L., Ustinova, K., Kutil, Z., Novakova, Z., Pavlicek, J., Mikesova, J., Trapl, D., Baranova, P., Havlinova, B., Hubalek, M., Lansky, Z. & Barinka, C. (2017) 'Human histone deacetylase 6 shows strong preference for tubulin dimers over assembled microtubules', *Sci Rep,* 7(1), pp. 11547.

Smith, E., Meyerrose, T. E., Kohler, T., Namdar-Attar, M., Bab, N., Lahat, O., Noh, T., Li, J., Karaman, M. W., Hacia, J. G., Chen, T. T., Nolta, J. A., Muller, R., Bab, I. & Frenkel, B. (2005) 'Leaky ribosomal scanning in mammalian genomes: significance of histone H4 alternative translation in vivo', *Nucleic Acids Res,* 33(4), pp. 1298-308.

Smith, R., Sellou, H., Chapuis, C., Huet, S. & Timinszky, G. (2018) 'CHD3 and CHD4 recruitment and chromatin remodeling activity at DNA breaks is promoted by early poly(ADP-ribose)-dependent chromatin relaxation', *Nucleic Acids Res,* 46(12), pp. 6087-6098.

Smoak, K. A. & Cidlowski, J. A. (2004) 'Mechanisms of glucocorticoid receptor signaling during inflammation', *Mech Ageing Dev,* 125(10-11), pp. 697-706.

Solomon, D. E. (2002) 'An in vitro examination of an extracellular matrix scaffold for use in wound healing', *Int J Exp Pathol,* 83(5), pp. 209-16.

Song, I. H. & Buttgereit, F. (2006) 'Non-genomic glucocorticoid effects to provide the basis for new drug developments', *Mol Cell Endocrinol,* 246(1-2), pp. 142-6.

Spinelli, S. L., Xi, X., McMillan, D. H., Woeller, C. F., Richardson, M. E., Cavet, M. E., Zhang, J. Z., Feldon, S. E. & Phipps, R. P. (2014) 'Mapracorat, a selective glucocorticoid receptor agonist, upregulates RelB, an anti-inflammatory nuclear factor-kappaB protein, in human ocular cells', *Exp Eye Res,* 127, pp. 290-8.

Stahn, C. & Buttgereit, F. (2008) 'Genomic and nongenomic effects of glucocorticoids', *Nat Clin Pract Rheumatol,* 4(10), pp. 525-33.

Stahn, C., Lowenberg, M., Hommes, D. W. & Buttgereit, F. (2007) 'Molecular mechanisms of glucocorticoid action and selective glucocorticoid receptor agonists', *Mol Cell Endocrinol,* 275(1-2), pp. 71-8.

Stamer, W. D., Hoffman, E. A., Kurali, E. & Krauss, A. H. (2013) 'Unique response profile of trabecular meshwork cells to the novel selective glucocorticoid receptor agonist, GW870086X', *Invest Ophthalmol Vis Sci,* 54(3), pp. 2100-7.

Stavreva, D. A., Muller, W. G., Hager, G. L., Smith, C. L. & McNally, J. G. (2004) 'Rapid glucocorticoid receptor exchange at a promoter is coupled to transcription and regulated by chaperones and proteasomes', *Mol Cell Biol,* 24(7), pp. 2682-97.

Stevens, A., Garside, H., Berry, A., Waters, C., White, A. & Ray, D. (2003) 'Dissociation of steroid receptor coactivator 1 and nuclear receptor corepressor recruitment to the human glucocorticoid receptor by modification of the ligand-receptor interface: the role of tyrosine 735', *Mol Endocrinol,* 17(5), pp. 845-59.

Stojadinovic, O., Sawaya, A., Pastar, I. & Tomic-Canic, M. (2013) 'Glucocorticoid receptor localizes to adherens junctions at the plasma membrane of keratinocytes', *PLoS One,* 8(4), pp. e63453.

Strehl, C. & Buttgereit, F. (2014) 'Unraveling the functions of the membrane-bound glucocorticoid receptors: first clues on origin and functional activity', *Ann N Y Acad Sci,* 1318, pp. 1-6.

Strehl, C., Gaber, T., Lowenberg, M., Hommes, D. W., Verhaar, A. P., Schellmann, S., Hahne, M., Fangradt, M., Wagegg, M., Hoff, P., Scheffold, A., Spies, C. M., Burmester, G. R. & Buttgereit, F.

(2011) 'Origin and functional activity of the membrane-bound glucocorticoid receptor', *Arthritis Rheum,* 63(12), pp. 3779-88.

Suino-Powell, K., Xu, Y., Zhang, C., Tao, Y. G., Tolbert, W. D., Simons, S. S., Jr. & Xu, H. E. (2008) 'Doubling the size of the glucocorticoid receptor ligand binding pocket by deacylcortivazol', *Mol Cell Biol,* 28(6), pp. 1915-23.

Sumi, T., Matsumoto, K., Takai, Y. & Nakamura, T. (1999) 'Cofilin phosphorylation and actin cytoskeletal dynamics regulated by rho- and Cdc42-activated LIM-kinase 2', *J Cell Biol,* 147(7), pp. 1519-32.

Sun, L. C., Lin, J. T., Li, W., Zhang, L., Zhou, T. L. & Zhang, X. Y. (2012) 'Nicotine inhibits histone deacetylase 6 activity and chaperone-dependent activation of the glucocorticoid receptor in A549 cells', *Chin Med J (Engl),* 125(4), pp. 662-6.

Sun, M. & Zaman, M. H. (2017) 'Modeling, signaling and cytoskeleton dynamics: integrated modeling-experimental frameworks in cell migration', *Wiley Interdiscip Rev Syst Biol Med,* 9(1).

Surjit, M., Ganti, K. P., Mukherji, A., Ye, T., Hua, G., Metzger, D., Li, M. & Chambon, P. (2011) 'Widespread negative response elements mediate direct repression by agonist-liganded glucocorticoid receptor', *Cell,* 145(2), pp. 224-41.

Tanaka, H., Shimizu, N. & Yoshikawa, N. (2017) 'Role of skeletal muscle glucocorticoid receptor in systemic energy homeostasis', *Exp Cell Res,* 360(1), pp. 24-26.

Tao, H., Chen, Y. Y., Sun, Z. W., Chen, H. L. & Chen, M. (2018) 'Silence of HDAC6 suppressed esophageal squamous cell carcinoma proliferation and migration by disrupting chaperone function of HSP90', *J Cell Biochem,* 119(8), pp. 6623-6632.

Tape, C. J., Worboys, J. D., Sinclair, J., Gourlay, R., Vogt, J., McMahon, K. M., Trost, M., Lauffenburger, D. A., Lamont, D. J. & Jorgensen,

C. (2014) 'Reproducible automated phosphopeptide enrichment using magnetic TiO2 and Ti-IMAC', *Anal Chem,* 86(20), pp. 10296-302.

Teng, Z., Zhang, M., Zhao, M. & Zhang, W. (2013) 'Glucocorticoid exerts its non-genomic effect on IPSC by activation of a phospholipase C-dependent pathway in prefrontal cortex of rats', *J Physiol,* 591(13), pp. 3341-53.

Thanomkitti, K., Fong-Ngern, K., Sueksakit, K., Thuangtong, R. & Thongboonkerd, V. (2018) 'Molecular functional analyses revealed essential roles of HSP90 and lamin A/C in growth, migration, and self-aggregation of dermal papilla cells', *Cell Death Discov,* 4, pp. 53.

Tiwari, M., Oasa, S., Yamamoto, J., Mikuni, S. & Kinjo, M. (2017) 'A Quantitative Study of Internal and External Interactions of Homodimeric Glucocorticoid Receptor Using Fluorescence Cross-Correlation Spectroscopy in a Live Cell', *Sci Rep,* 7(1), pp. 4336.

Trebble, P. J., Woolven, J. M., Saunders, K. A., Simpson, K. D., Farrow, S. N., Matthews, L. C. & Ray, D. W. (2013) 'A ligand-specific kinetic switch regulates glucocorticoid receptor trafficking and function', *J Cell Sci,* 126(Pt 14), pp. 3159-69.

Tu, G. W., Shi, Y., Zheng, Y. J., Ju, M. J., He, H. Y., Ma, G. G., Hao, G. W. & Luo, Z. (2017) 'Glucocorticoid attenuates acute lung injury through induction of type 2 macrophage', *J Transl Med,* 15(1), pp. 181.

Tu, J., Stoner, S., Fromm, P. D., Wang, T., Chen, D., Tuckermann, J., Cooper, M. S., Seibel, M. J. & Zhou, H. (2018) 'Endogenous glucocorticoid signaling in chondrocytes attenuates joint inflammation and damage', *FASEB J,* 32(1), pp. 478-487.

Turney, M. K. & Kovacs, W. J. (2001) 'Function of a truncated glucocorticoid receptor form at a negative glucocorticoid response

element in the proopiomelanocortin gene', *J Mol Endocrinol,* 26(1), pp. 43-9.

Tyanova, S., Temu, T., Sinitcyn, P., Carlson, A., Hein, M. Y., Geiger, T., Mann, M. & Cox, J. (2016) 'The Perseus computational platform for comprehensive analysis of (prote)omics data', *Nat Methods,* 13(9), pp. 731-40.

Uings, I. J., Needham, D., Matthews, J., Haase, M., Austin, R., Angell, D., Leavens, K., Holt, J., Biggadike, K. & Farrow, S. N. (2013) 'Discovery of GW870086: a potent anti-inflammatory steroid with a unique pharmacological profile', *Br J Pharmacol,* 169(6), pp. 1389-403.

Valenzuela-Fernandez, A., Cabrero, J. R., Serrador, J. M. & Sanchez-Madrid, F. (2008) 'HDAC6: a key regulator of cytoskeleton, cell migration and cell-cell interactions', *Trends Cell Biol,* 18(6), pp. 291-7.

van de Garde, M. D., Martinez, F. O., Melgert, B. N., Hylkema, M. N., Jonkers, R. E. & Hamann, J. (2014) 'Chronic exposure to glucocorticoids shapes gene expression and modulates innate and adaptive activation pathways in macrophages with distinct changes in leukocyte attraction', *J Immunol,* 192(3), pp. 1196-208.

van den Heuvel, J. K., Boon, M. R., van Hengel, I., Peschier-van der Put, E., van Beek, L., van Harmelen, V., van Dijk, K. W., Pereira, A. M., Hunt, H., Belanoff, J. K., Rensen, P. C. & Meijer, O. C. (2016) 'Identification of a selective glucocorticoid receptor modulator that prevents both diet-induced obesity and inflammation', *Br J Pharmacol,* 173(11), pp. 1793-804.

van der Burg, B., Liden, J., Okret, S., Delaunay, F., Wissink, S., van der Saag, P. T. & Gustafsson, J. A. (1997) 'Nuclear factor-kappa B repression in antiinflammation and immunosuppression by glucocorticoids', *Trends Endocrinol Metab,* 8(4), pp. 152-7.

Vanden Berghe, W., Francesconi, E., De Bosscher, K., Resche-Rigon, M. & Haegeman, G. (1999) 'Dissociated glucocorticoids with anti-inflammatory potential repress interleukin-6 gene expression by a nuclear factor-kappaB-dependent mechanism', *Mol Pharmacol,* 56(4), pp. 797-806.

Vittorio, C. C. & Werth, V. P. (2000) 'Preventive techniques to limit glucocorticoid-induced side effects', *Adv Dermatol,* 16, pp. 273-97; discussion 298.

Vockley, C. M., D'Ippolito, A. M., McDowell, I. C., Majoros, W. H., Safi, A., Song, L., Crawford, G. E. & Reddy, T. E. (2016) 'Direct GR Binding Sites Potentiate Clusters of TF Binding across the Human Genome', *Cell,* 166(5), pp. 1269-1281 e19.

Volk, A. & Crispino, J. D. (2015) 'The role of the chromatin assembly complex (CAF-1) and its p60 subunit (CHAF1b) in homeostasis and disease', *Biochim Biophys Acta,* 1849(8), pp. 979-86.

Vollmer, T. R., Stockhausen, A. & Zhang, J. Z. (2012) 'Anti-inflammatory effects of mapracorat, a novel selective glucocorticoid receptor agonist, is partially mediated by MAP kinase phosphatase-1 (MKP-1)', *J Biol Chem,* 287(42), pp. 35212-21.

Wai, D. C. C., Szyszka, T. N., Campbell, A. E., Kwong, C., Wilkinson-White, L. E., Silva, A. P. G., Low, J. K. K., Kwan, A. H., Gamsjaeger, R., Chalmers, J. D., Patrick, W. M., Lu, B., Vakoc, C. R., Blobel, G. A. & Mackay, J. P. (2018) 'The BRD3 ET domain recognizes a short peptide motif through a mechanism that is conserved across chromatin remodelers and transcriptional regulators', *J Biol Chem,* 293(19), pp. 7160-7175.

Wallace, A. D. & Cidlowski, J. A. (2001) 'Proteasome-mediated glucocorticoid receptor degradation restricts transcriptional signaling by glucocorticoids', *J Biol Chem,* 276(46), pp. 42714-21.

Waltner-Law, M., Duong, D. T., Daniels, M. C., Herzog, B., Wang, X. L., Prasad, R. & Granner, D. K. (2003) 'Elements of the glucocorticoid and retinoic acid response units are involved in cAMP-mediated expression of the PEPCK gene', *J Biol Chem,* 278(12), pp. 10427-35.

Wang, H., Aslanian, R. & Madison, V. S. (2008) 'Induced-fit docking of mometasone furoate and further evidence for glucocorticoid receptor 17alpha pocket flexibility', *J Mol Graph Model,* 27(4), pp. 512-21.

Wang, X. & DeFranco, D. B. (2005) 'Alternative effects of the ubiquitin-proteasome pathway on glucocorticoid receptor down-regulation and transactivation are mediated by CHIP, an E3 ligase', *Mol Endocrinol,* 19(6), pp. 1474-82.

Wang, Z., Chen, W., Kono, E., Dang, T. & Garabedian, M. J. (2007) 'Modulation of glucocorticoid receptor phosphorylation and transcriptional activity by a C-terminal-associated protein phosphatase', *Mol Endocrinol,* 21(3), pp. 625-34.

Watson, L. C., Kuchenbecker, K. M., Schiller, B. J., Gross, J. D., Pufall, M. A. & Yamamoto, K. R. (2013) 'The glucocorticoid receptor dimer interface allosterically transmits sequence-specific DNA signals', *Nat Struct Mol Biol,* 20(7), pp. 876-83.

Weber, S. G. (1984) 'Chromatographic band broadening theory using a random walk with a step-length distribution', *Anal Chem,* 56(12), pp. 2104-9.

Weikum, E. R., de Vera, I. M. S., Nwachukwu, J. C., Hudson, W. H., Nettles, K. W., Kojetin, D. J. & Ortlund, E. A. (2017) 'Tethering not required: the glucocorticoid receptor binds directly to activator protein-1 recognition motifs to repress inflammatory genes', *Nucleic Acids Res,* 45(14), pp. 8596-8608.

Weinstein, S. P., Paquin, T., Pritsker, A. & Haber, R. S. (1995) 'Glucocorticoid-induced insulin resistance: dexamethasone

inhibits the activation of glucose transport in rat skeletal muscle by both insulin- and non-insulin-related stimuli', *Diabetes,* 44(4), pp. 441-5.

Werkstrom, V., Prothon, S., Ekholm, E., Jorup, C. & Edsbacker, S. (2016) 'Safety, Pharmacokinetics and Pharmacodynamics of the Selective Glucocorticoid Receptor Modulator AZD5423 after Inhalation in Healthy Volunteers', *Basic Clin Pharmacol Toxicol,* 119(6), pp. 574-581.

Whirledge, S., Kisanga, E. P., Taylor, R. N. & Cidlowski, J. A. (2017) 'Pioneer Factors FOXA1 and FOXA2 Assist Selective Glucocorticoid Receptor Signaling in Human Endometrial Cells', *Endocrinology,* 158(11), pp. 4076-4092.

White, J. T., Li, J., Grasso, E., Wrabl, J. O. & Hilser, V. J. (2018) 'Ensemble allosteric model: energetic frustration within the intrinsically disordered glucocorticoid receptor', *Philos Trans R Soc Lond B Biol Sci,* 373(1749).

Winkler, R., Benz, V., Clemenz, M., Bloch, M., Foryst-Ludwig, A., Wardat, S., Witte, N., Trappiel, M., Namsolleck, P., Mai, K., Spranger, J., Matthias, G., Roloff, T., Truee, O., Kappert, K., Schupp, M., Matthias, P. & Kintscher, U. (2012) 'Histone deacetylase 6 (HDAC6) is an essential modifier of glucocorticoid-induced hepatic gluconeogenesis', *Diabetes,* 61(2), pp. 513-23.

Wu, B., Li, P., Liu, Y., Lou, Z., Ding, Y., Shu, C., Ye, S., Bartlam, M., Shen, B. & Rao, Z. (2004) '3D structure of human FK506-binding protein 52: implications for the assembly of the glucocorticoid receptor/Hsp90/immunophilin heterocomplex', *Proc Natl Acad Sci U S A,* 101(22), pp. 8348-53.

Wu, D. Y., Ou, C. Y., Chodankar, R., Siegmund, K. D. & Stallcup, M. R. (2014) 'Distinct, genome-wide, gene-specific selectivity patterns of four glucocorticoid receptor coregulators', *Nucl Recept Signal,* 12, pp. e002.

Wu, S. Z. & Bezanilla, M. (2018) 'Actin and microtubule cross talk mediates persistent polarized growth', *J Cell Biol*.

Wust, S., Tischner, D., John, M., Tuckermann, J. P., Menzfeld, C., Hanisch, U. K., van den Brandt, J., Luhder, F. & Reichardt, H. M. (2009) 'Therapeutic and adverse effects of a non-steroidal glucocorticoid receptor ligand in a mouse model of multiple sclerosis', *PLoS One,* 4(12), pp. e8202.

Xing, K., Gu, B., Zhang, P. & Wu, X. (2015) 'Dexamethasone enhances programmed cell death 1 (PD-1) expression during T cell activation: an insight into the optimum application of glucocorticoids in anti-cancer therapy', *BMC Immunol,* 16, pp. 39.

Yang, H., Ganguly, A. & Cabral, F. (2010) 'Inhibition of cell migration and cell division correlates with distinct effects of microtubule inhibiting drugs', *J Biol Chem,* 285(42), pp. 32242-50.

Yang, J., Liu, J. & DeFranco, D. B. (1997) 'Subnuclear trafficking of glucocorticoid receptors in vitro: chromatin recycling and nuclear export', *J Cell Biol,* 137(3), pp. 523-38.

Yang, N., Baban, B., Isales, C. M. & Shi, X. M. (2017) 'Role of glucocorticoid-induced leucine zipper (GILZ) in inflammatory bone loss', *PLoS One,* 12(8), pp. e0181133.

Yoon, Y., Noh, S., Jeong, J. & Park, K. (2018) 'An accuracy improvement method for the topology measurement of an atomic force microscope using a 2D wavelet transform', *Ultramicroscopy,* 188, pp. 70-76.

Yoshikawa, N., Shimizu, N., Sano, M., Ohnuma, K., Iwata, S., Hosono, O., Fukuda, K., Morimoto, C. & Tanaka, H. (2008) 'Role of the hinge region of glucocorticoid receptor for HEXIM1-mediated transcriptional repression', *Biochem Biophys Res Commun,* 371(1), pp. 44-9.

Yu, S., Cai, X., Wu, C., Liu, Y., Zhang, J., Gong, X., Wang, X., Wu, X., Zhu, T., Mo, L., Gu, J., Yu, Z., Chen, J., Thiery, J. P., Chai, R. & Chen, L. (2017) 'Targeting HSP90-HDAC6 Regulating Network Implicates Precision Treatment of Breast Cancer', *Int J Biol Sci,* 13(4), pp. 505-517.

Yumura, S., Itoh, G., Kikuta, Y., Kikuchi, T., Kitanishi-Yumura, T. & Tsujioka, M. (2013) 'Cell-scale dynamic recycling and cortical flow of the actin-myosin cytoskeleton for rapid cell migration', *Biol Open,* 2(2), pp. 200-9.

Zaret, K. S. & Carroll, J. S. (2011) 'Pioneer transcription factors: establishing competence for gene expression', *Genes Dev,* 25(21), pp. 2227-41.

Zeng, R., Lin, C., Lin, Z., Chen, H., Lu, W., Lin, C. & Li, H. (2018) 'Approaches to cutaneous wound healing: basics and future directions', *Cell Tissue Res,* 374(2), pp. 217-232.

Zhang, L., Liu, N., Xie, S., He, X., Zhou, J., Liu, M. & Li, D. (2014) 'HDAC6 regulates neuroblastoma cell migration and may play a role in the invasion process', *Cancer Biol Ther,* 15(11), pp. 1561-70.

Zhang, X., Yuan, Z., Zhang, Y., Yong, S., Salas-Burgos, A., Koomen, J., Olashaw, N., Parsons, J. T., Yang, X. J., Dent, S. R., Yao, T. P., Lane, W. S. & Seto, E. (2007) 'HDAC6 modulates cell motility by altering the acetylation level of cortactin', *Mol Cell,* 27(2), pp. 197-213.

Zhang, Y., Li, N., Caron, C., Matthias, G., Hess, D., Khochbin, S. & Matthias, P. (2003) 'HDAC-6 interacts with and deacetylates tubulin and microtubules in vivo', *EMBO J,* 22(5), pp. 1168-79.

Zhao, Z., Xu, H. & Gong, W. (2010) 'Histone deacetylase 6 (HDAC6) is an independent deacetylase for alpha-tubulin', *Protein Pept Lett,* 17(5), pp. 555-8.

Zhou, G. L., Zhang, H., Wu, H., Ghai, P. & Field, J. (2014) 'Phosphorylation of the cytoskeletal protein CAP1 controls its association with cofilin and actin', *J Cell Sci,* 127(Pt 23), pp. 5052-65.

Zhou, J. & Cidlowski, J. A. (2005) 'The human glucocorticoid receptor: one gene, multiple proteins and diverse responses', *Steroids,* 70(5-7), pp. 407-17.

Zou, W., Yang, S., Zhang, T., Sun, H., Wang, Y., Xue, H. & Zhou, D. (2015) 'Hypoxia enhances glucocorticoid-induced apoptosis and cell cycle arrest via the PI3K/Akt signaling pathway in osteoblastic cells', *J Bone Miner Metab,* 33(6), pp. 615-24.